UC Santa Cruz
UC Santa Cruz Electronic Theses and Dissertations

Title
A Comparative Study of Passive versus Dynamic Sea-Level Rise Inundation Models for the Island of Kauai

Permalink
https://escholarship.org/uc/item/37m1084z

Author
Bezore, Rhiannon Victoria Ann

Publication Date
2014

Peer reviewed|Thesis/dissertation

eScholarship.org Powered by the California Digital Library
University of California

UNIVERSITY OF CALIFORNIA

SANTA CRUZ

A Comparative Study of Passive versus Dynamic Sea-Level Rise Inundation Models for the Island of Kauai

A thesis submitted in partial satisfaction
of the requirements for the degree of

MASTER OF SCIENCE

in

EARTH SCIENCES

by

Rhiannon Bezore

September 2014

The Thesis of Rhiannon Bezore
is approved:

Professor Gary Griggs, Chair

Professor Noah Finnegan

Curt Storlazzi

Tyrus Miller
Vice Provost and Dean of Graduate Studies

Copyright © by

Rhiannon Bezore

2014

Table of Contents

List of Figures

List of Tables

List of Appendices

Abstract

A COMPARATIVE STUDY OF PASSIVE VERSUS DYNAMIC SEA-LEVEL RISE INUNDATION MODELS FOR THE ISLAND OF KAUAI

by

Rhiannon Bezore

Using ArcGIS, a sea-level rise inundation comparison was conducted using four different techniques under five sea-level rise conditions for the Kauai, Hawaii, towns of Hanalei Bay, Kapa'a, and Waimea. Sea-level rise was mapped in 0.5 m increments from 0.0 m of rise to 2.0 m of rise. Datasets used in the analysis include a digital elevation model (DEM) layer, wave height data, tidal elevation data, and land cover data. The four techniques illustrating projected inundation serve as a comparison of passive versus dynamic models. The primary goals of this study were to not only compare passive and dynamic sea-level rise inundation models, but also to provide a realistic representation of what future sea-level rise will look like on Kauai, and which areas would be inundated at specific future water surface levels. The results of this analysis can be used to aid Kauai government officials in planning for the future and to aid in prioritizing where and what infrastructure and development will need to be considered before actual sea-level rise impacts occur.

Acknowledgements

I would like to thank Gary Griggs, who has not only been an amazing adviser but also a mentor who has helped shape both my academic and career paths. A wholehearted thank you is owed to Curt Storlazzi of USGS, as well, for all of his guidance and help during the process of completing this project. Finally, I would like to sincerely thank my family for their encouragement throughout my academic career and for their continued support in all of my endeavors.

Introduction

Sea level has been rising steadily since the beginning of the 20th Century at a rate of about 1.8 mm /yr, with the rates increasing to about 3.0 mm/yr since 2000 (NRC, 2012; Board on Atmospheric Sciences and Climate, 2010. P.238) (**Figure 1**). Prior to 1993, sea level measurements were taken from tide gauges, which provide only local values, but since then satellite altimetry has become the primary method of measurement, which provides global values. According the latest IPCC report on sea-level rise and climate change, under IPCC AR5 scenarios and within the 95% confidence range, global sea level is projected to rise by 0.80 m between 1996 and 2100 (Church et.al, 2013. P.1184). Between the years of 2081 and 2100, the fifth IPCC report also projects the rate of global mean sea-level rise to range from 4.4 mm/yr to 11.2 mm/yr (P.1181). For the Hawaiian Islands, however, sea level is projected to increase by about 0.82 m (~2.6 ft) from 1990 levels by the year 2100 (Codiga and Wager, 2011. P.2).

This local increase in sea level and global sea-level rise can be attributed to the increase in anthropogenic carbon dioxide (CO_2) that has been observed and documented (**Figure 2**) since the Industrial Revolution in the late 19th Century and subsequent drastic increase in the burning of fossil fuels (Board on Atmospheric Sciences and Climate, 2010. P.185). Carbon dioxide from anthropogenic sources enhances Earth's greenhouse effect by trapping long-wave radiation emitted from Earth's surface. As the atmosphere warms, sea- level rises as a result of two main factors, the melting of land ice and the thermal expansion of seawater. The first raises sea level by adding mass to the ocean in the form of melting terrestrial ice, compared to the melting of sea ice, which does not have an effect on sea level. The second factor is a function of water's unique physical properties, in that as water warms, it expands. Sea-level rise is not uniform across the globe and is actually projected to decrease in some regions due to tectonic uplift and other regional effects. Sea level surrounding the Hawaiian Islands tends to rise more slowly than the global average rate, possibly due to wind patterns in the Pacific Ocean and the piling of warm water to the western Pacific, which raises sea level in that region relative to the rest of the Pacific. Hawaii has had an average 0.15 cm/yr increase in sea level over the last century, but the islands are still very susceptible to the impacts of rise (Fletcher, 2012).

Figure 1 Sea-level change for 1870-2014, with data shown in blue being based on tide gages and data shown in red being based on satellite altimetry (Church 2006, and University of Colorado, 2014).

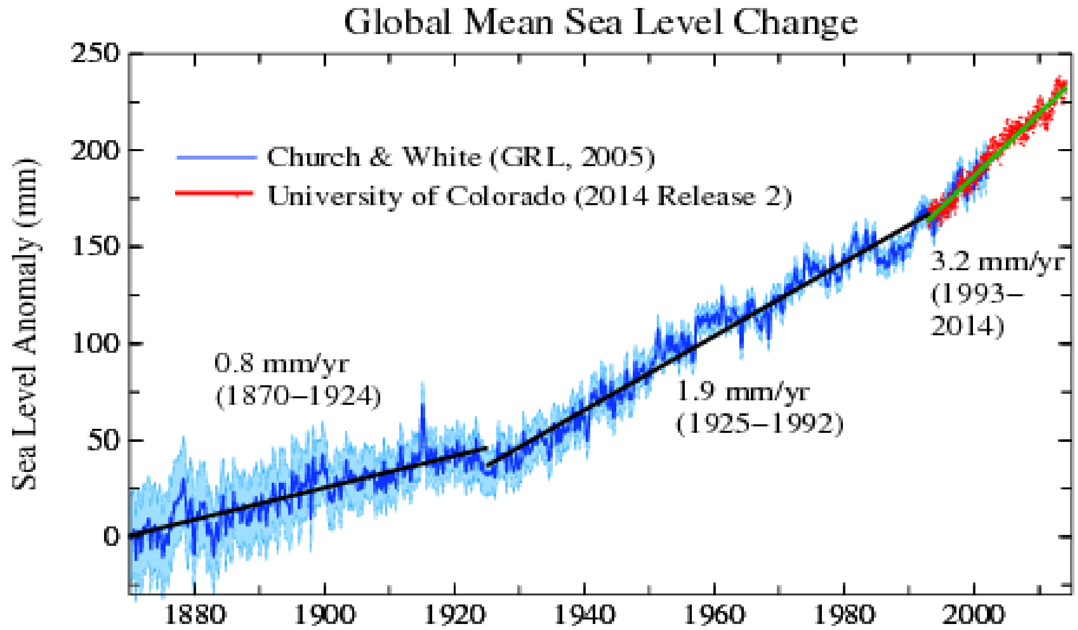

Figure 2 The Keeling Curve showing atmospheric carbon dioxide measured at the Mauna Loa Observatory from 1960 to 2014 (keelingcurve.ucsd.edu).

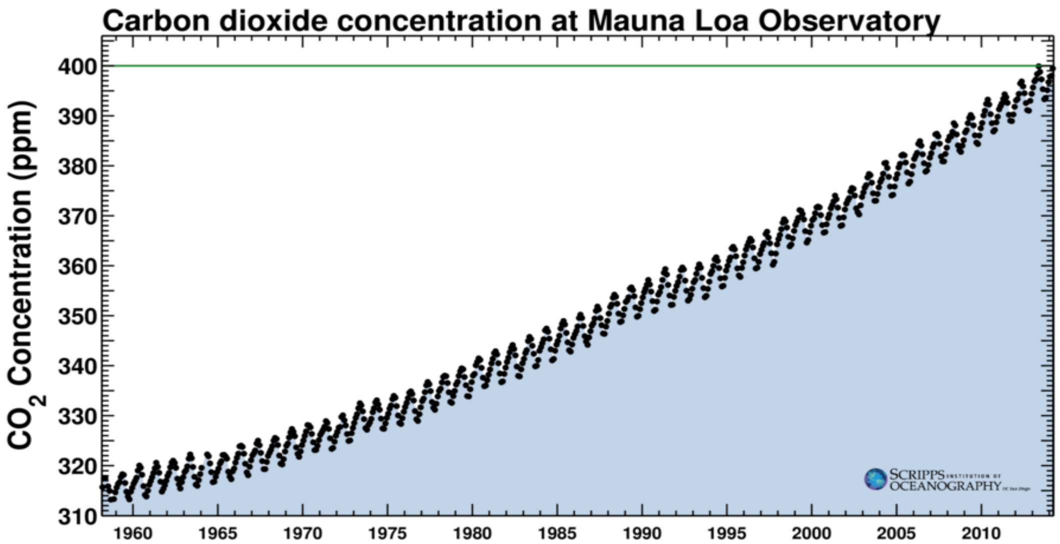

The most common type of sea-level rise inundation mapping is what is known as passive or “bathtub modeling,” in that it “represents a reference level and depicts the amount of inundation due to sea-level rise only,” much like filling up a bathtub (Storlazzi, 2013. P.13). The simplest way to illustrate inundation in a passive model is to show any low-lying elevation that is likely to be inundated by a rise in sea level. The next simplest passive method is to use sea surface height specific to the region, from tidal data, to show inundation due to sea-level rise combined with high tides. This is best shown using mean higher high tides, so as to show the maximum impact.

Neither type of passive model takes into account dynamic forces, such as wave height, wave shoaling, wave set-up, or wave run-up (**Figure 3**). Wave height is measured offshore at a given depth, and the wave face will steepen as the wave propagates through shallower water, shoaling over the fringing reef that is found on the outer edges of the bay, and run-up the beach as it breaks. These processes will act to amplify the effects of sea-level rise, especially when mapped on top of a tidal surface. This study compares two types of passive inundation models: one showing low-lying areas susceptible to inundation and one showing tidal surfaces with sea-level rise. Two types of dynamic models are also analyzed: one showing sea-level rise with wave set-up and one showing sea-level rise with wave set-up and wave run-up. Both of the dynamic models also incorporate tidal sea surface height at mean higher high water.

Figure 3 Visual representation of passive versus dynamic inundation models, including various components of inundation calculations for each (Storlazzi, 2013. P.4).

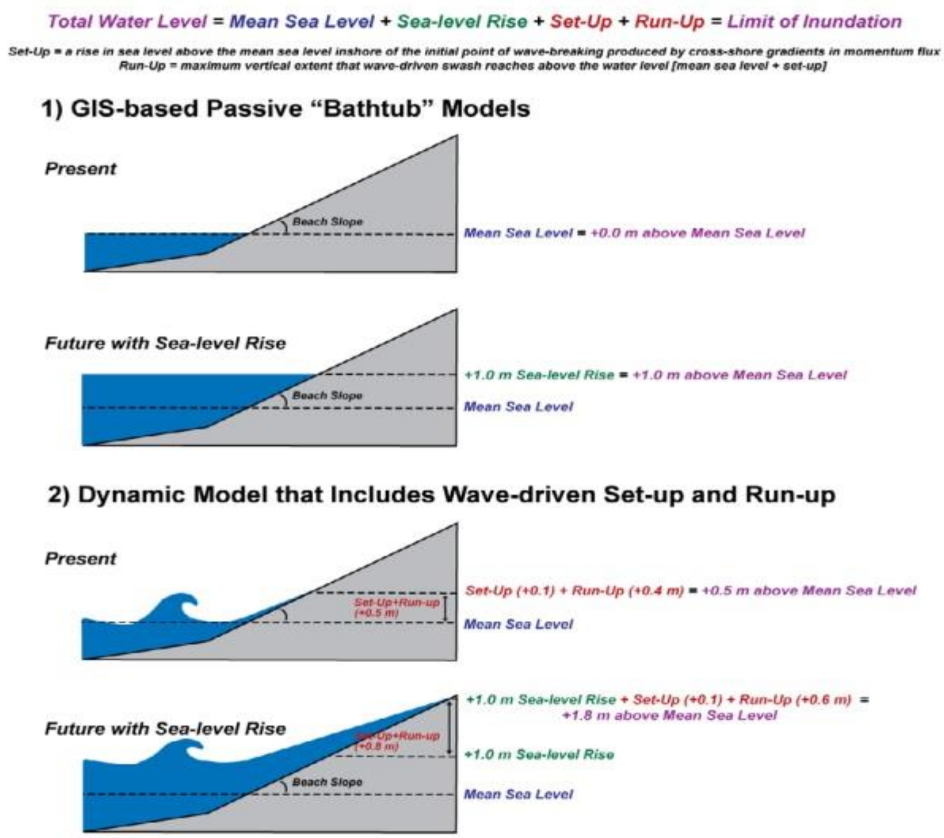

Study Area

The Hawaiian-Emperor Seamount Chain is an intra-plate volcanic chain that sits over an inferred hotspot, which is believed to be the rising of a magma plume stemming from as deep as the core-mantle boundary, although some argue that the magma source is from the shallow asthenosphere (Courtillot, et al., 2003). This hotspot is currently located underneath the Big Island of Hawaii (**Figure 4**), which accounts for the ongoing volcanism on the island. The seamount chain extends over 6,000 kilometers from the Big Island of Hawaii to the Aleutian Trench and increase in age farther away from the hotspot (Watson 1999). The seamounts are shield volcanoes formed from low viscosity, very fluid basaltic lava flows. The Hawaiian Islands sit south of the bend and showcase the expected behavior of westward Pacific Plate motion and an inferred hotspot (Clague and Dalrymple, 1989), although more recent work suggests that the bend in the chain is more likely due to a moving hot spot rather than a shift in plate motion (Tarduno, et al., 2009).

Figure 4 Depiction of hotspot volcanism that currently lies under Hawaii, increasing age away from the hotspot, and north-west movement of the Pacific Plate. (Eruptions of Hawaiian Volcanoes: Past, Present, and Future: U.S. Geological Survey General Interest Publication).

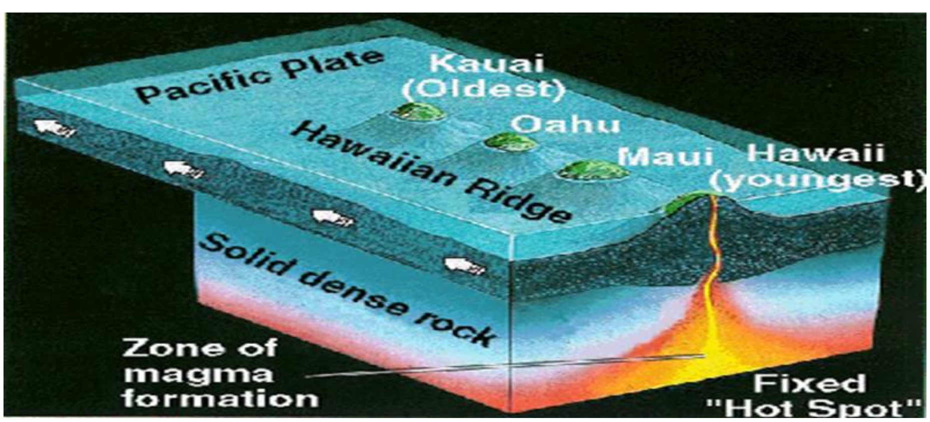

Kauai is the northern-most and oldest inhabited island in the Hawaiian Island Chain, at 477 km from Hawaii and about 5.7 million years old (SOEST). It has 75 km of sandy beaches, 71% of which show signs of erosion, classified as temporary or permanent decrease in beach width, rather than cliff erosion, over the past 86 years (Fletcher, et al, 2012, P.21). One factor that impacts Kauai's high percentages of beach erosion is that it is a volcanic island. The igneous rocks that make up the island are resistant to the eroding processes, such as wind, rain, and flowing rivers, that would carry sediment from inland to the beaches. The sediment supply from inland is limited to said beaches, and when sediment supply does not equal or surpass sediment loss, beaches erode. The decrease in beach widths will only continue with an increase in sea-level unless inland migration of the beaches is allowed to occur as it would without anthropogenic influence. It is believed that "areas lying within 32 cm (1ft) of modern mean higher high water (MHHW) are especially vulnerable to the impacts of SLR by mid-century while those lying between O.75 and 1.9 m (2.5-6.2ft) will be vulnerable in the latter half of the century" (SOEST, 2008).

Three specific locations on the island of Kauai were chosen for this study: Hanalei, Kapa'a, and Waimea (**Figure 5**). These locations were chosen to represent different conditions and to serve as case studies for passive regional versus dynamic regional inundation models. Each site has different on- and offshore conditions, including wave height and direction, bathymetry, topography, beach slope, and land cover types. All three locations were also identified as areas of interest to the County of Kauai after conferring with Sea Grant Hawaii and the County of Kauai Planning Department (2013).

Figure 5 Study area showing Kauai as the northernmost island of the Hawaiian Islands and the three specific study sites: Hanalei on the northern coast, Kapa'a on the east, and Waimea in the southwest

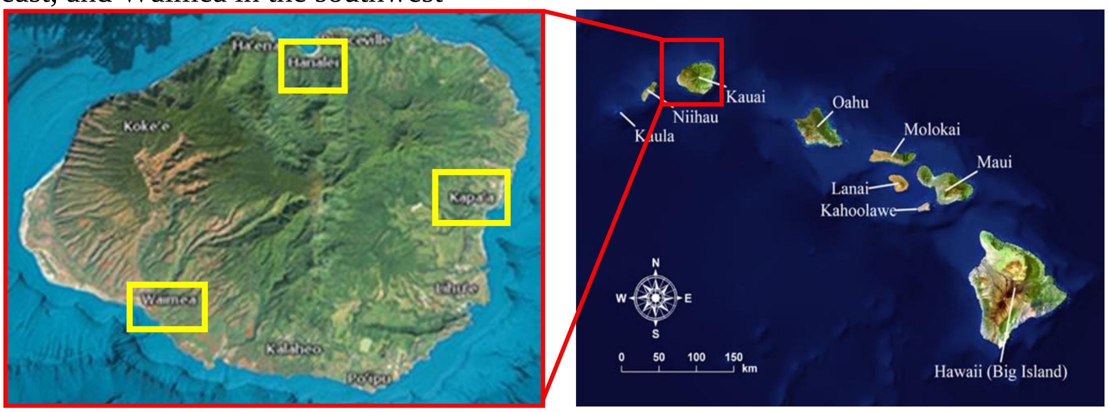

The town of Hanalei (**Figure 5**) is located on the north shore of Kauai in between the towns of Haena to the west and Princeville to the east and is situated on the Hanalei Bay. The town is bounded by the Waioli Stream on the west and the Hanalei River on the east, and the beaches of Hanalei are primarily made of carbonate and terrigenous sediments. Hanalei beaches (**Figure 6**) are experiencing an average accretion rate of

0.0 m/yr to 1.4 m/yr, but can experience large erosional events during winter swells and can experience greater accretion during calm summer months (Fletcher, et al., 2011).

Figure 6 Hanalei facing east towards the Hanalei Pier, showing conditions during Summer 2013.

Kapa’a is on the east side of Kauai (**Figure 5**) and is confined by what is left of the Kealia Landing to the north and the Waikaea Canal to the south (Kauai Shoreline Study Erosion Maps, 2008). The average long-term (1927-2008) erosion rate for Kapa’a is -0.19 m/yr to -0.15 m/y., while the average short-term (1950-2008) erosion rate is -0.10 m/yr to -0.06 m/yr (Fletcher, 2011). There are already several protection measures in place to slow erosion along this section of coast, including rip rap and groins placed along the shoreline, as well as barrier fences sectioning off highly erodible sections of the coast in hopes of limiting human access, which tends to increase erosion (**Figure 7**).

Figure 7 Kapa'a showing conditions during Summer 2012 and Summer 2014, respectively. Note the proximity of infrastructure to the beach and the existence of a temporary fence to slow erosion of the coast along this section.

Waimea is located on the southwest shore of Kauai (**Figure 5**) and is subject to Kona storm waves, which occur mostly from October through April, are generated by southerly and southwesterly winds, and reach heights of 3-5 m; trade wind waves; and southern swell, as well as being exposed to inundation up to 300 m inland from hurricanes such as Iwa (1982) and Iniki (1992) (Fletcher, 2012. P.25). Waimea is confined by the Kikiaola Small Boat Harbor, built in 1959, in the west and the Waimea River in the east, both of which lead to a maximum trend of 0.7 m/yr to 2.1 m/yr of accretion on Waimea's beaches. The river supplies the majority of the sediment, and the jetties that bound both sides of the harbor trap sand on the east side of the harbor as it flows to the west (Fletcher, et al., 2011) (**Figure 8**).

Figure 8 Looking east on Waimea Beach from the Waimea State Recreation Pier (Google Earth, 2012)

According to the last countywide census that included all of the census designated places (CDP), of Kauai County’s 67, 090 residents, 450 live in Hanalei, 10,699 live in Kapa’a, and 9,212 live in Waimea (US Census, 2010). The majority of these residents live at or near sea level. In addition, Kauai’s economy is almost entirely dependent upon tourism, which in turn is dependent upon the beaches. With sea-level rise, one can expect to see damage to buildings and infrastructure, beach erosion, inundation of low lying areas, and increased impacts during storm events, none of which are conducive to living near the coast or to supporting an economy reliant on tourist who come primarily for the beach experience (Fletcher, et al, 2010, P.16). Examining and analyzing future impacts from sea level rise before the impacts are actually occurring is a worthwhile and useful endeavor, whether or not it is known exactly when the sea-level rise will occur (Fletcher, et al, 2010, P.15).

Methods

Four different methods in ArcGIS were used in this study to show inundation due to 0.0 m, 0.5 m, 1.0 m, 1.5 m, and 2.0 m of sea-level rise. All of the methods used a 3 m digital elevation model (DEM) obtained from NOAA that is referenced vertically to local mean sea level (LMSL) and horizontally to the North American Datum of 1983 (NAD83) (NOAA, 2010). This is the same DEM that is used in NOAA's Hawaii Edition of the Digital Coast Sea-level rise and Coastal Flooding Impacts Viewer. Methods in this study were based in part off of the methods used in Storlazzi et. al's (2013) comparative study of passive versus dynamic inundation models and NOAA's Detailed Methodology for Mapping Sea-Level Rise Inundation (NOAA, 2012).

The first method was to simply show any elevation less than each of the stated increments of sea-level rise, which was done by using a conditional statement within the map algebra raster calculator tool to create a binary raster. This process was completed for each of the three locations with accompanying maps showing the results of each increment of sea-level rise.

The second method included tidal data for each location to show not only low-lying areas susceptible to inundation, as was the case in the first method, but also to give a more realistic inundation scenario as well as the increased impact that high tides can have on inundation. The tidal data was retrieved from NOAA, both from the Digital Coast Sea-level rise and Coastal Flooding Impacts data set, and from the Tides and Currents database for verification of sea surface elevation for the three locations. The tidal data used was all in the mean higher high water tidal datum, which is the average of the higher high water height of each tidal day observed over the National Tidal Datum Epoch, so as to create a tidal surface that would provide maximum inundation values (NOAA, 2012). This average mean higher high water value for each location was then added to each sea-level rise increment. This again was done using a conditional statement within ArcMaps' math algebra tool to create a binary raster layer for each sea- level rise scenario. These layers were combined into a map to show each level of inundation.

For the third method, not only was the tidal surface at mean higher high water included in the calculations, but the wave run-up for each location at each rise of sea-level were also used. The run-up was calculated by first using the assumptions that the average depth of coral reefs near shore is 1.0 m, and that a wave breaking over coral reefs can only be 1.0 m high then, since breaking wave heights are depth dependent with a ratio of $\gamma = \frac{H_B}{\bar{h}} = 0.73 - 1.03 \approx 1.0$, where H_B is the height of the breaking wave and $\bar{h}$ is the depth of the water column (Komar, 1976. P.174). Therefore, as sea-level rises, the depth of the water column will increase over the reefs, and the height of waves shoaling over the reefs will increase, while still maintaining an assumed ratio of $\gamma = 1.0$. Method #3 uses this assumption to find the wave set-up for sea-level rise increments of 0.0-2.0 m using wave heights of 1.0-3.0 m, as well as the mean higher high water elevations used in Method #2. Method #3 represents a spatially-uniform approach to modeling inundation, which may not show what inundation will actually look like in the three locations used in this study, since the bathymetry varies spatially within all three study areas. For instance, wave set-up will likely be greater over zones of shallower reefs than modeled and will likely be less than modeled in areas of deeper reef flats or near paleo-stream channels in the reefs.

The average beach slope for each location was then found using beach profiles compiled by Gibbs, et al. with elevations in meters above the local tidal datum (Gibbs, et al., 2008). A shoaling factor, which is controlled by the deep water wave steepness and the slope of the beach, of 1.52 was used, as the beaches classified as having moderate slopes (roughly 1:33 slope), which was then added to each wave height to get the shoaling breaker height. The wave set-up was then calculated as being ten percent of the shoaling breaker height, as the shoaling of the wave energy decreases the set-up height by 85-90% (UCAR, 2009). This set-up height was then added to the tidal height and each increment of sea-level rise using the map algebra tool again for the Hanalei, Kapa'a, and Waimea and maps showing inundation were created.

The fourth and final method incorporated wave run-up. The wave run-up elevations were calculated using the Stockdon equation (Stockdon et. al, 2006), which gives the two percent exceedance run-up and is defined as:

$$R_{2\%} = 1.1(0.35\beta_f(H_0L_0)^{\frac{1}{2}} + \frac{[H_0L_0(0.563\beta_f{}^2+0.004)]^{\frac{1}{2}}}{2}).$$

Here β_f is the slope of the beach, H_0 is the significant wave height, L_0 is the wavelength, and $R_{2\%}$ is the 2% exceedance run-up elevation. The beach slopes and wave heights used in Method #4 were the same as those used in Method #3. As with Method #3, the wave run-up values calculated with Method #4 will likely be lower than would be seen with a spatially varying model for shallow areas and will be higher over deep areas than would be seen with a more realistic model. The run-up elevations were then added to the tidal surface and the wave set-up elevations using the map algebra tool to create binary rasters. These rasters were used to create a map of maximum inundation for each sea-level rise scenario.

To create the inundation maps, images from each of the three locations were obtained and prepared for use within ArcMap as detailed below. The images for Hanalei and Kapa'a were obtained through Google Earth and were chosen to represent the most recent satellite view with the least cloud coverage possible. These both needed to be georeferenced in ArcMap by using control points and adding coordinates obtained from Google Earth. The image for Waimea was taken in 2006 and was obtained from University of Hawaii's SOEST Coastal Geology Group from the Kauai Ortho-Rectified Historical Shoreline Mosaics page (www.soest.hawaii.edu/coasts/erosion/kauai/mosaics). The Google Earth image for Waimea was not used because it did not have the desired exposure or lack of cloud coverage, and the ArcGIS Online Imagery was not used for any of the locations because it did best show the towns or coverage by the inundation maps but was used to verify the georeferencing.

The first set of maps were created by layering the different sea-level rise rasters from largest sea-level rise increment (2.0 m) to smallest sea-level rise increment (0.0 m) on top of the images of each location for each given method. The transparency of each layer was adjusted to provide easier viewing of where the current coastline was beneath the individual sea levels. A polyline shapefile of the coastline was then added to the maps to show the inland extent of the inundation and provide a reference point. These maps were meant to show extent of inundation based on each sea-level rise value, rather than to compare the different methods. The second set of inundation maps was created to show differences between methods. As such, each map depicts a given sea-level rise inundating the land based on all four methods. This technique is meant to provide context on how the methods differ.

Each raster layer was then converted to a polygon shape file to find the area of inundation. A raster dataset showing land cover types was then added to the maps, converted to polygon shape files, and clipped to the sea-level rise scenario polygons for each of the four methods. These data were collected and mapped by the Coastal Change Analysis Program (C-CAP, 2009) with Quickbird imagery from January 2009 obtained for this project through NOAA's Digital Coast Data Viewer website. The area of each type of land cover was then calculated from the clipped polygons.

Results

Mean higher high water elevation at present sea level is 0.55 m in Hanalei (**Figure 9**) and Kapa'a (**Figure 10**) and 0.49 m in Waimea (**Figure 11**).

For all three locations, a mean wave period of 6.0 seconds and a mean wavelength of 11.5 m were used. Hanalei had the greatest average beach slope at 0.47, while Kapa'a had the second steepest average beach slope at 0.32, and Waimea came in with the gentlest slope at 0.28. Wave set-up for all three locations was 0.3 m for 0.0 m of sea-level rise and 0.7 m for all other sea-level rise increments. The two percent exceedance wave run-up was greatest in Hanalei at 2.18 m, second greatest in Kapa'a at 1.48 m and the smallest in Waimea at 1.31 m, all under the 2.0 m sea-level rise scenario. All of these results are compiled in **Table 1**.

Mean Higher High Water Tide Results

Figure 9 Hanalei showing mean higher high water tidal inundation (0.55 m) at current sea level.

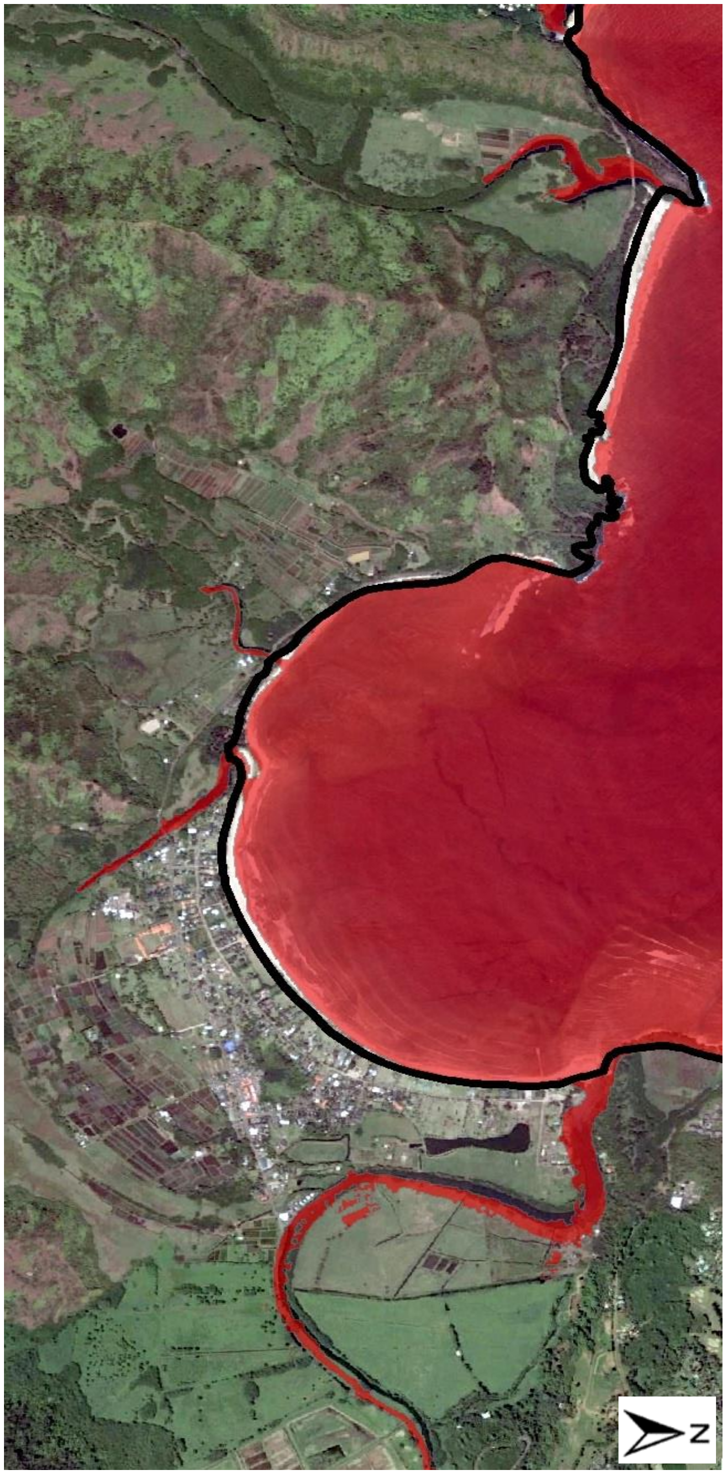

Figure 10 Kapa'a showing mean higher high water tidal inundation (0.55 m) at current sea level.

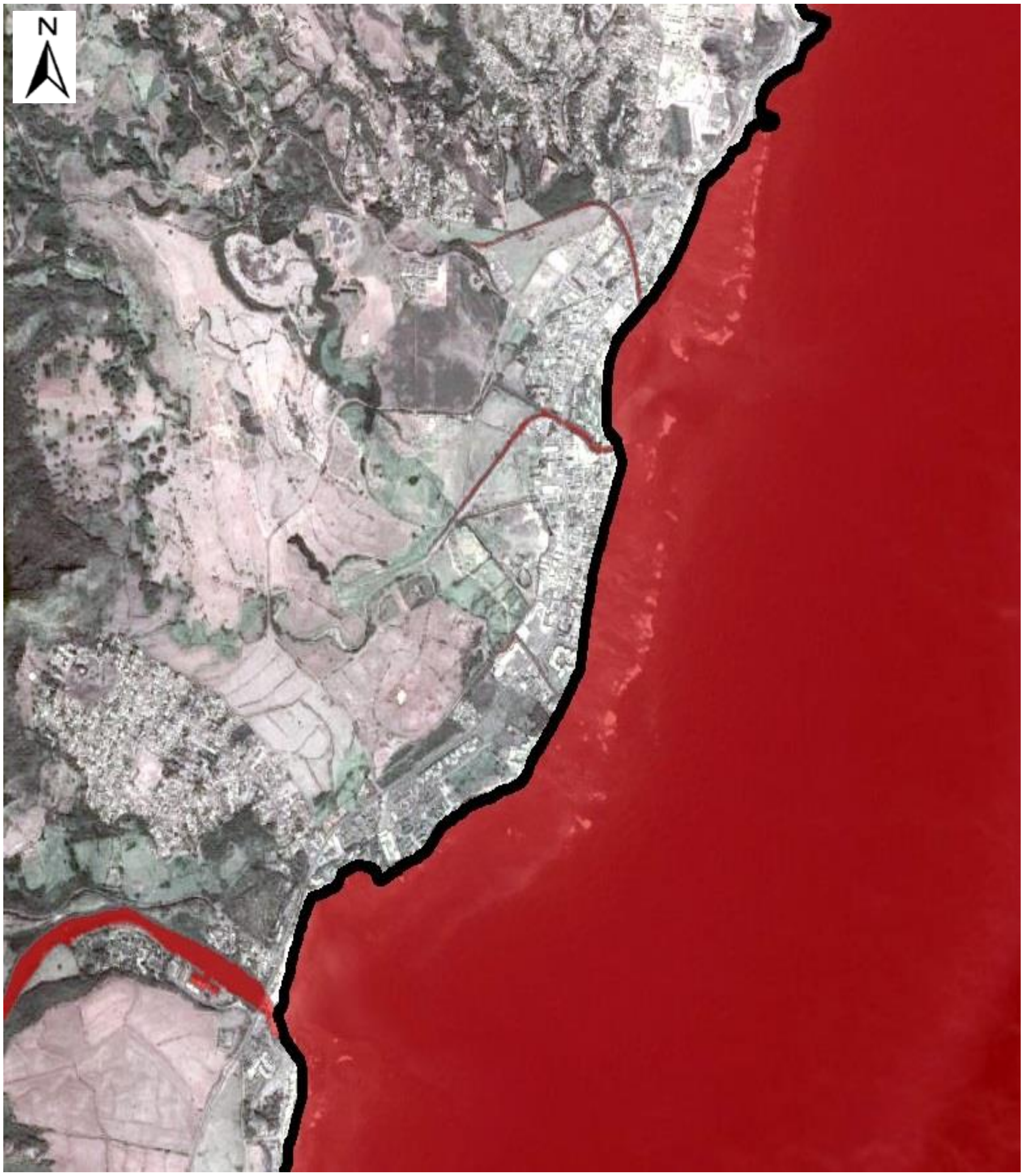

Figure 11 Waimea showing mean higher high water tidal inundation (0.49 m) at current sea level.

As expected, Method #1 shows the least inundation with each incremental rise in sea level, then Method #2 and Method #3 respectively, with Method #4 showing the greatest extent of inundation. Hanelei (**Figure 12-15**) had the second greatest percentage of area inundated compared to the total mapped land area for each sea-level rise increment and method, with Kapa'a (**Figures 16-19**) showing the least percent of inundation, and Waimea (**Figures 20-23**) showing the greatest across all methods and increments of sea-level rise.

For Hanalei, the minimum percent of coverage was 4.1% under Method #1 and 0.0 m of sea-level rise, and the maximum was 51.8% under Method #4 with 2.0 m of sea-level rise (**Table 2**). Kapa'a had the lowest percentage of inundation with 0.0 m of sea-level rise using Method #1 at 1.8%, and the greatest percentage with 2.0 m of sea-level rise using Method #4 at 30.3% (**Table 3**). The lowest percent coverage by inundation for Waimea was under 0.0 m of sea-level rise using Method #1 at 0.02%, and the greatest was with 2.0 m of sea-level rise using Method #4 at 94.0% (**Table 4**). The statistics for percent of total area studied inundated are also represented visually in **Figures 24-27** for Hanalei, **Figures 28-31** for Kapa'a, and **Figures 32-35** for Waimea.

Hanalei Result Maps

Figure 12 Hanalei sea-level rise inundation using Method #1

Figure 13 Hanalei sea-level rise inundation using Method #2

Figure 14 Hanalei sea-level rise inundation using Method #3

Figure 15 Hanalei sea-level rise inundation using Method #4

Kapa’a Result Maps

Figure 16 Kapa’a sea-level rise inundation using Method #1

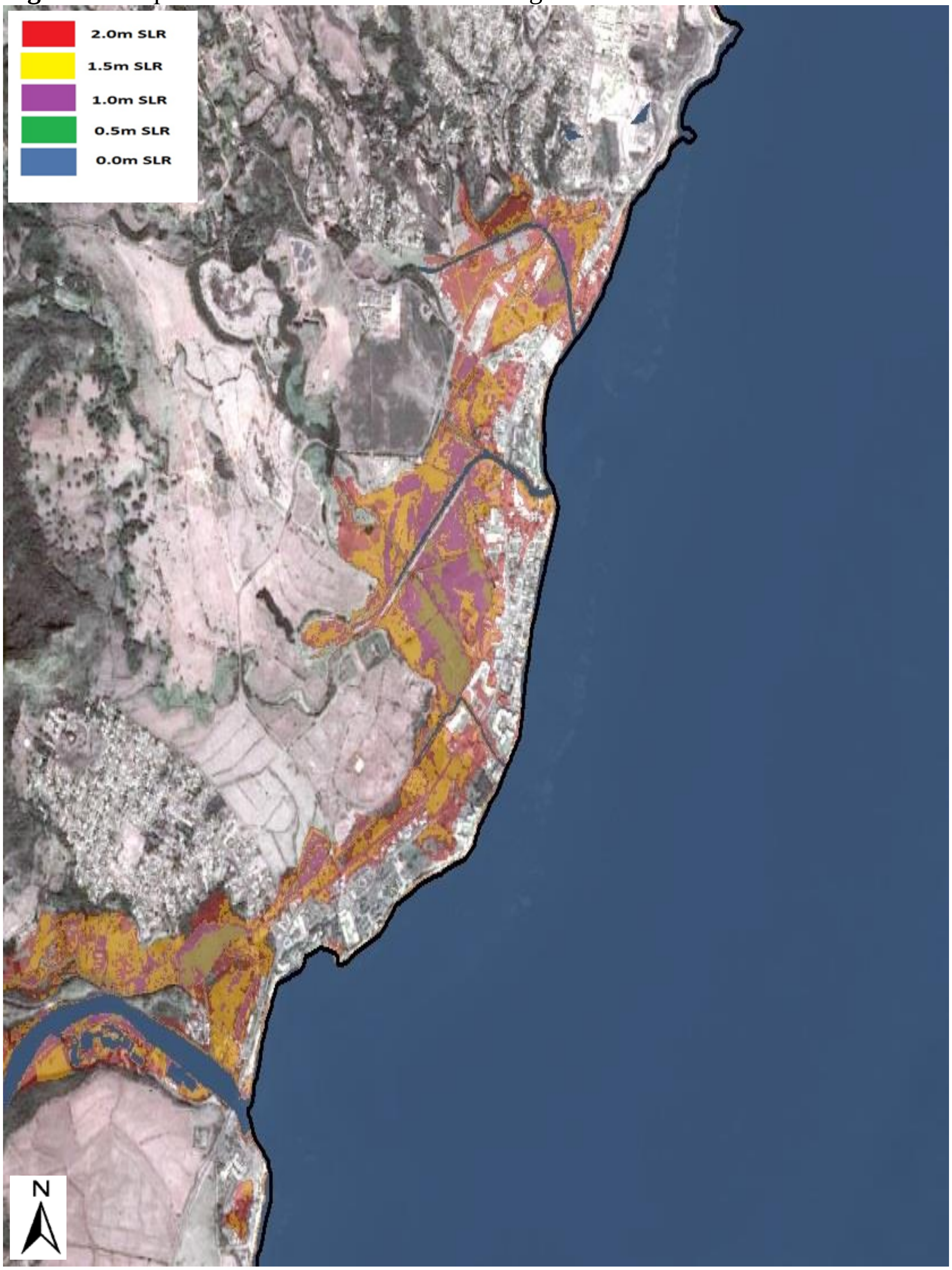

Figure 17 Kapa'a sea-level rise inundation using Method #2

Figure 18 Kapa'a sea-level rise inundation using Method #3

Figure 19 Kapa’a sea-level rise inundation using Method #4

Waimea Result Maps

Figure 20 Waimea sea-level rise inundation using Method #1

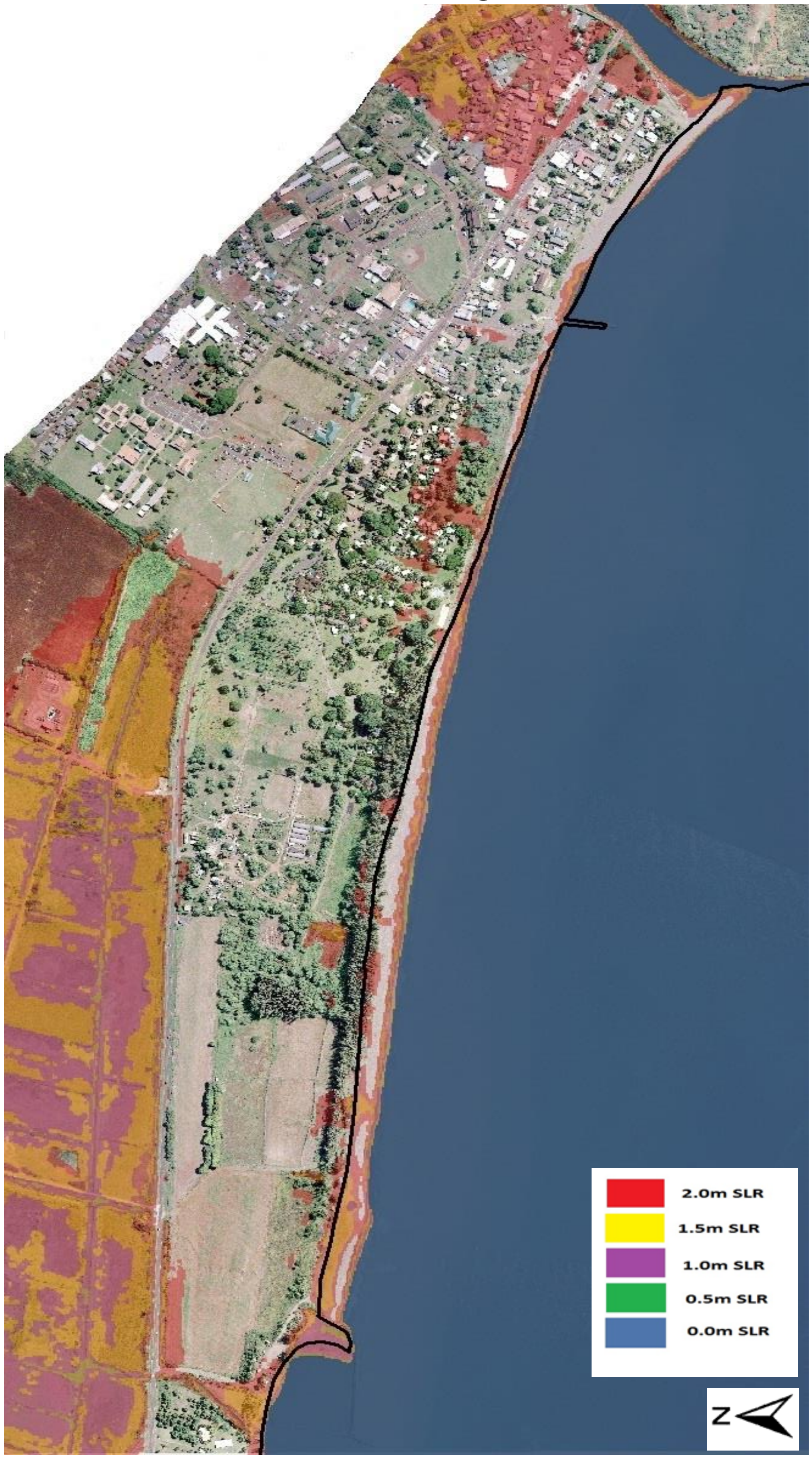

Figure 21 Waimea sea-level rise inundation using Method #2

Figure 22 Waimea sea-level rise inundation using Method #3

Figure 23 Waimea sea-level rise inundation using Method #4

The land cover data analysis shows that the land cover types that will be most affected by inundation will be wetlands, grasslands/pastures, and areas near open water. In Hanalei (**Figure 36**), impervious surfaces made up the land type least affected by inundation with each incremental rise in sea level, while in Kapa'a (**Figure 37**) and Waimea (**Figure 38**), cultivated croplands are the least affected land type. The percentage of total land area covered by bare land that was inundated under each sea-level rise scenario ranges from 0.8% to 2.3% for Hanalei, 0.4% to 1.4% for Kapa'a, and 1.0% to 8.4% for Waimea. Cultivated crops that are inundated made up 0.002% to 6.3% of the total land area in Hanalei, 0.0% to 0.08% in Kapa'a, and 0.0% to 4.4% in Waimea. Inundated land classified as developed, open space made up 0.09% to 4.4% of the total land area in Hanalei, 0.04% to 4.3% in Kapa'a, and 0.0% to 19.9 % in Waimea. Of the inundated total land area 0.02% to 6.8% is classified as evergreen forest in Hanalei, 0.06% to 2.9% in Kapa'a, and 0.03% to 13.8% in Waimea. The inundated area consisting of Grassland/pasture makes up 0.06% to 12.9% of Hanalei's total area, 0.07% to 7.5% of Kapa'a's total area, and 0.0% to 48.0% of Waimea's total area. Of the total area of Hanalei, 0.07% to 3.0% is inundated impervious surfaces, while the ranges are 0.1% to 4.8% in Kapa'a and 0.04% to 13.9% in Waimea. Open water, which includes any areas of water with less than 30% cover of trees and other plant life, that is inundated by sea-level rise comprises 6.3% to 6.8% of the total land area in Hanalei, 5.2% to 5.5% in Kapa'a, and 16.5% to 18.5% for Waimea. Land classified as wetlands inundated by sea level ranges from 0.3% to 16.4% in Hanalei (**Appendix VII**), 0.2% to 6.2% in Kapa'a

(**Appendix VIII**), and 0.0% to 0.0% in Waimea (**Appendix IX**). The statistics for land cover data can be found in **Tables 5 - 16**.

Hanalei Percent Inundation Results

Figure 24 Percent of total Hanalei land area in study site inundated by each sea-level rise increment for Method #1

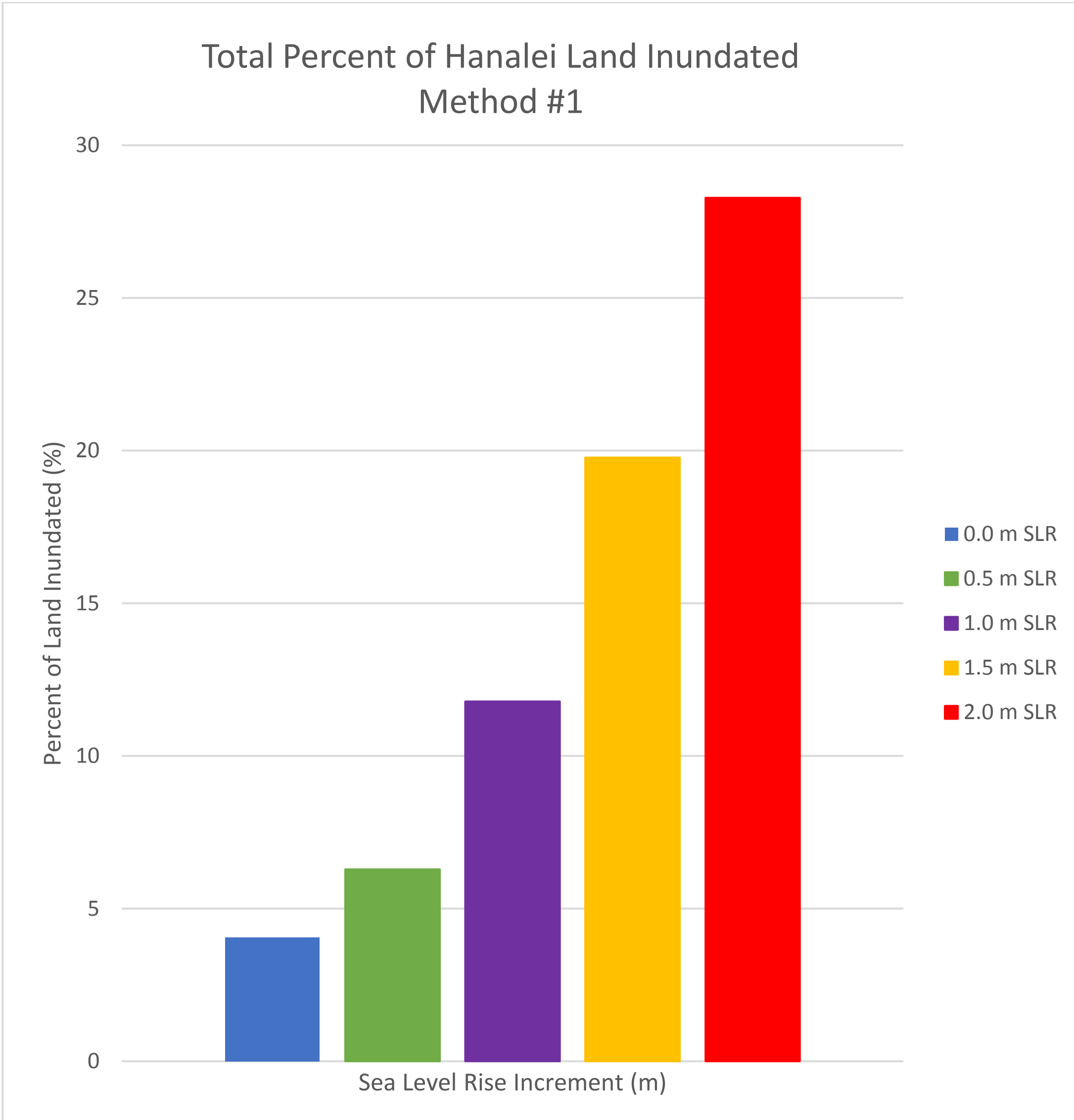

Figure 25 Percent of total Hanalei land area in study site inundated by each sea-level rise increment for Method #2

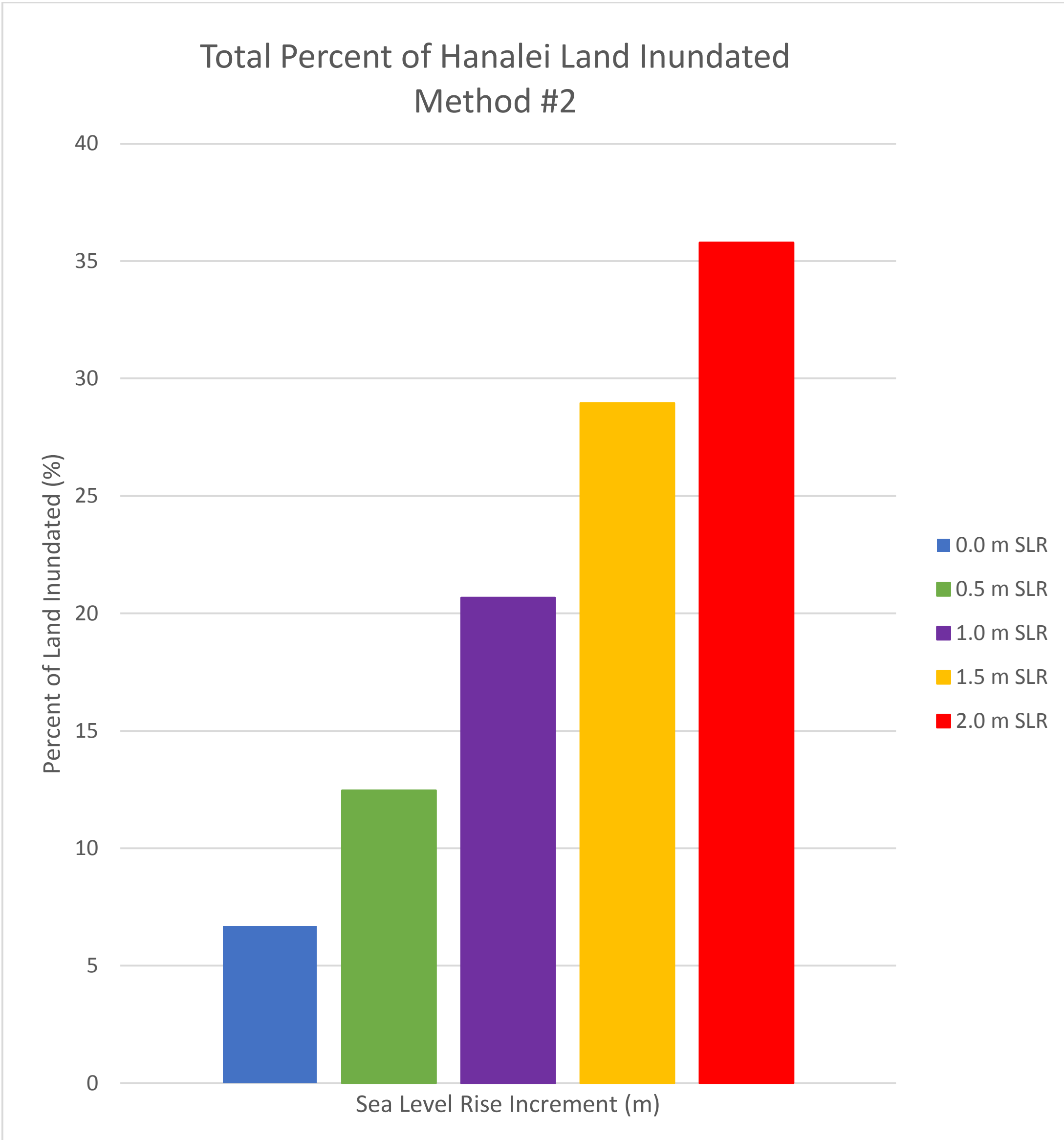

Figure 26 Percent of total Hanalei land area in study site inundated by each sea-level rise increment for Method #3

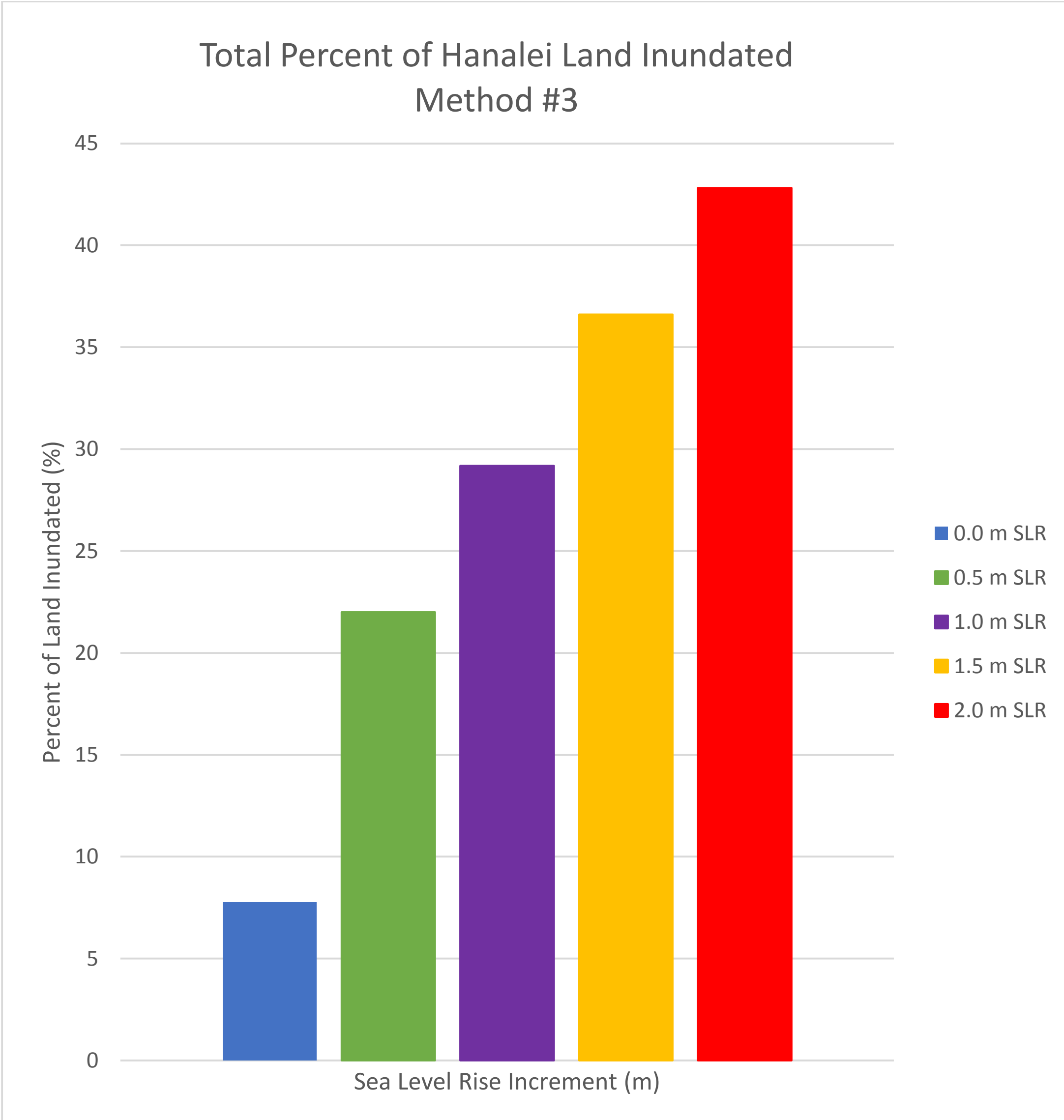

Figure 27 Percent of total Hanalei land area in study site inundated by each sea-level rise increment for Method #4

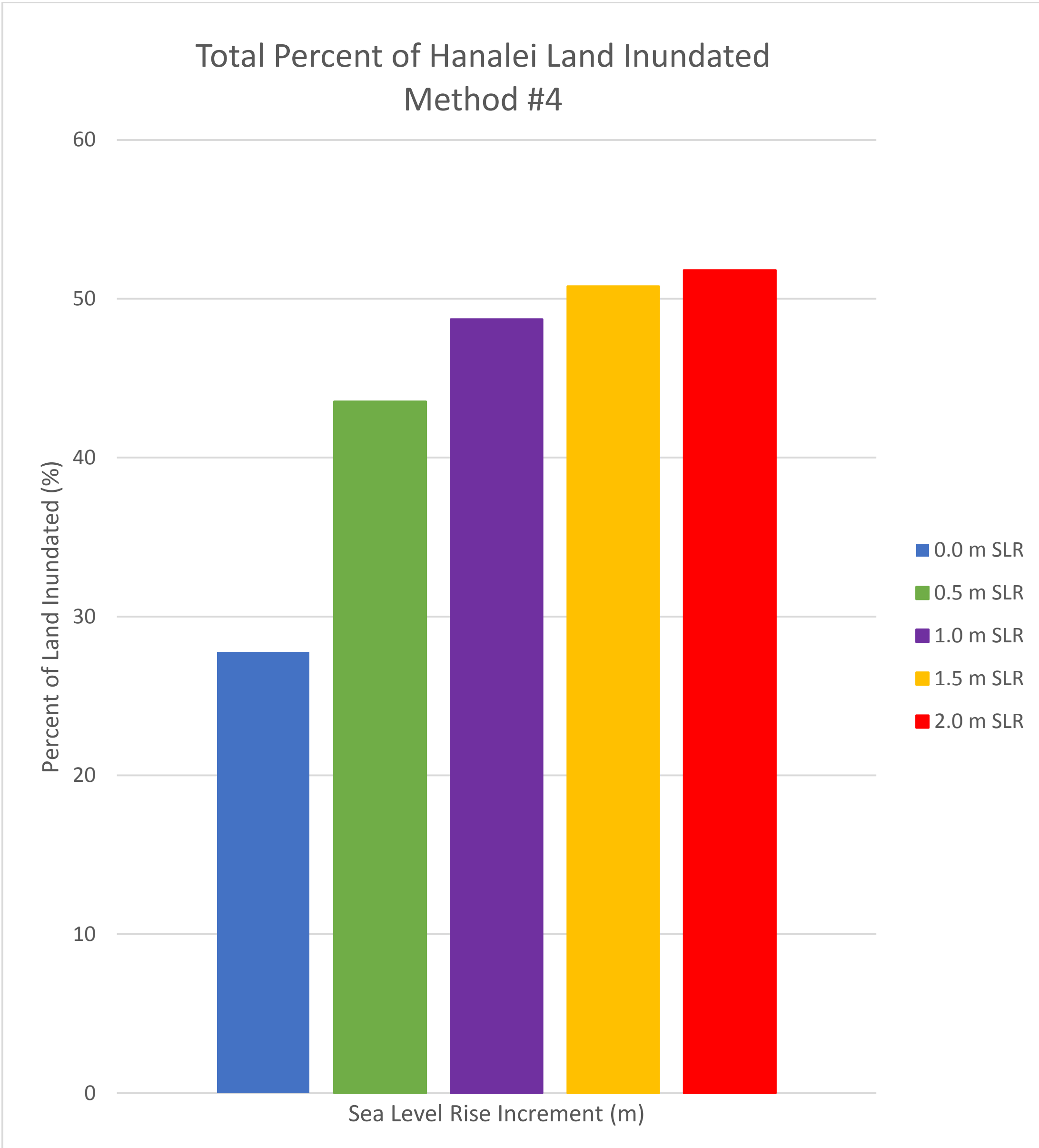

Kapa’a Percent Inundation Results

Figure 28 Percent of total Kapa’a land area in study site inundated by each sea-level rise increment for Method #1

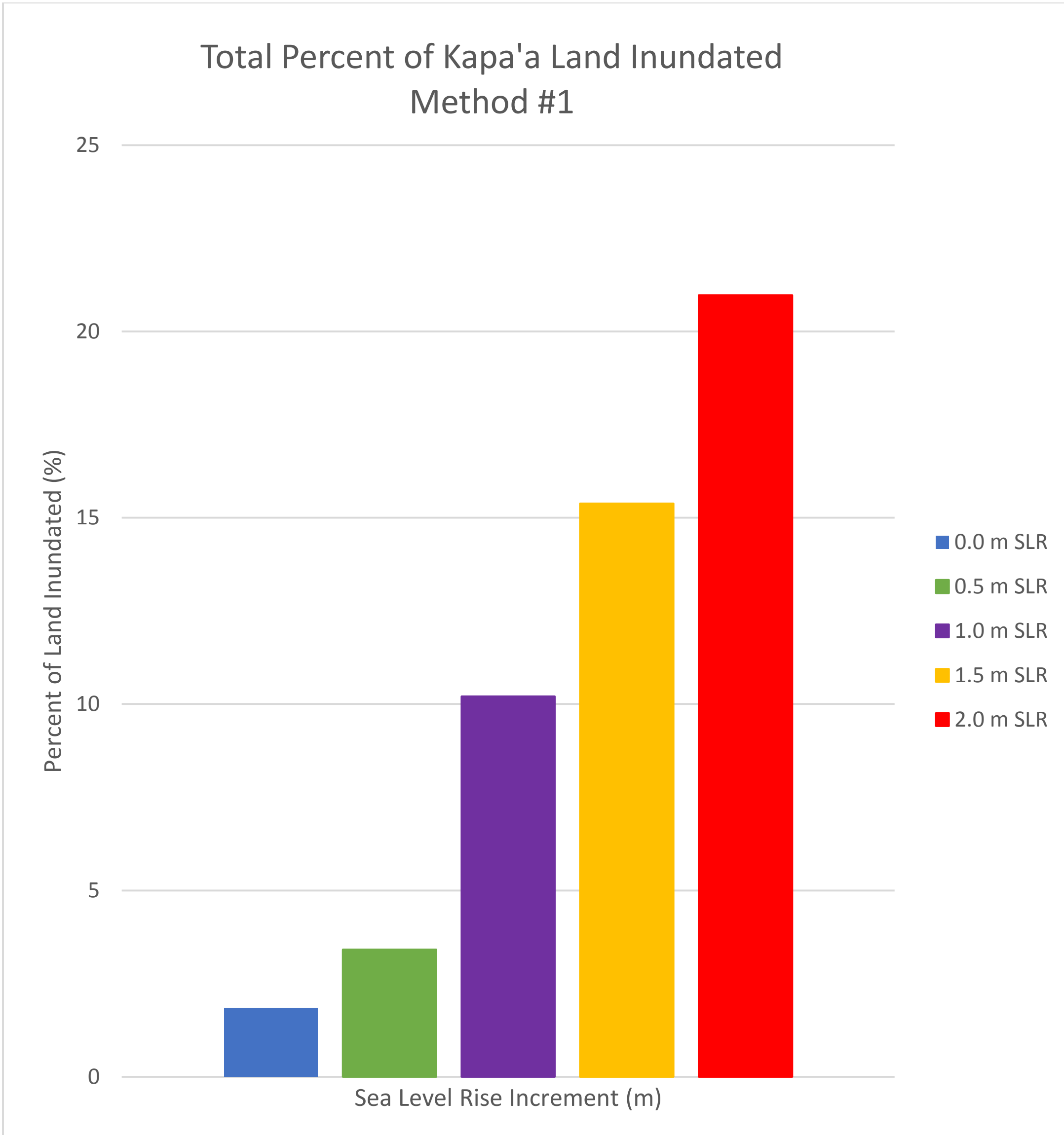

Figure 29 Percent of total Kapa'a land area in study site inundated by each sea-level rise increment for Method #2

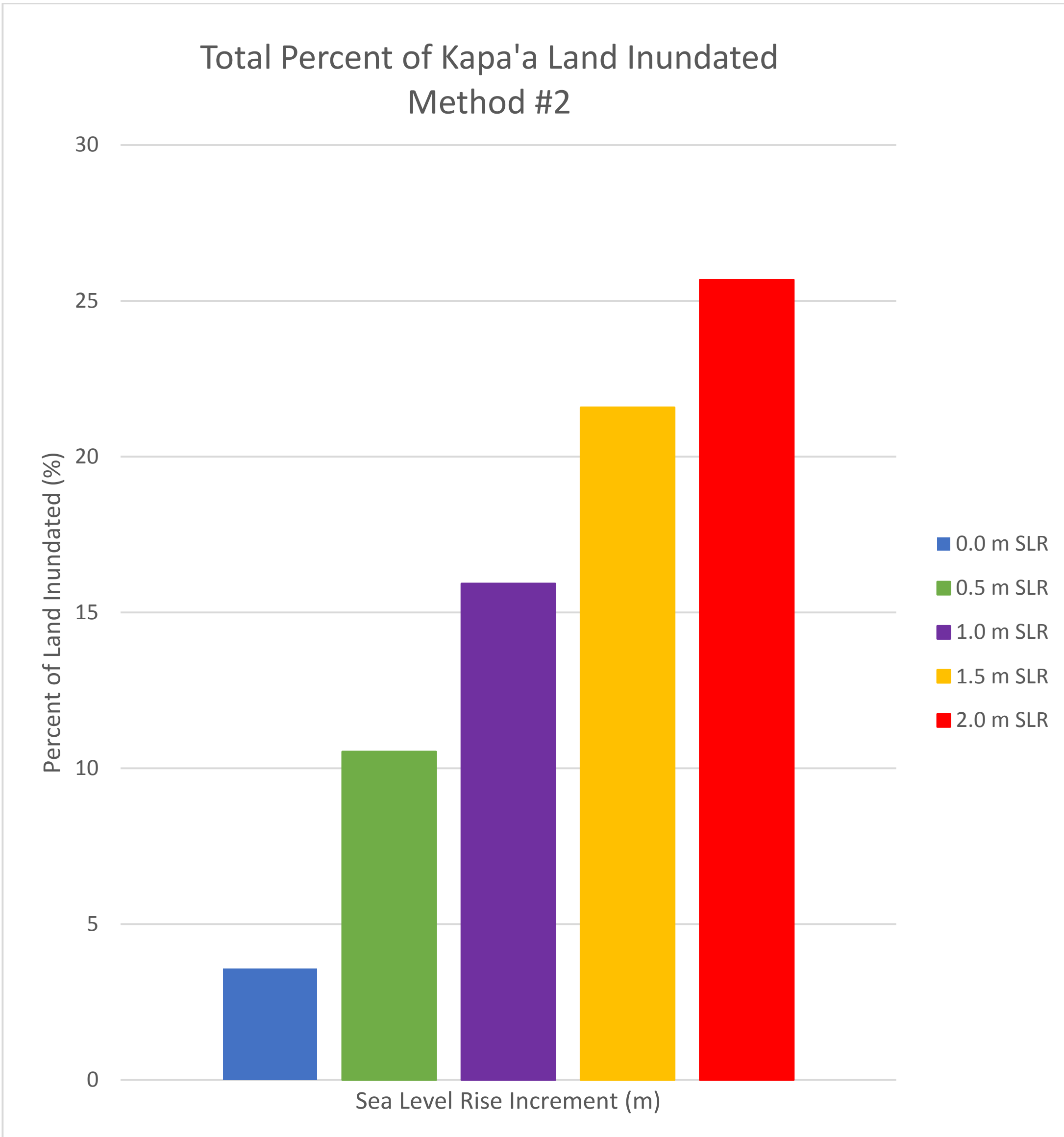

Figure 30 Percent of total Kapa’a land area in study site inundated by each sea-level rise increment for Method #3

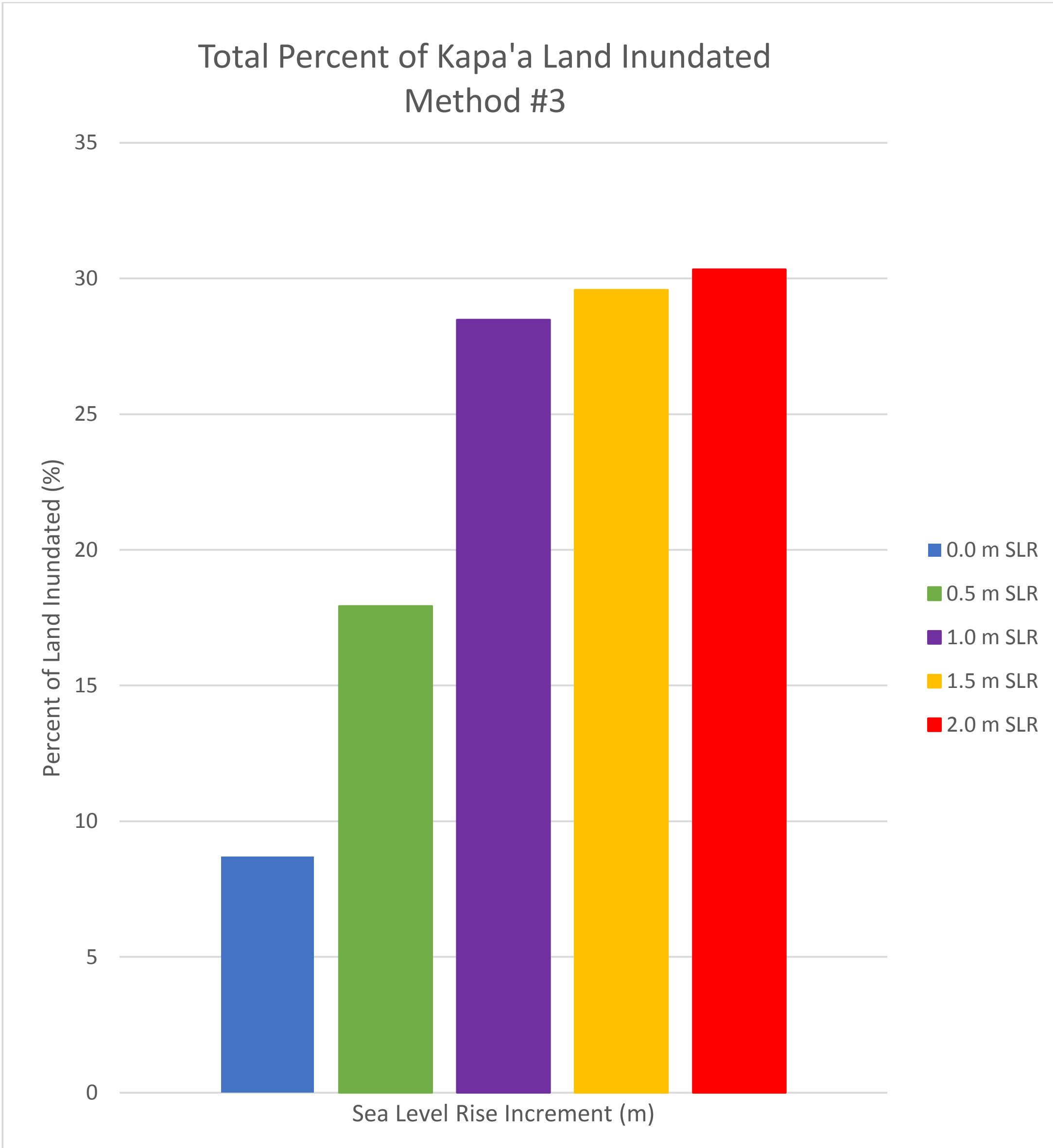

Figure 31 Percent of total Kapa'a land area in study site inundated by each sea-level rise increment for Method #4

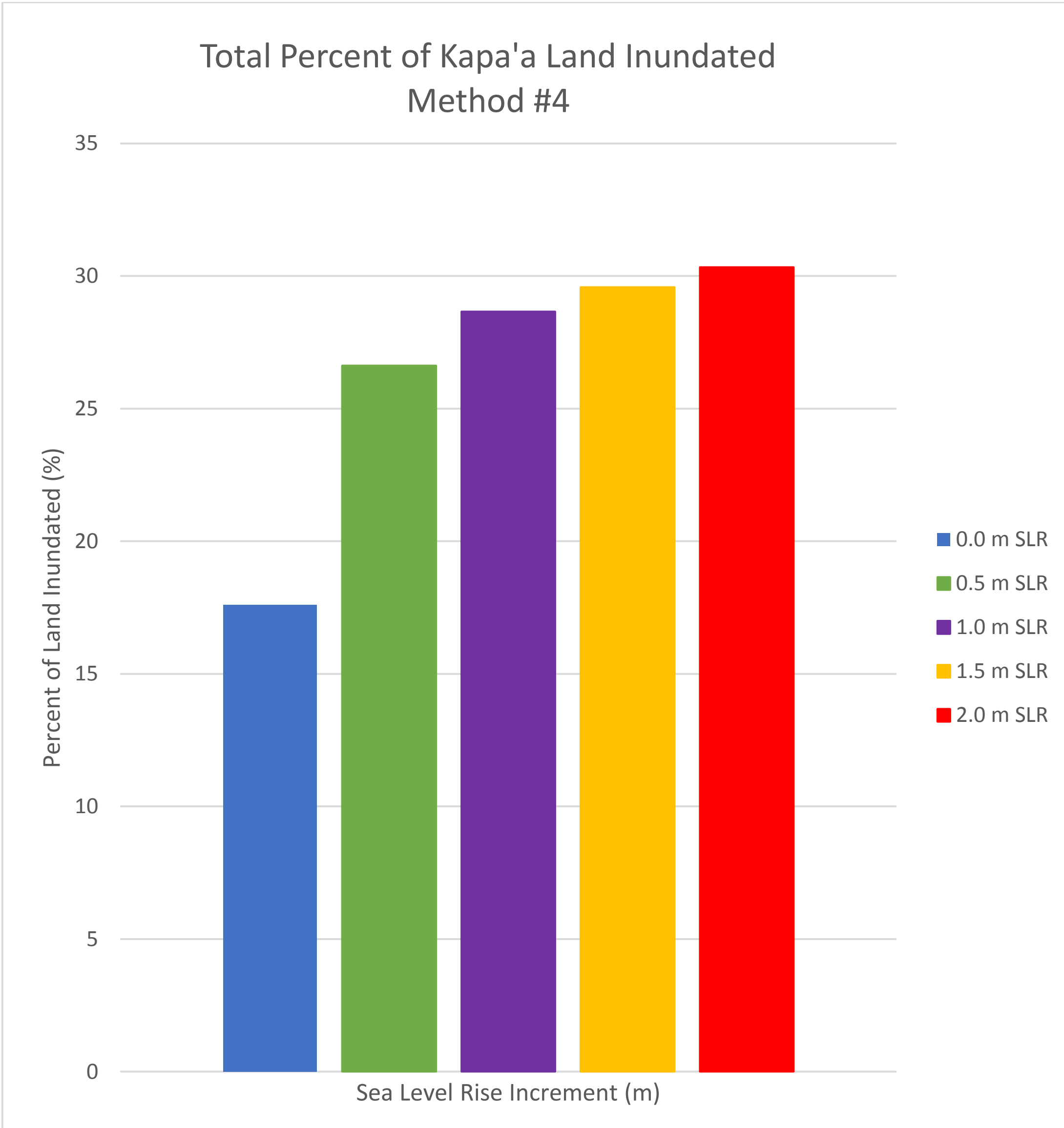

Waimea Percent Inundation Results

Figure 32 Percent of total Waimea land area in study site inundated by each sea-level rise increment for Method #1

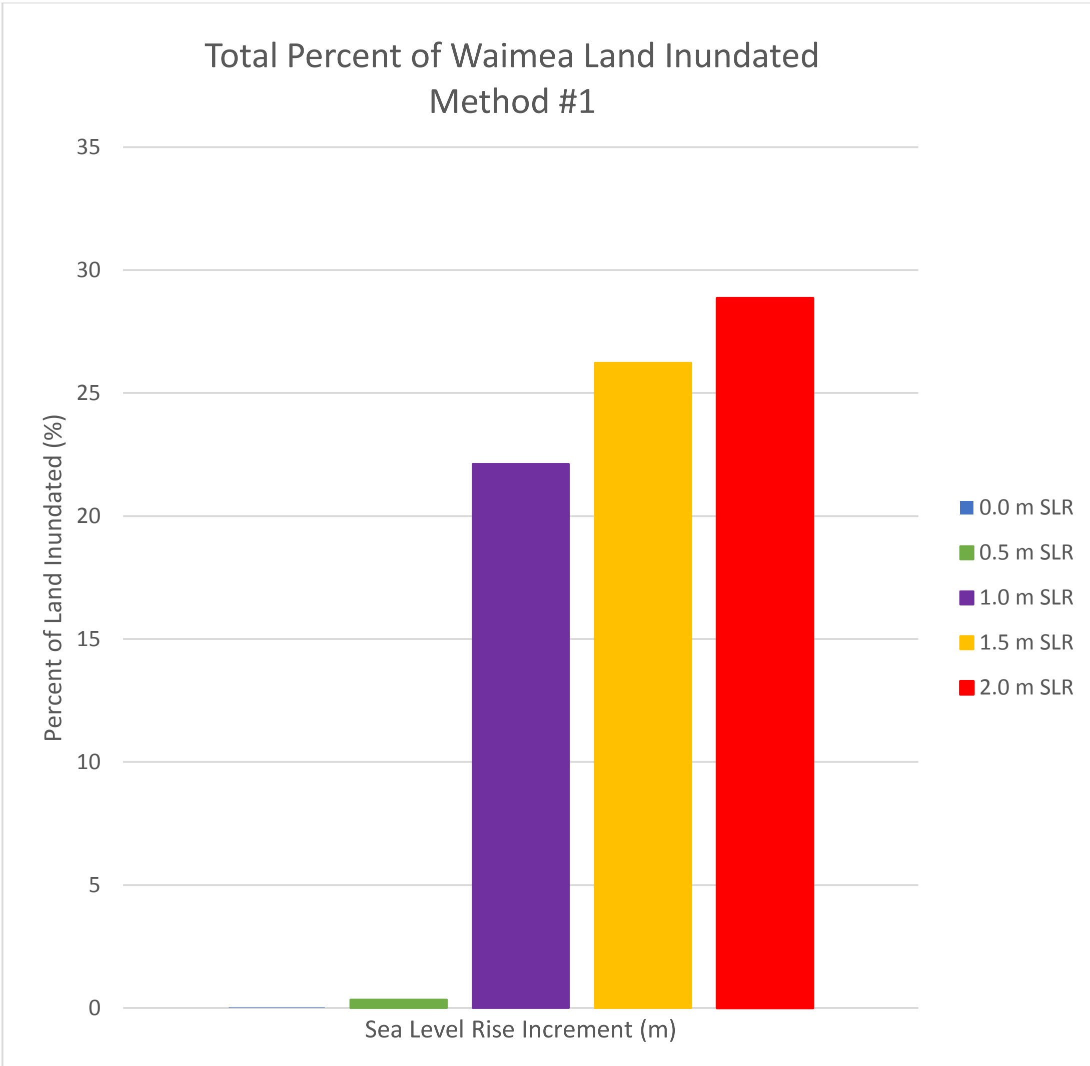

Figure 33 Percent of total Waimea land area in study site inundated by each sea-level rise increment for Method #2

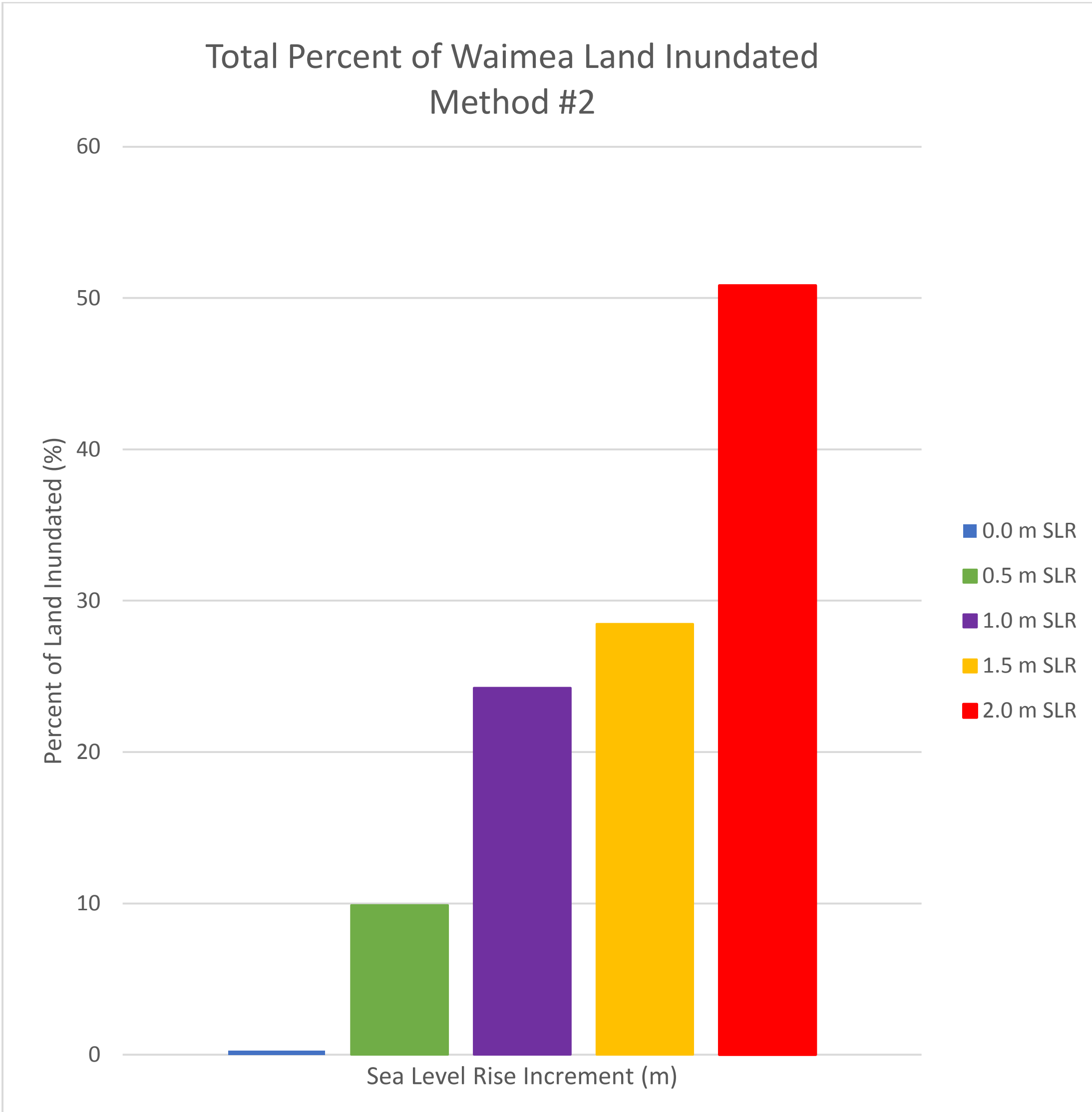

Figure 34 Percent of total Waimea land area in study site inundated by each sea-level rise increment for Method #3

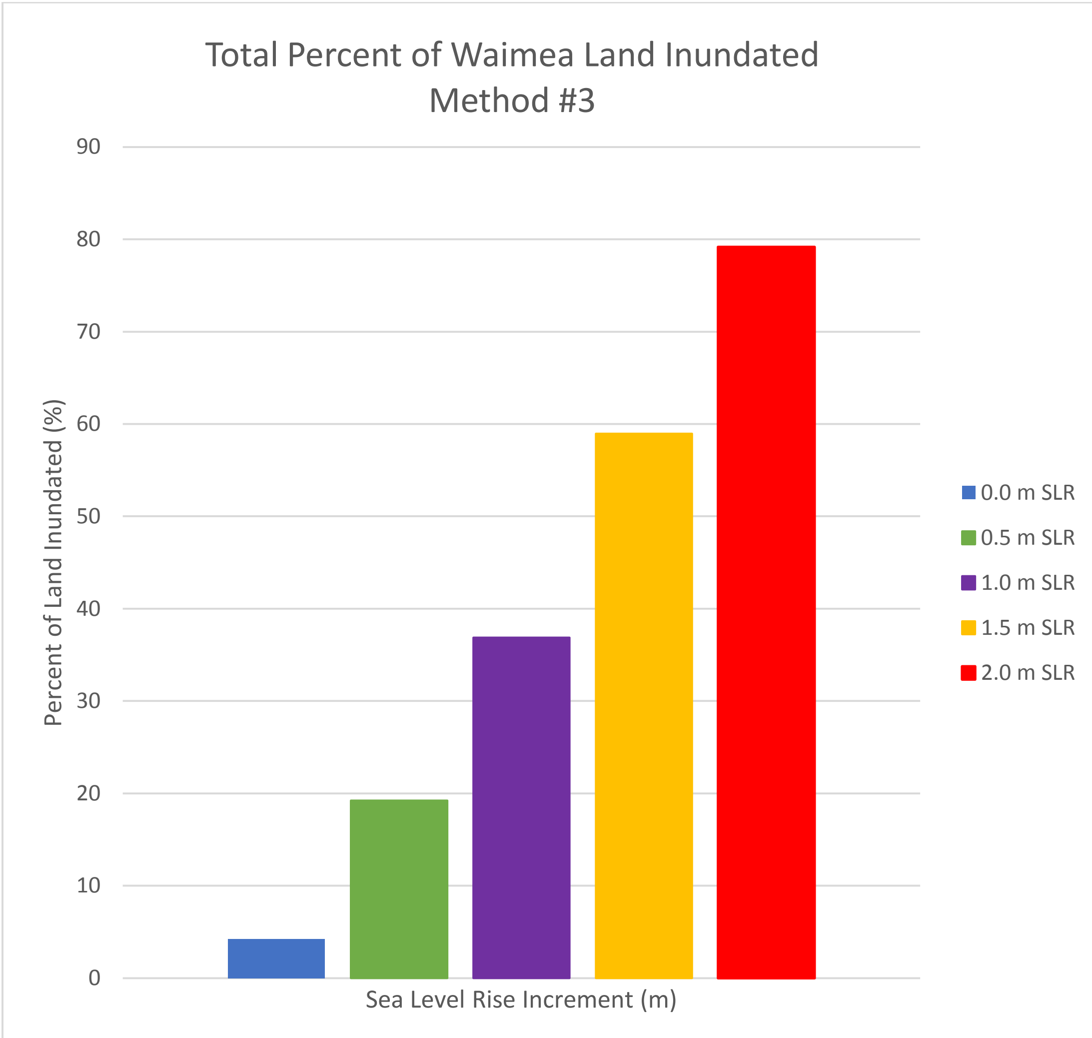

Figure 35 Percent of total Waimea land area in study site inundated by each sea-level rise increment for Method #4

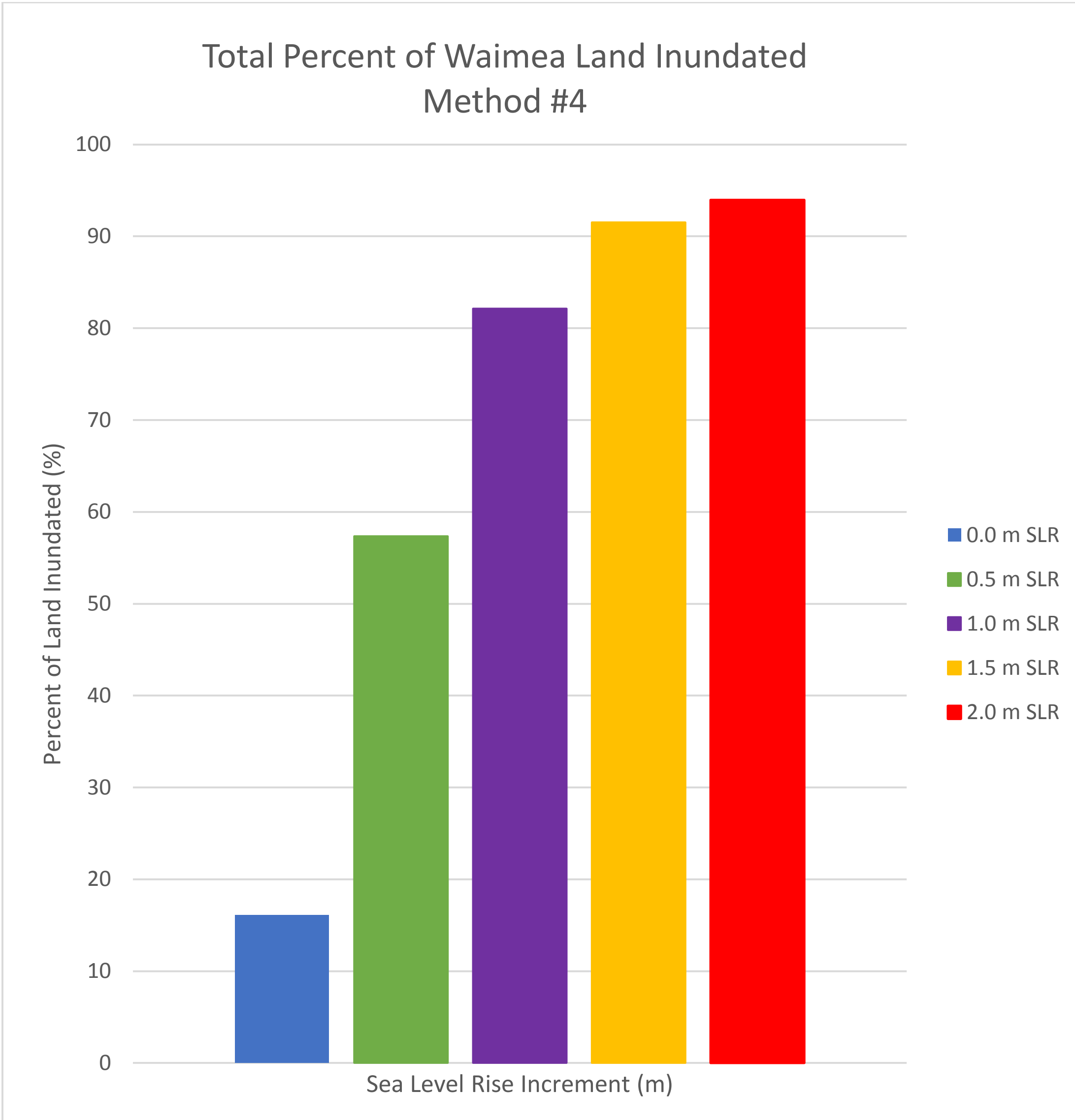

Land Cover Classification Results

Figure 36 Land cover classifications for Hanalei

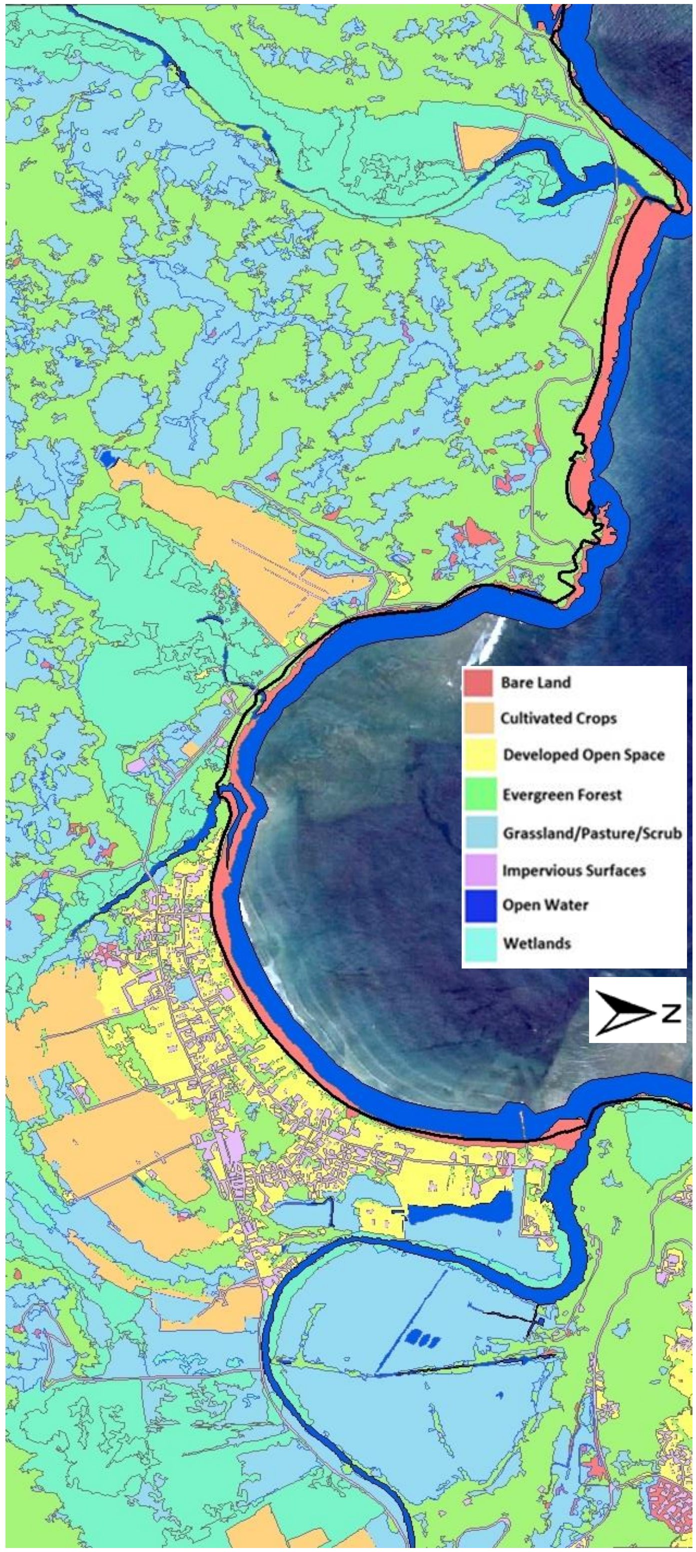

Figure 37 Land cover classifications for Kapa'a

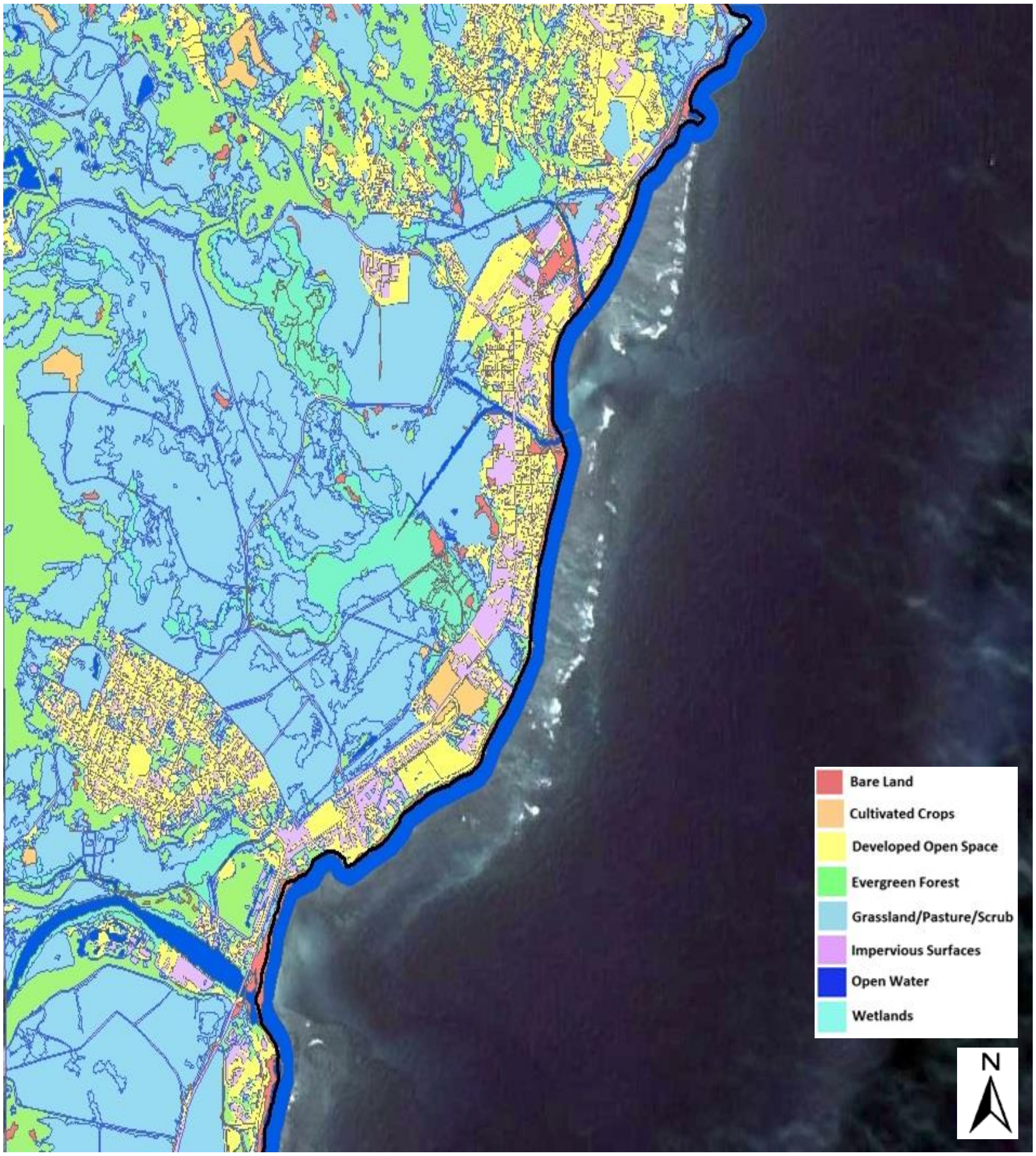

Figure 38 Land cover classifications for Waimea

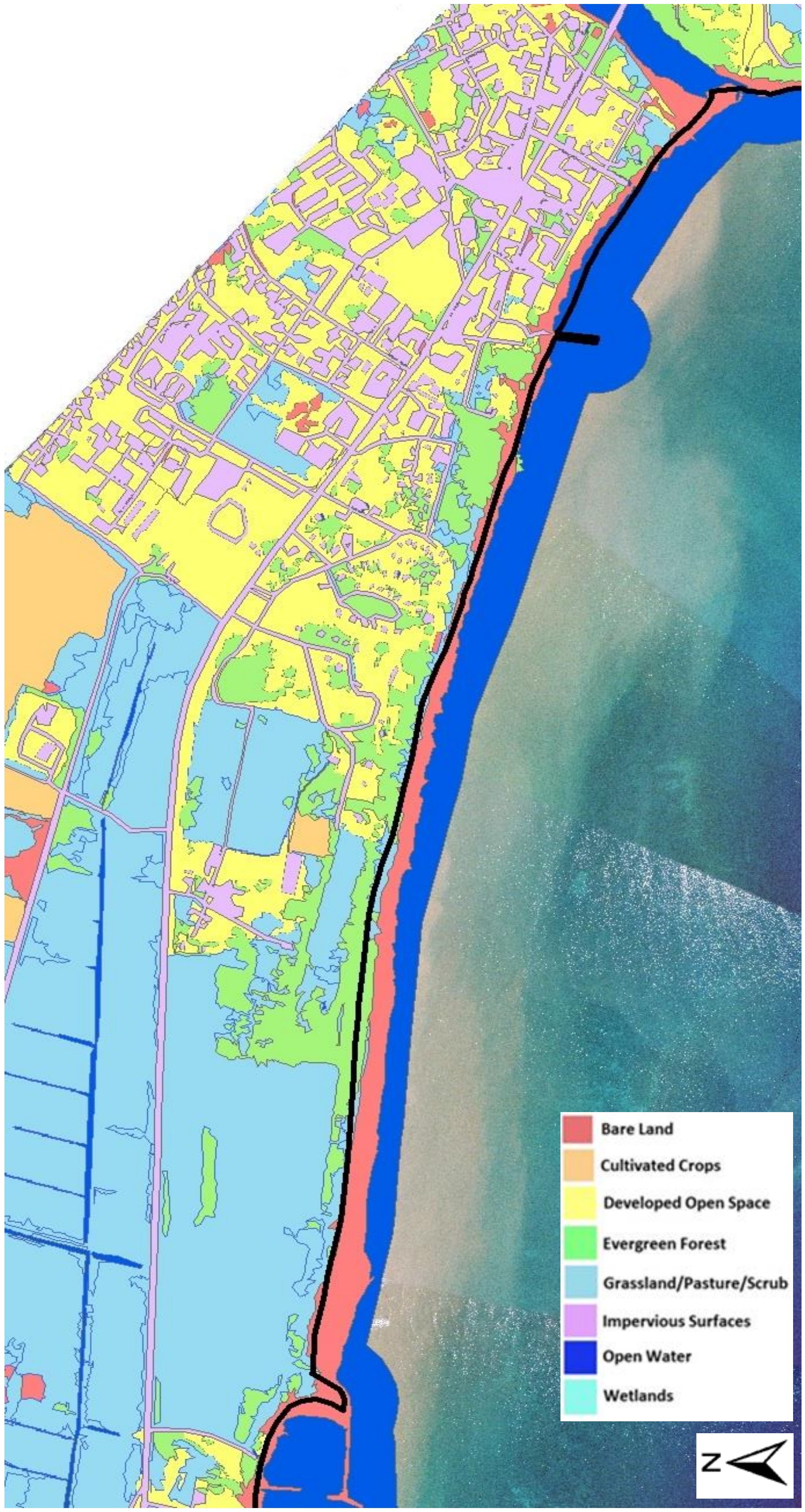

Discussion

Although all methods of inundation modeling have limitations, using all four of the methods can provide a range of inundation scenarios, including upper and lower bounds. For example, the passive modeling techniques used in Methods #1 and #2 might be too conservative to show the furthest extent of inundation under each sea-level rise scenario, but the models can act as a lower bound for future planning on Kauai. These passive models can be used to represent everyday conditions at each location under the sea-level rise increments used, such as during low tides and low wave energy conditions. At the other end of the spectrum, the dynamic modeling techniques used in Methods #3 and #4 are not meant to show everyday conditions but rather extreme conditions, as they show wave set-up on top of mean higher high water levels and the 2% exceedance run-up values. The areas shown as being inundated under each sea-level rise increment in Methods #3 and #4 may only be inundated during storm and swell events with longer recurrence intervals, and thus, these methods can be used as an upper bound on planning for future inundation events.

Regardless of whether the inundation model being used is passive, dynamic, or some combination of the two, it is important to use a regional model, rather than a global model. Global models, which use methods most similar to Method #1, do not take into account any of the local conditions that can greatly impact the extent of inundation, except for topographic elevation. These models do not include important features such as wave conditions, bathymetry, local tidal levels, beach morphology, tectonics, isostasy, or regional onshore land uses. Regional models, such as those used in Methods #1-4, are appropriate for specific locations and therefore give the most accurate results for each site.

In this study, the importance of local effects in a model can be seen by the increasing levels of inundation from Method #1 to Method #4. For instance, Kapa’a showed the least amount of inundation as a percentage of the total land area studied, while Waimea showed the greatest amount of inundation across all sea-level rise increments and using all methods, with a 43.2% difference between the two locations in inundation under Method #4 and 2.0 m of sea level rise (**Tables 3 and 4**). These differences can be attributed to conditions specific to each of the three locations.

While Waimea had the lowest run-up values, it also had the lowest foreshore beach slope, which could be responsible for the greater extent of inundation. Although Hanalei had the greatest wave run-up values, its steeper beach face slope and wider beach width are most likely responsible for protecting it from inundation compared to Kapa’a. Kapa’a had a steeper beach slope than Waimea, which may explain the greater protection from inundation events, even though the wave set-up values are greater than in Waimea. Another reason for the order of least to greatest inundation is most likely the topography of the land, with Waimea having lower inland elevations, and Kapa’a having higher inland elevations. If this study had been completed using a global model, the differences in inundation would have been much smaller, and the peculiarities of each location, even on an island as small as Kauai, would have been lost.

The land cover results were also site-specific and provide valuable information about what types of features will be inundated. There are two broad, overarching types of land cover that are important when conducting a sea-level rise study, resilient features and non-resilient features. Resilient land cover types are anything that can easily and quickly recover from inundation events without much interference by or cost to humans. These features include parks, grasslands, wetlands, and even parking lots. Non-resilient land cover types are those that may take much longer to recover naturally or may not withstand inundation events at all. These include many man-made features, such as homes, hotels, hospitals, and any other building type that will most likely be damaged by inundation and not able to recover without human intervention. In the case of non-resilient features, human intervention could be in the form of pumping out water from the buildings after being inundated, repairing damages, building protective structures before the next inundation event, or even relocating the structure. All of these efforts to help restore non-resilient features cost money and time, and depending on which plan of action is taken, the restoration might be a continuous or ongoing cost to whoever owns that property.

By knowing what types of land cover will be inundated by each rise in sea-level, planners in the County of Kauai will have a clearer idea of when and where the greatest impacts might be in the future, in that inundation is less of a cause for concern in areas with more resilient features and more of a cause for concern in areas of non-resilient land cover. For example, using Method #4 in Hanalei shows that impervious surfaces, the non-resilient land cover type in this study, ranged from 0.1%

to 3.0% of the total land area studied for the five sea-level rise scenarios. When comparing that to Method #4 results for Waimea, where the percent of total land area classified as inundated impervious surfaces ranged from 0.04% at 0.0 m sea-level rise to 13.9% at 2.0 m sea-level rise, planners might be more concerned about sea-level rise in Waimea than in Hanalei. Thus, the results from the land cover portion of this study can be used to create a ranking system as to which locations may need more attention, resources, concern, and adaptation planning. Once these regions of concern have been identified, planners and the County of Kauai as a whole should create a plan of action for how the island will adapt to future sea level changes. There a few options that will be outlined below, and the merits and drawbacks of each will be discussed.

The first option in responding to future sea-level rise is to do nothing and wait until the changes are at hand to react. This is often a popular reaction, as future issues are not thought to be problems until they affect the general population, at which point people are forced to play catch up in reacting to the problem. This technique may seem like an easy solution at the present time, but it leaves little to no time for planning in the future and can lead to further problems as people try to react in the midst of the problem rather than plan ahead. This method of non-reaction also can confound the issue at hand in the future. Costs to plan and to protect will only rise over time, making communities more financially vulnerable as well as physically vulnerable to inundation in the future. Planning also takes time, and implementing changes, such as set-back laws, can take even longer, meaning that by the time people get around to dealing with sea-level rise, it might be too late to provide much relief to coastal communities.

Another option is to continue to enforce and possibly strengthen building set-back laws on the island. Since 2008, Kauai has had the "most progressive setback standards in Hawaii," and while in Hawaii "state law requires setbacks of not less than 20 feet and not more than 40 feet, Kauai's ordinance requires that structures in Kauai be setback a minimum of 40 feet from the certified shoreline" (Office of Ocean and Coastal Resource Management, 2012). These setback laws are based on average depth of the lot, building footprints, and erosion rates in front of the property. For lots with an average depth less than 160 ft, the setback is a function of the depth. For example, lots with a depth less than 100 ft, the minimum setback is 40 ft, and for every 20 ft increase in depth means an increase of 10 ft in setback. For lots with a depth of greater than 160 ft and less than 5,000 square feet, including decks, pools, etc., the setback is 40 ft plus 70 times the annual erosion rate. Finally, for lots greater than 5,000 square feet, the setback is 40 feet plus 100 times the annual erosion rate (Office of Ocean and Coastal Resource Management, 2012).

These setbacks limit the number of coastal protection structures needed to prevent damage to coastal buildings as well as maintaining adequate public access to the beach. In the future, with sea-level rise, the setback laws should be upheld and modified as needed, and will probably need to become even more stringent in order to protect existing structures from inundation. It might also become necessary to remove grandfather clauses that currently allow houses built prior to the passing of these setback laws to be rebuilt at their previous location on lots but on stilts or pilings to protect from future inundation. With increased sea levels, such buildings might need to be relocated further inland rather than rebuilt higher off of the ground.

A third option is to continue to permit and build coastal protection structures, such as rip rap, seawalls, groins, and breakwaters, as needed. There is a level of hesitation at this time to building additional protection structures unless there is definitive proof that the property or structure is in danger of being damaged. As of the summer of 2013, there were roughly 350 coastal structures, including seawalls, riprap, groins, and jetties, in place around the island, but there will likely be more petitions to build more as sea level continues to rise. Protection structures are far from a perfect solution, however, and can exacerbate problems on either side of the structure or even further downshore.

Erosion, both passive and active, is a common concern when it comes to building new coastal protection structures. Passive erosion occurs when an armoring structure fixes the bluff or cliff position behind it and diminishes the beach width in front of it, while the beach on either side of the structure continues to erode and migrate inland (Griggs, 2005; Stamski, 2005. P.9). This loss of beach in front of the structure and inland migration on either side can create an artificial headland and will occur regardless of structure type. Active erosion includes scouring at the base of structures or increased erosion on either side of the structure (P.10). The results of an eight-year study of over 2,000 beach profiles along the central California coast on seawall backed beaches and adjacent control beaches, however, showed that no significant scouring took place directly in front of any of the seawalls or rip rap monitored (Griggs, et. al., 1997).

There is also the is the issue of the visual impact of structures that do not look natural, which is primarily a concern for beach goers and the owners of neighboring properties who do not wish to look at unsightly structures on an otherwise pristine natural landscape. Newer structure types, such as soil nail walls, which can blend in fairly well with the natural cliff, are less of an eyesore, but none of the three locations used in this study are backed by cliffs and would thus require structures such as sea walls or riprap. These more traditional protection structures are usually less popular with the public because they can encroach upon the beach, which is public land, and can restrict access to the beach in some cases, especially during high tide or large wave events. Other less permanent structures, such as geotextile bags, may be a more widely accepted option, as they are more easily moved or removed as needed.

An alternative to protection structures is beach nourishment, which is the importing of sand on to a beach to replenish a lack of sand. The beaches of Waikiki have historically been nourished periodically, with inland waters being diverted in order to prolong the residence time of the imported sands on the beaches (Feirstein and Fletcher, 2004). Kuhio Beach in Waikiki, Oahu was the site of a beach nourishment project in 2006, in which 10,000 cubic yards of sand were dredged from offshore sand deposits and pumped onto heavily eroded sections of the beach. The project temporarily added up to 15m in width and about 1m in height to the beach at a cost of $475,000 (Eversole and Lemmo, 2007). The coastline of Kauai is much less armored than the coastline of Waikiki, however, and therefore sand will not have as many manmade obstacles, such as groins and breakwaters to trap the sand from moving farther downshore or offshore once it is placed on the beaches. There are, however, two nourishment projects being proposed for the island of Kauai, one in the Poipu region and one in the Kekaha region, which encompasses Waimea. Both locations currently have preliminary regional sediment management plans that detail the sediment budgets and littoral cell dynamics. The proposed plan for the Poipu region is to import sand from offshore to widen the beach with the hopes of also rebuilding a once natural tombolo that acted to trap sand from moving downshore. The plan for the Kekaha region is to bypass the sand that gets trapped in the Kikialoa Harbor by dredging (Garvey, et al, 2012). Beach nourishment is not without its drawbacks though, such as possible environmental impacts both to the dredging sites and the pumping locations, the loss of imported sand to either storm activity or natural littoral drift, and the potential financial cost of having to periodically re-nourish beaches in order to maintain the results.

One more option of how to respond to future sea-level rise is planned or managed retreat. This may not initially have the public's vote, as people tend to want to move closer to the coast rather than farther inland, especially when the future effects of sea-level rise are not yet evident. However, as inundation events become more frequent and intense and the coastline begins to migrate inland, coastal residents might have to follow suit. There could potentially be a system emplaced in which the county of Kauai or state of Hawaii encourages people to sell their private property within a given distance of the mean higher high water line to the county. In this way, the government could keep beachfront property as public space and ensure that resilient land cover types are used to act as a buffer against impacts from inundation.

There are two types of data that were purposefully not included in this study, one being specific dates for each sea-level rise increment and the other being population data. No dates were assigned to each sea-level rise scenario because there are many models that show a wide range of predictions for how much sea level will increase by a given year. For example, Rahmstorf et al. predict a range in increase of global sea level from 0.68-1.24m between 1986-2005 and 2081-2100 under Scenario RCP4.5 with 95% confidence (Church et al., 2013. P.1184). The IPCC AR5 Scenario RCP4.5 on the other hand predicts an increase during that same time period of 0.63m with 95% confidence (P.1184). The purpose of this study was not to show the results of one specific climate model as it pertains to inundation on Kauai, but rather to show multiple increases in sea level using different methods and allow the county of Kauai or whomever uses the results to then choose a prediction model of their liking and be able to visualize what inundation will look like under those conditions. Several important considerations in deciding which scenario or level to use include: what structures or infrastructure are potentially at risk, what is the monetary value or cost of replacement or relocation of the structures or facilities, and what is the social cost failure, loss or inundation of the structure. The loss associated with a home, a park, a road or highway, a hotel, or a sewage treatment plant would all be quite different from one to the next.

By not including specific future time lines or dates in this study, it was also deemed inappropriate to include population data. The population of Kauai is not steady and changes from year to year, generally increasing over time. If the population data from the last census, which was in 2011, was used, it would show the population of the island only at that time. This snapshot of the where and how many people were living in the three study sites would thus only be a single point in time and would not represent the population dynamics in the future, when the inundation will be occurring. Even if the population data were extrapolated into the future using the rate of change between the last two census polls, it would still not be useful in this study, as no dates were assigned to each increase of sea-level. Thus, extrapolating the population of Waimea, for instance, to the year 2100, would not have any meaning in looking at the inundation maps created for that area, since this study leaves the assigning of dates to the users' discretion.

There are limitations in the how the results from this study should be used, and it is important to note that the results are not an exact description of what future conditions will be like, as there are uncertainties and invalidities in the data and methods used. For instance, the use of the wave set-up and Stockdon wave run-up equations introduce error into the calculations due to the fact that Kauai's offshore bathymetry is highly variable, causing wave height gradients in the alongshore direction. In Hanalei Bay, there is a large patch reef called King's Reef offshore as well as a fringing reef on both sides of the bay. These reefs create significant mass gradients for both wave height and wave energy alongshore, making the calculation of wave set-up and wave run-up values inexact. Therefore, the values obtained for wave set-up and wave run-up in this study may be higher or lower than the actual future values. For instance, the fringing reefs on both sides of the bay will dissipate wave energy and decrease wave run-up and set-up, while the region in the center of the bay may have higher than calculated values due to channeling of wave energy. By using the assumptions that the depth dependence of breaking wave height over fringing reefs has an original ratio of 1:1 and that as the depth of the water column increases with sea-level rise so will the wave height over that water, this study provides not perfect or exact results but rather provides insight into what future conditions may look like.

Further work on this study will include use of the Deltares SWAN model, which is a spatially varying physics based wave model. The SWAN model provides realistic and valid wave field data that could then be used as more accurate and exact inputs for the set-up and run-up calculations. A Boussinesq model will also be used to verify the results of the SWAN model, since SWAN may not accurately model the steepness and refractive qualities of nearshore fringing reefs for long wavelengths (Hoeke, et al., 2011. P. 17). Airborne LiDAR (Light Detection and Ranging) remote sensing datat will also be used to generate a realistic bathymetric surface in order to better model the nearshore wave field in both the SWAN and Boussinesq models.

Conclusions

All evidence to date indicates that sea-level rise and shoreline inundation is no longer a what if question but rather a when question. Answering this question is becoming increasingly important for coastal communities and residents, especially on islands, where space and resources are limited. In order to do this effectively, realistic models that use reliable and region-specific data must be used to map potential future areas of inundation. While passive models should not be used alone, they can provide a useful lower bound for expected inundation and can give a realistic preview of what everyday conditions could look like in the future. Dynamic inundation models, on the other hand, show what the maximum extent of inundation under extreme conditions will likely be, and thus they should be used as an upper bound for inundation and possibly for zoning and hazard planning purposes.

Much like passive models not providing a complete picture of future inundation conditions under rising sea level, global models also do not offer enough information for region-specific planning. Regional and local conditions are very important in understanding and planning for future inundation, making regional inundation models much more effective and informative than global models. Topography, offshore bathymetry, wave characteristics, and tidal data can all help to make a model more complete and should be used whenever possible.

Land cover data is also site-specific, and the analysis of different land cover types can be a useful tool in planning for future inundation. Knowing whether an area projected to be inundated is likely to recover quickly or to be damaged and need help recovering can help planners have an idea of where they will need to allocate resources or pay more attention in preparing for future sea-level rise. This can save time and money and also ensure that areas that will not easily recover from inundation events get protected or relocated first.

The island of Kauai should begin planning when and how they will prepare for future sea-level rise, and assessing regional vulnerabilities is an important first step in doing so (Russell and Griggs, 2012). No two shoreline will be affected identically by sea-level rise, but a regional assessment can help prioritize where to concentrate resources. By using the results of these passive and dynamic models, the county of Kauai and state of Hawaii can act now to lessen future impacts of sea-level rise around the island.

Appendex I
Hanalei Inundation Maps
Figure 39 Hanalei Bay with 0.0 m of sea-level rise using Methods #1-4

Figure 40 Hanalei Bay with 0.5 m of sea-level rise using Methods #1-4

Figure 41 Hanalei Bay with 1.0 m of sea-level rise using Methods #1-4

Figure 42 Hanalei Bay with 1.5 m of sea-level rise using Methods #1-4

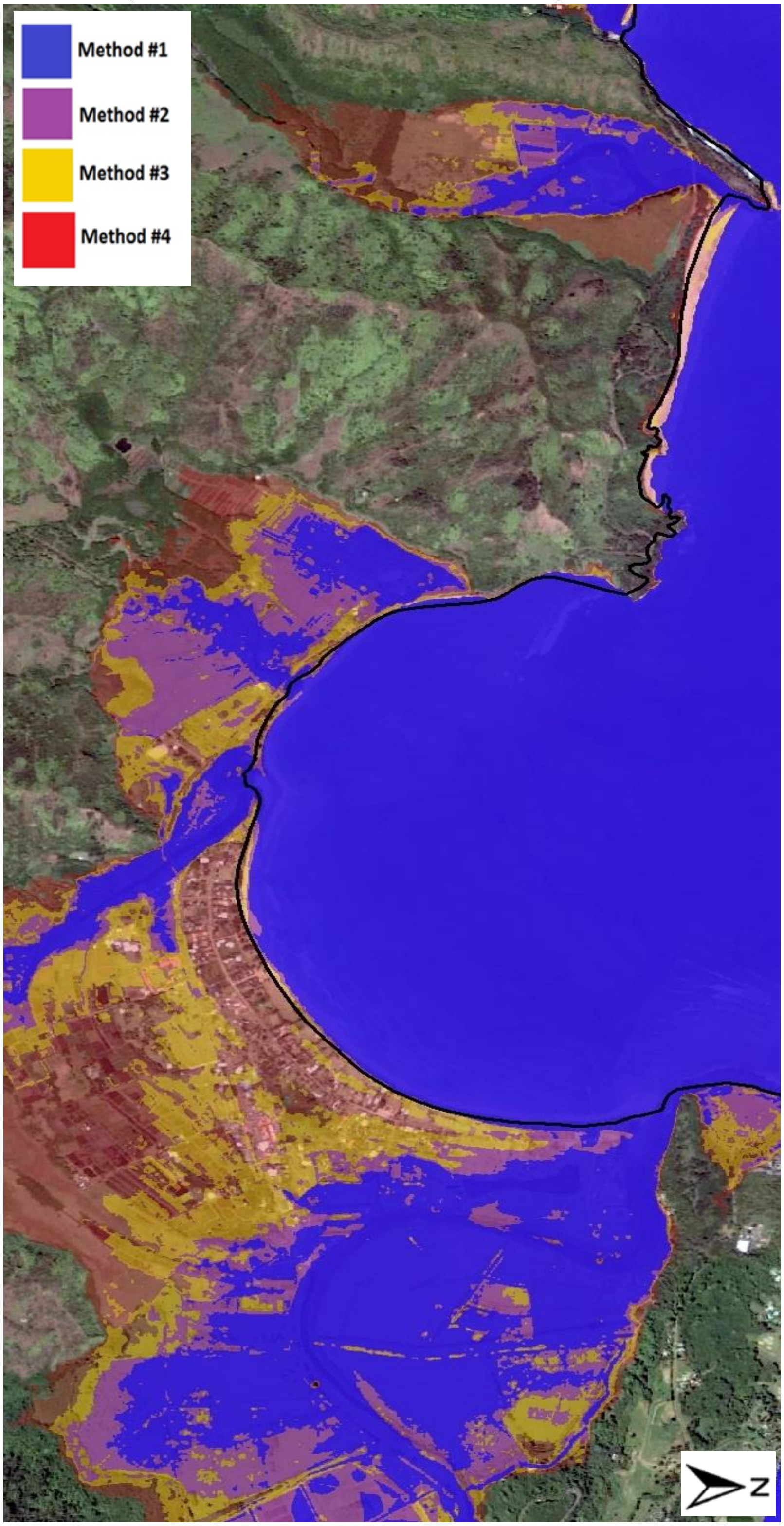

Figure 43 Hanalei Bay with 2.0 m of sea-level rise using Methods #1-4

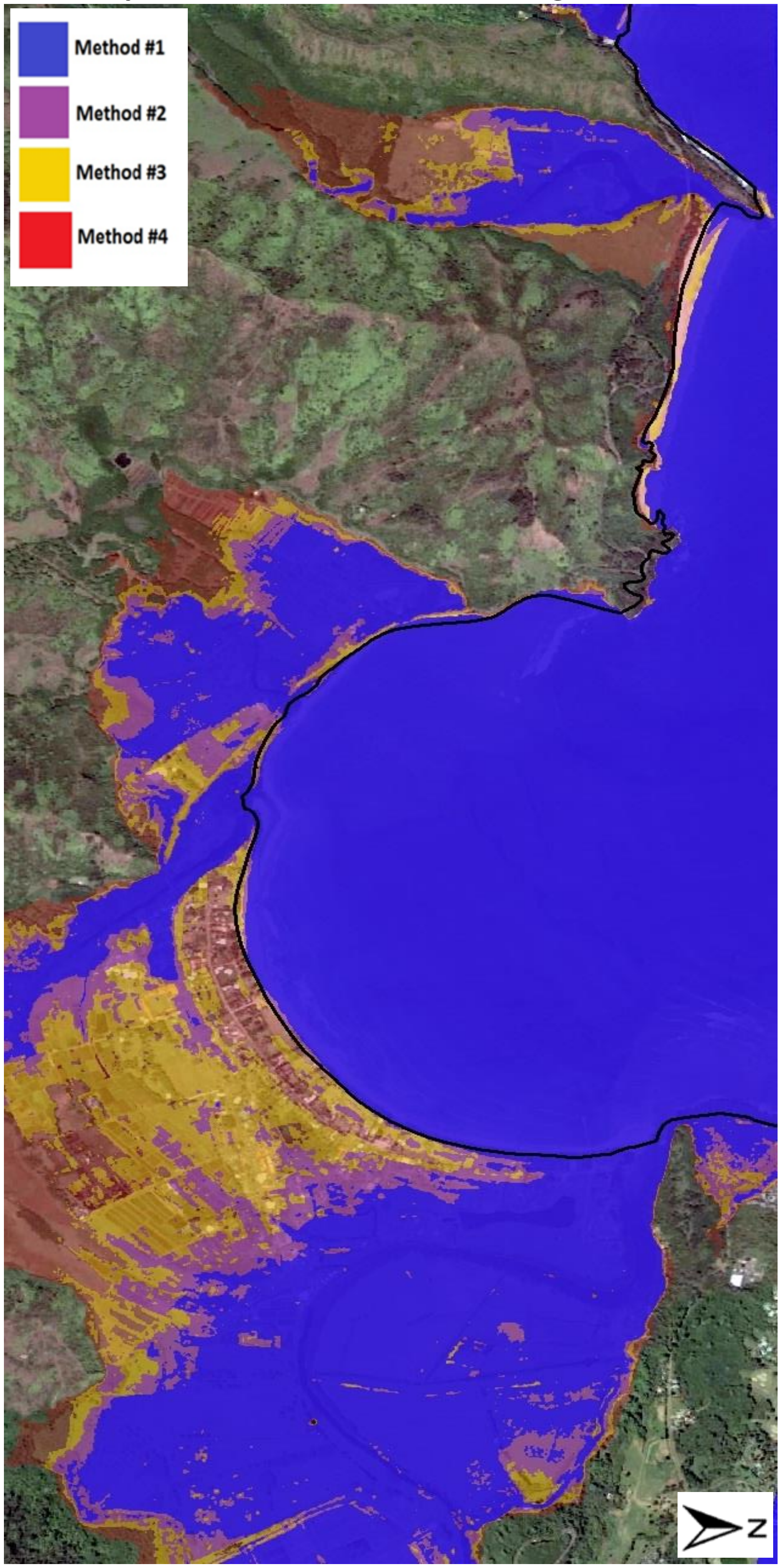

Appendix II
Kapa’a Inundation Maps
Figure 44 Kapa’a with 0.0 m of sea-level rise using Methods #1-4

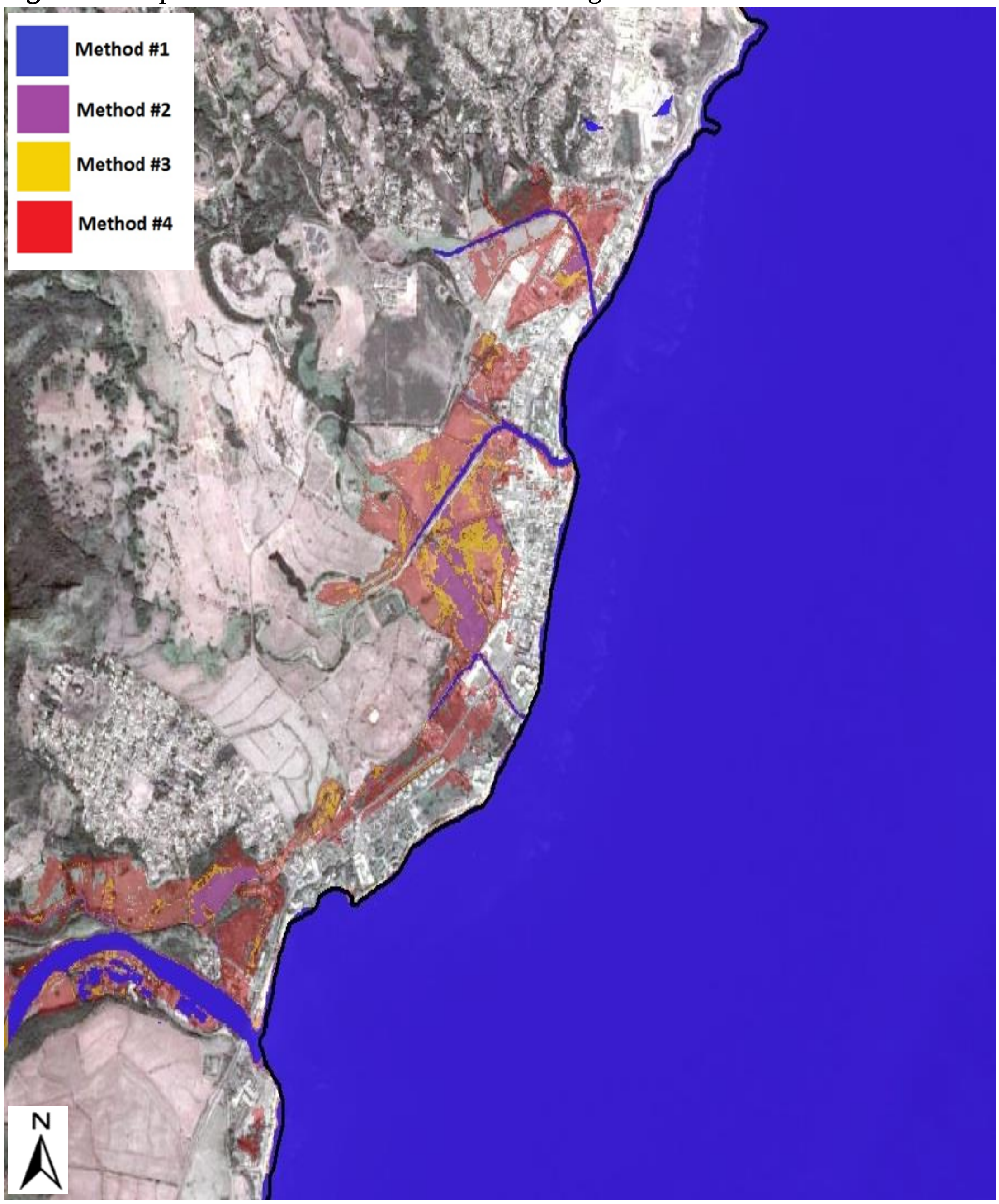

Figure 45 Kapa’a 0.5 m of sea-level rise using Methods #1-4

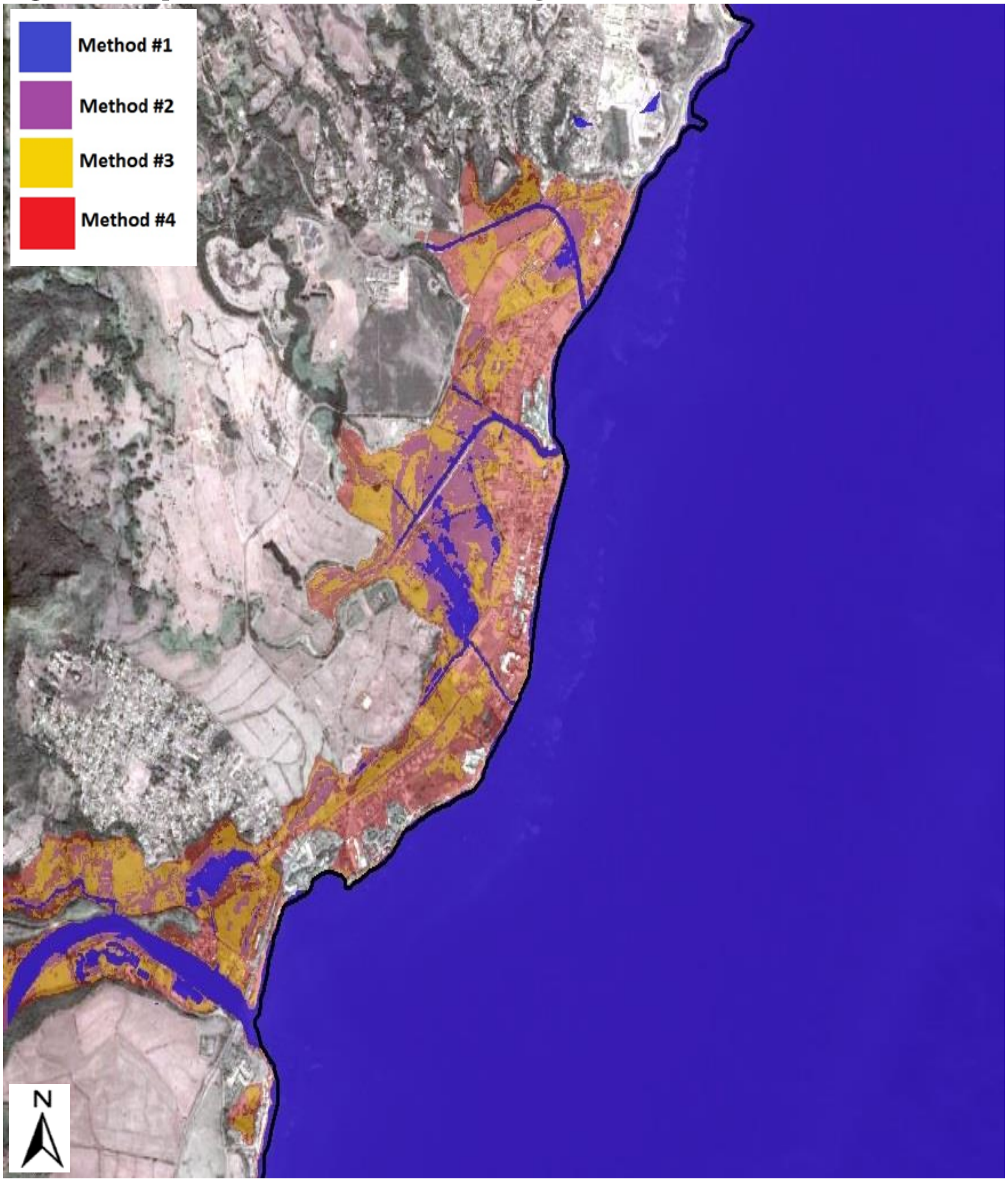

Figure 46 Kapa'a with 1.0 m of sea-level rise using Methods #1-4

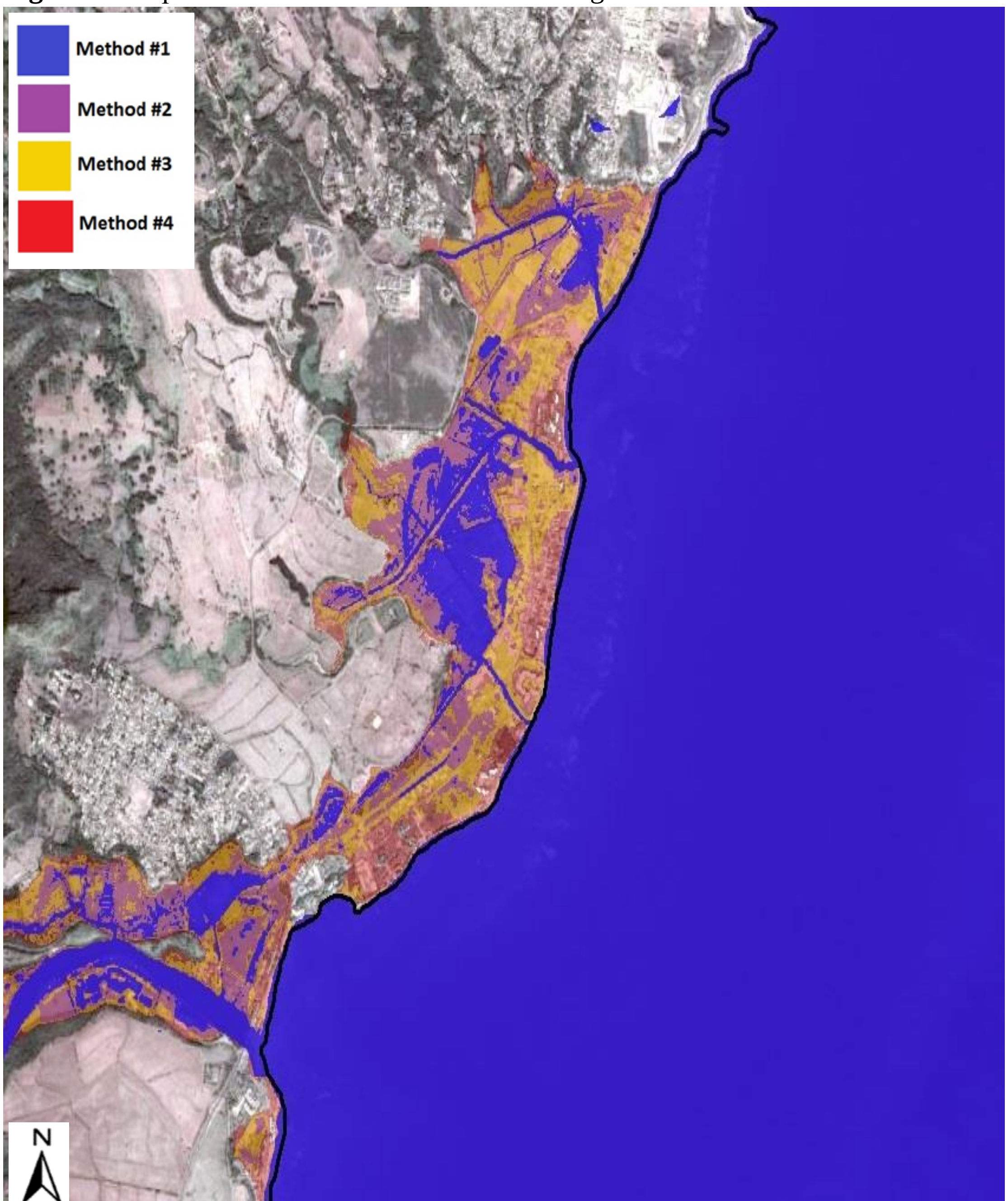

Figure 47 Kapa'a with 1.5 m of sea-level rise using Methods #1-4

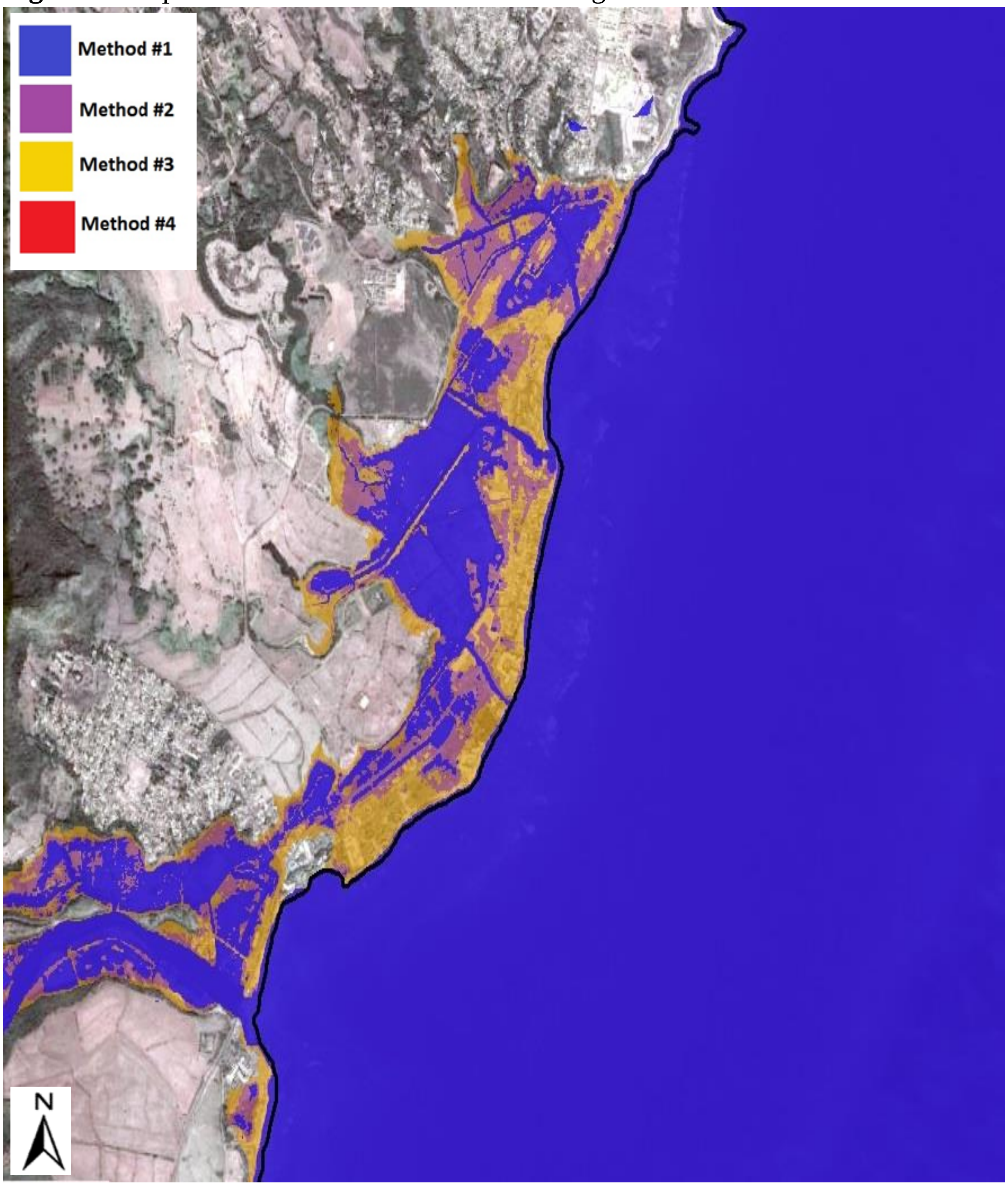

Figure 48 Kapa'a with 2.0 m of sea-level rise using Methods #1-4

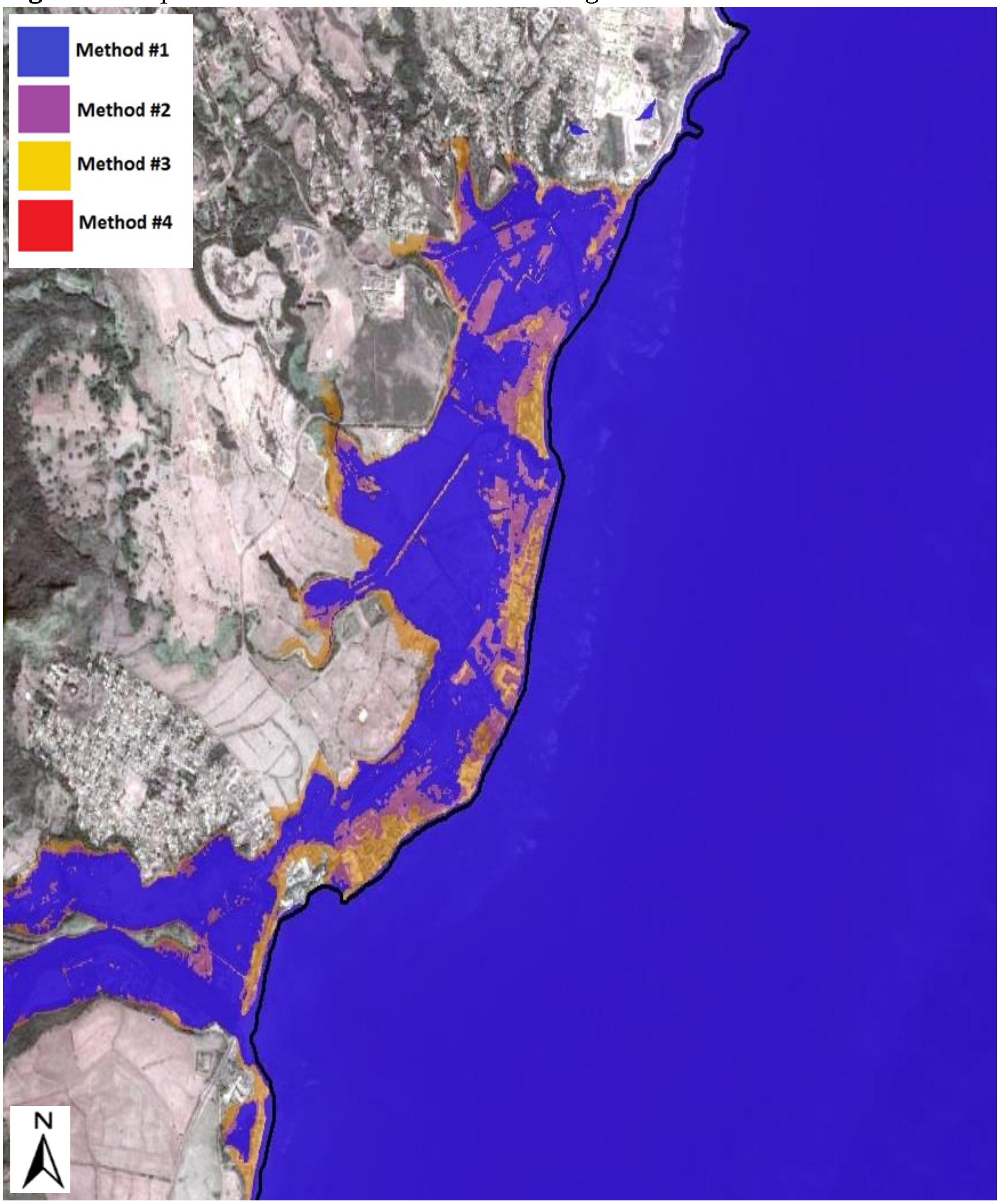

Appendix III
Waimea Inundation Maps
Figure 49 Waimea with 0.0 m of sea-level rise using Methods #1-4

Figure 50 Waimea with 0.5 m of sea-level rise using Methods #1-4

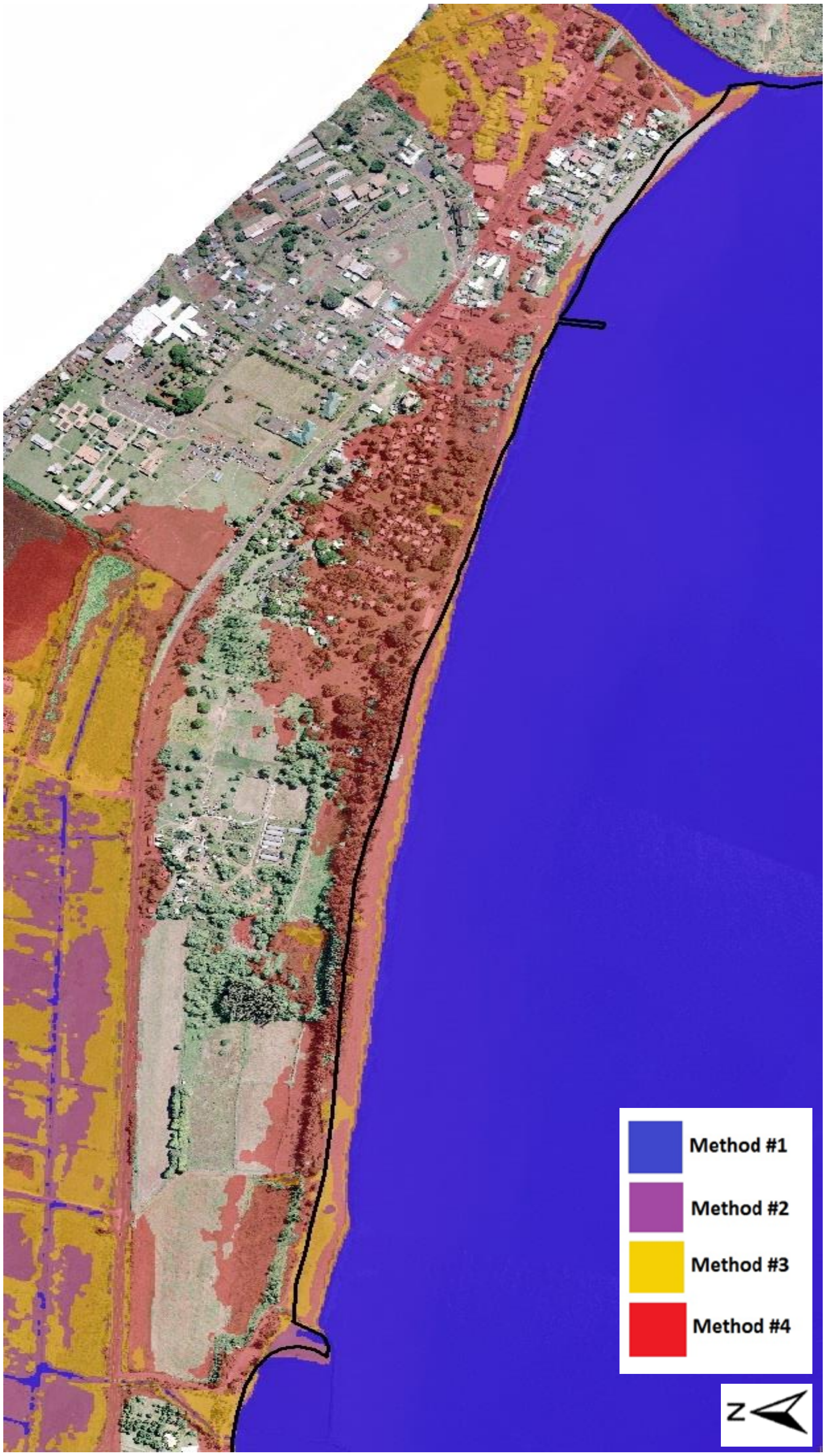

Figure 51 Waimea with 1.0 m of sea-level rise using Methods #1-4

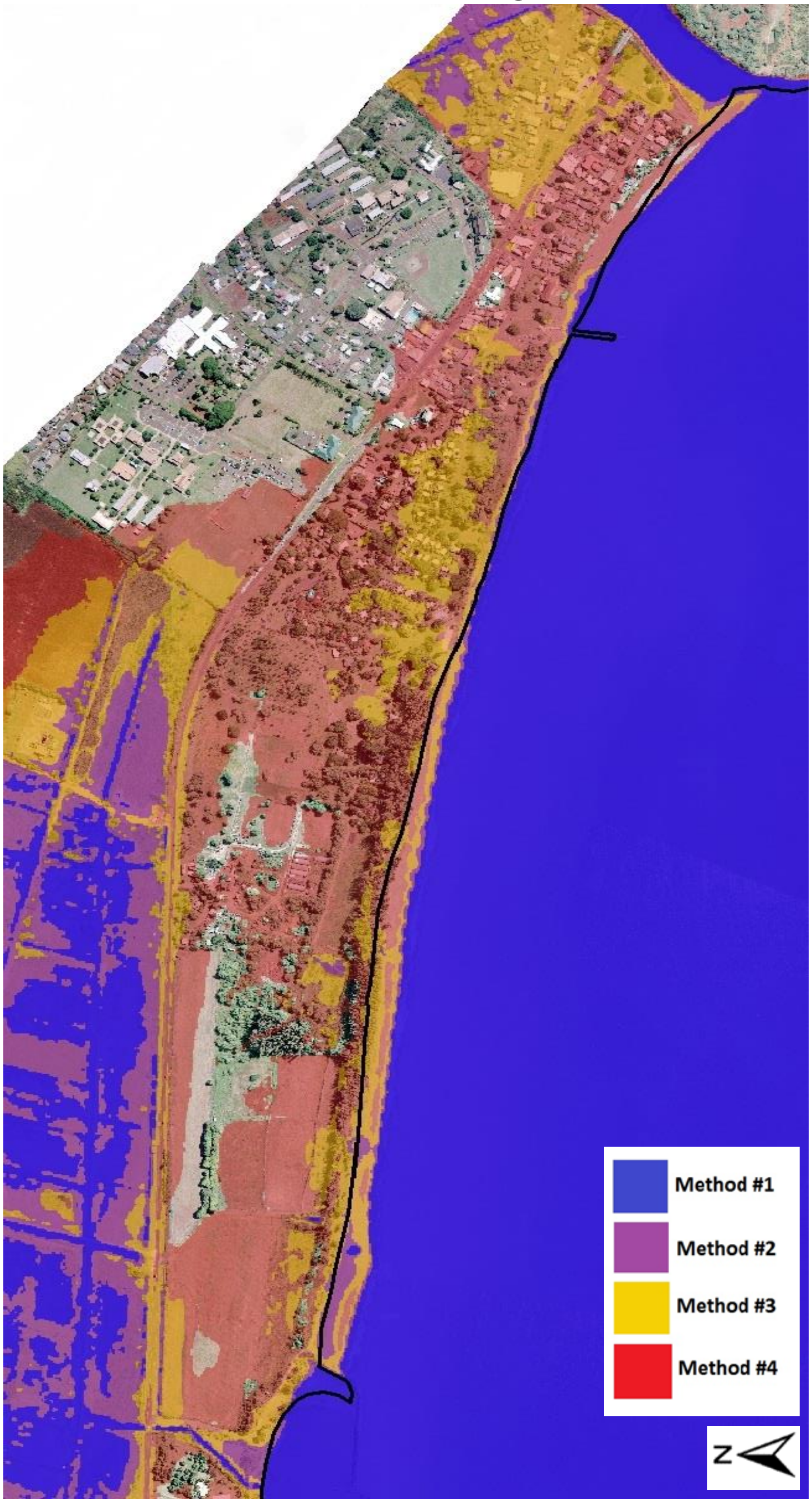

Figure 52 Waimea with 1.5 m of sea-level rise using Methods #1-4

Figure 53 Waimea inundation with 2.0 m of sea-level rise using Methods #1-4

Appendix IV
Hanalei Percent Inundation Graphs
Figure 54 Percent of total Hanalei land area in study site inundated by 0.0 m of sea-level rise using Methods #1-#4

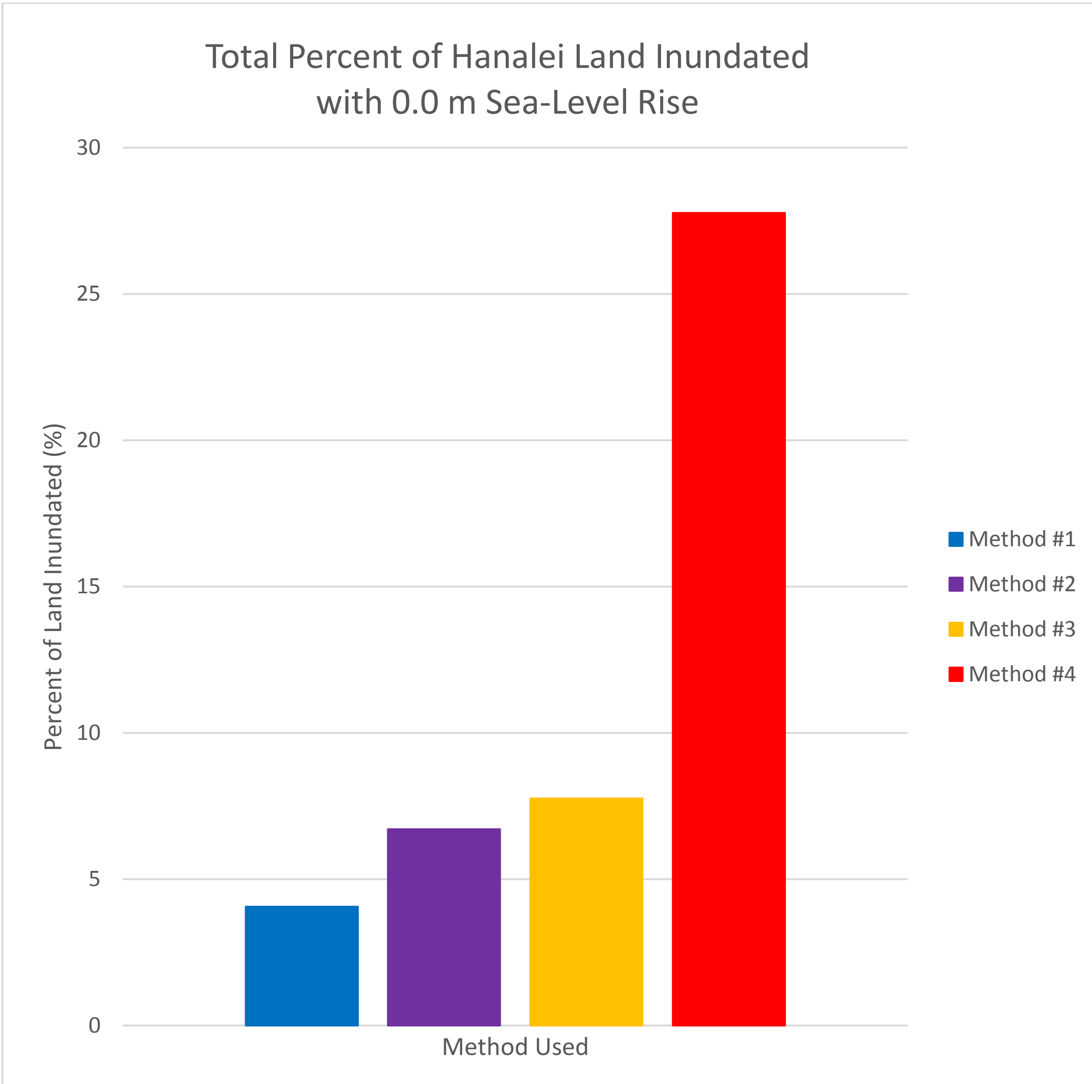

Figure 55 Percent of total Hanalei land area in study site inundated by 0.5 m of sea-level rise using Methods #1-#4

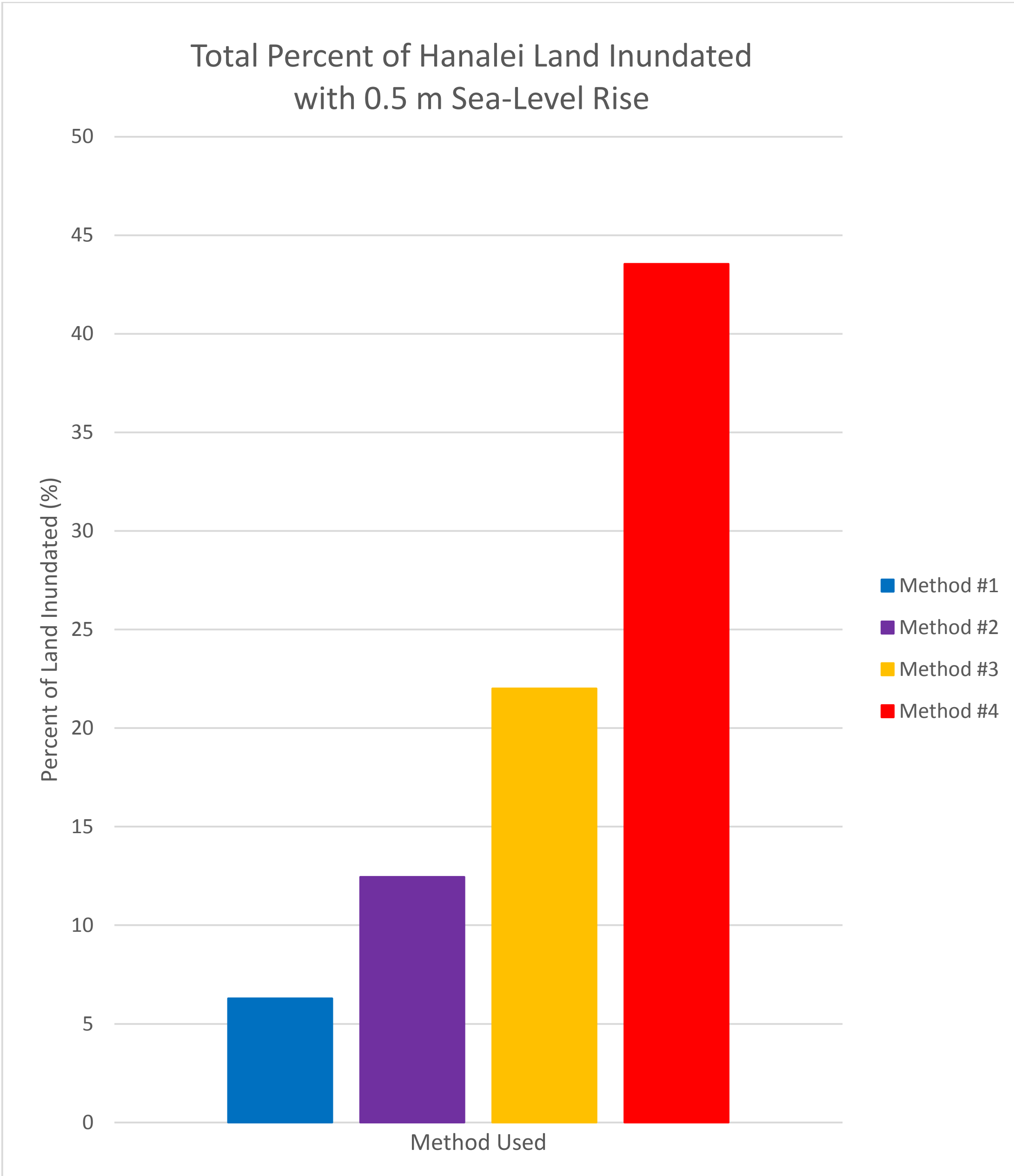

Figure 56 Percent of total Hanalei land area in study site inundated by 1.0 m of sea-level rise using Methods #1-#4

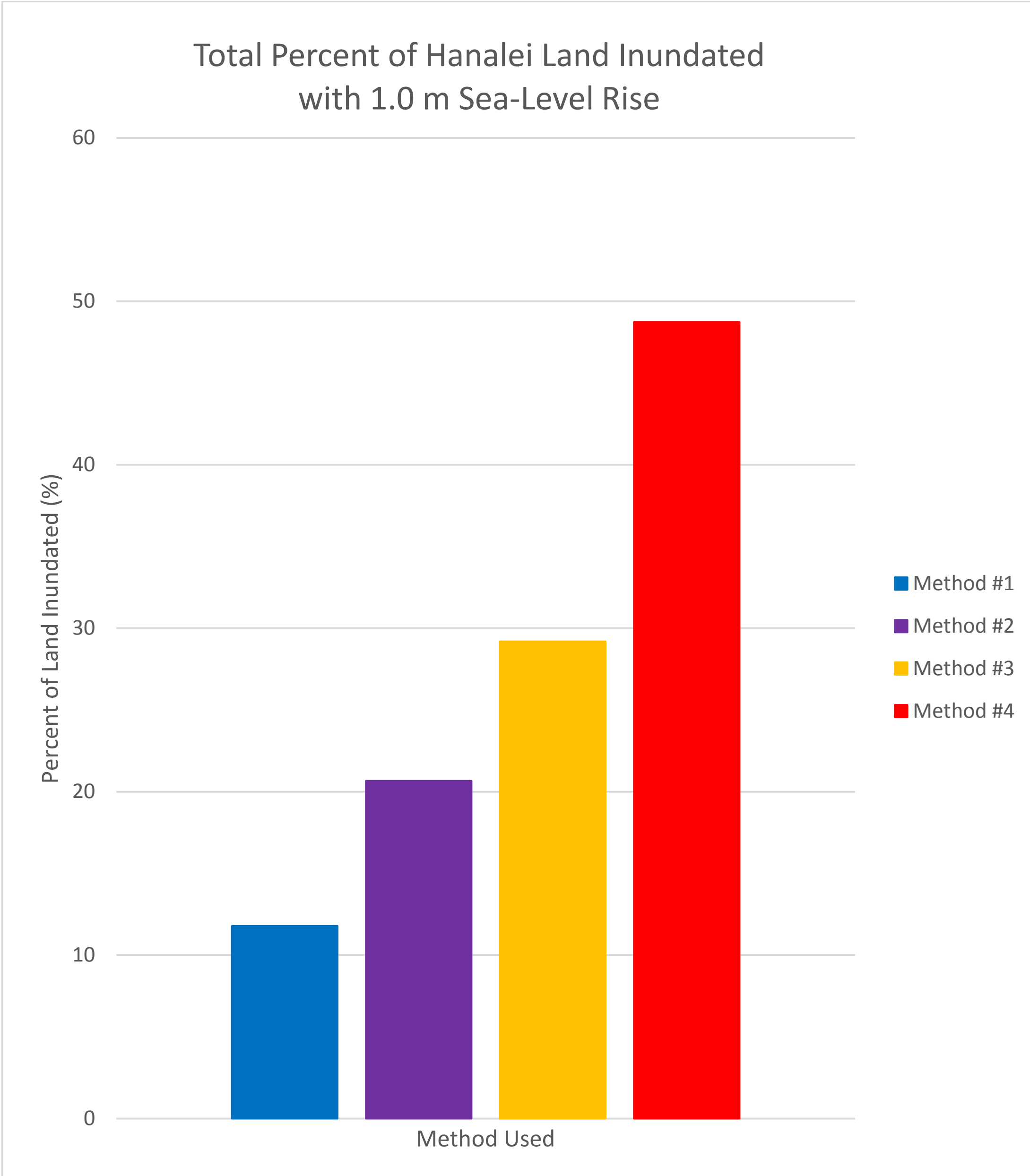

Figure 57 Percent of total Hanalei land area in study site inundated by 1.5 m of sea-level rise using Methods #1-#4

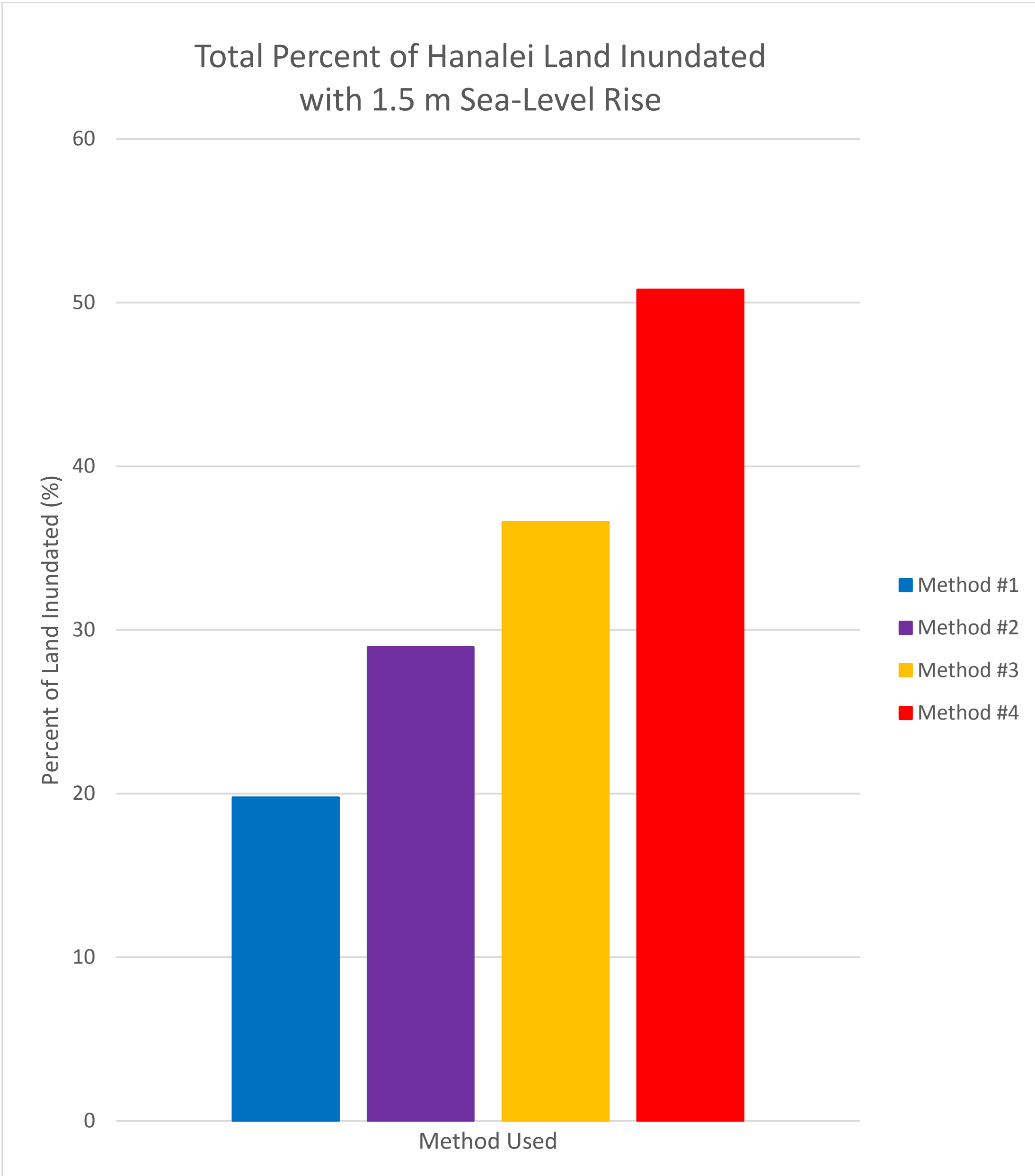

Figure 58 Percent of total Hanalei land area in study site inundated by 2.0 m of sea-level rise using Methods #1-#4

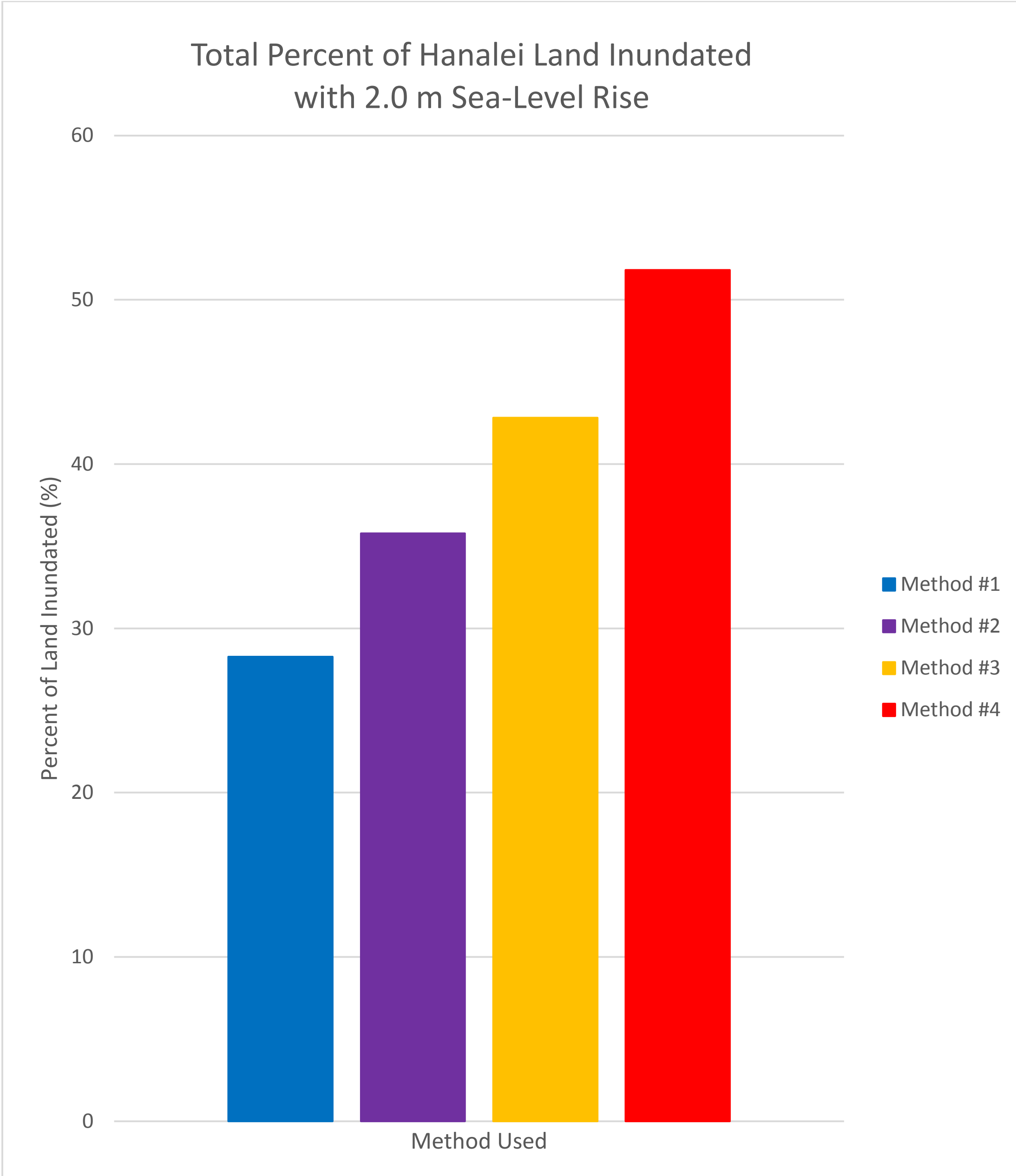

Appendix V
Kapa'a Percent Inundation Graphs
Figure 59 Percent of total Kapa'a land area in study site inundated by 0.0 m of sea-level rise using Methods #1-#4

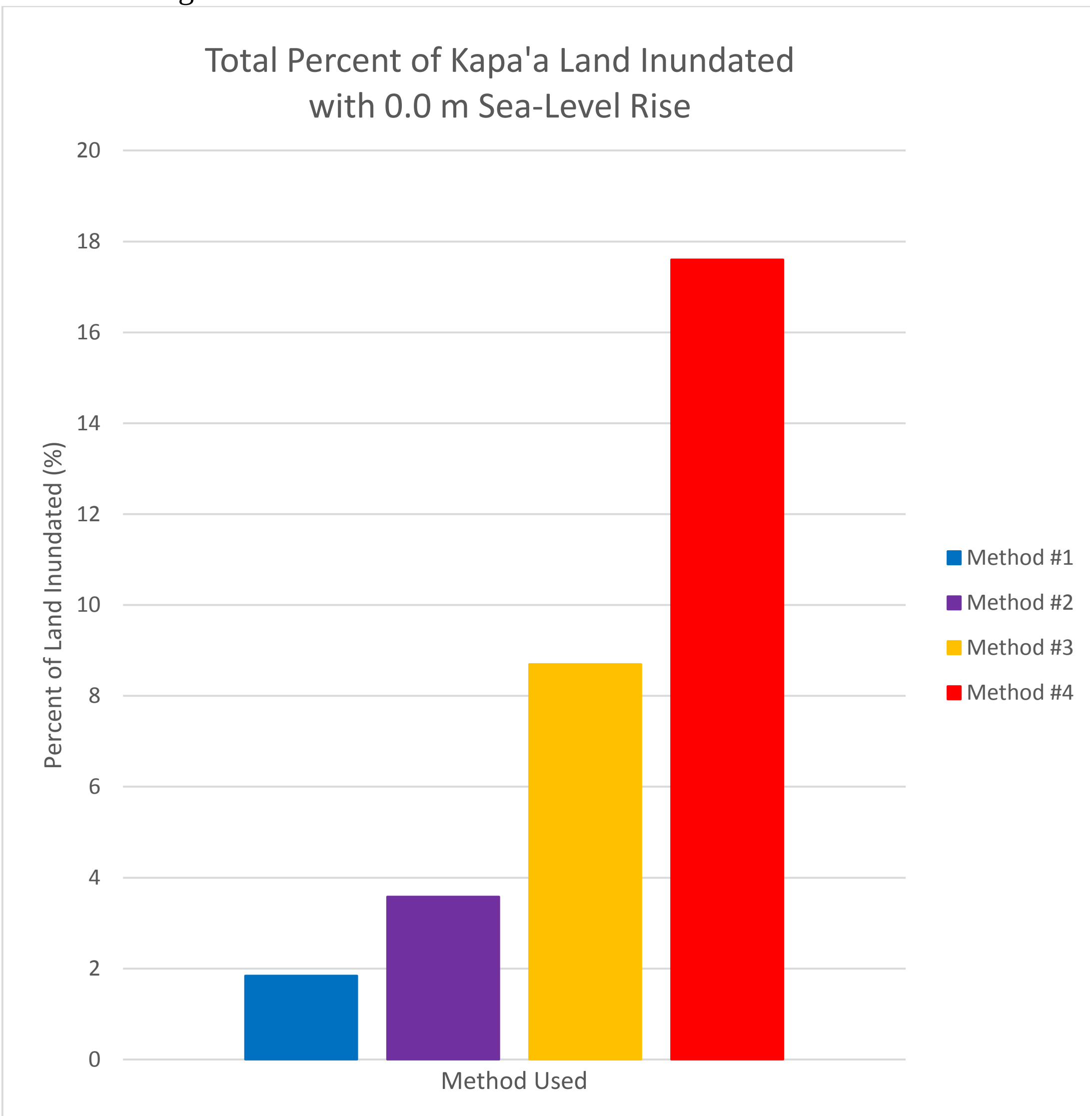

Figure 60 Percent of total Kapa’a land area in study site inundated by 0.5 m of sea-level rise using Methods #1-#4

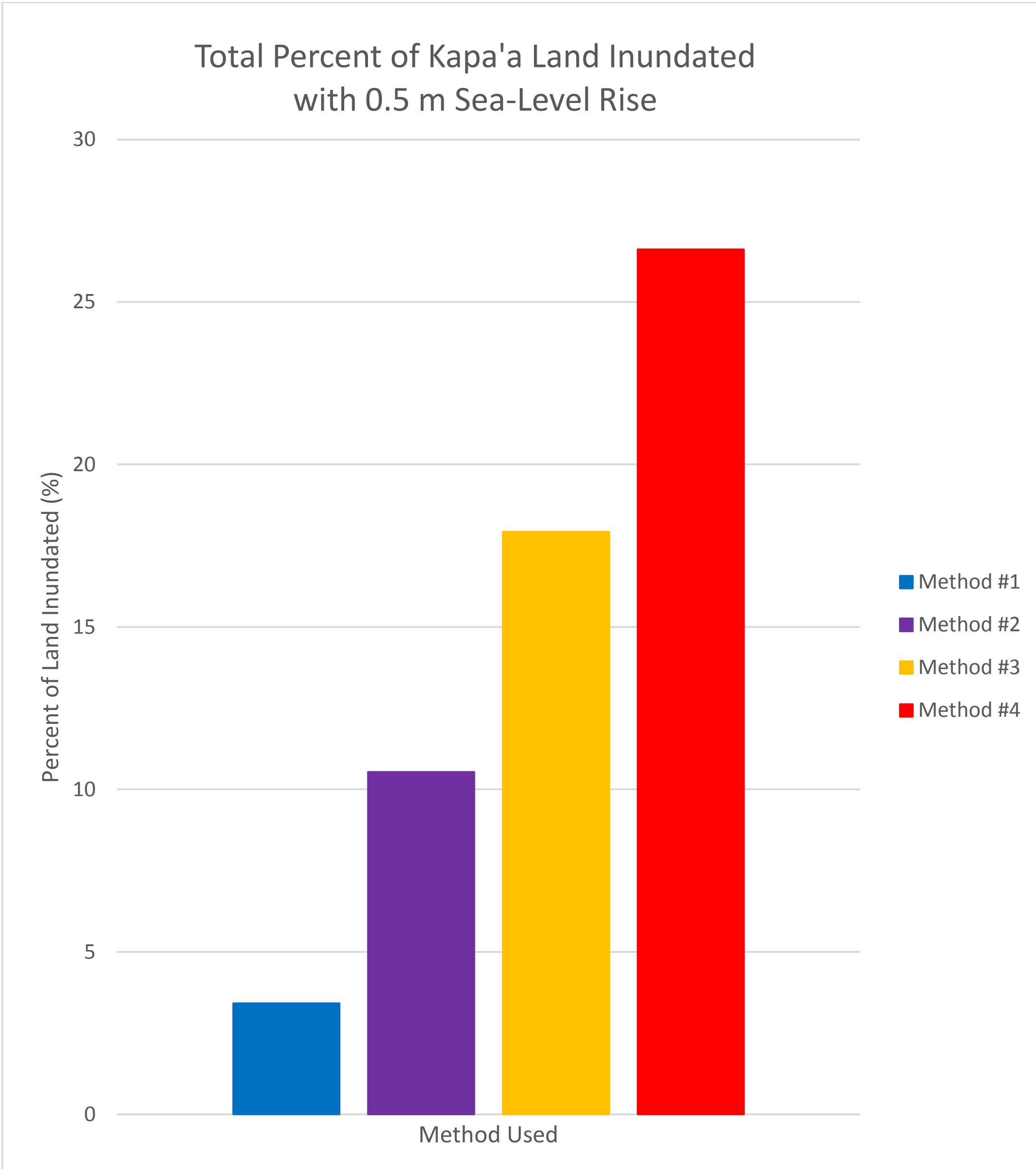

Figure 61 Percent of total Kapa'a land area in study site inundated by 1.0 m of sea-level rise using Methods #1-#4

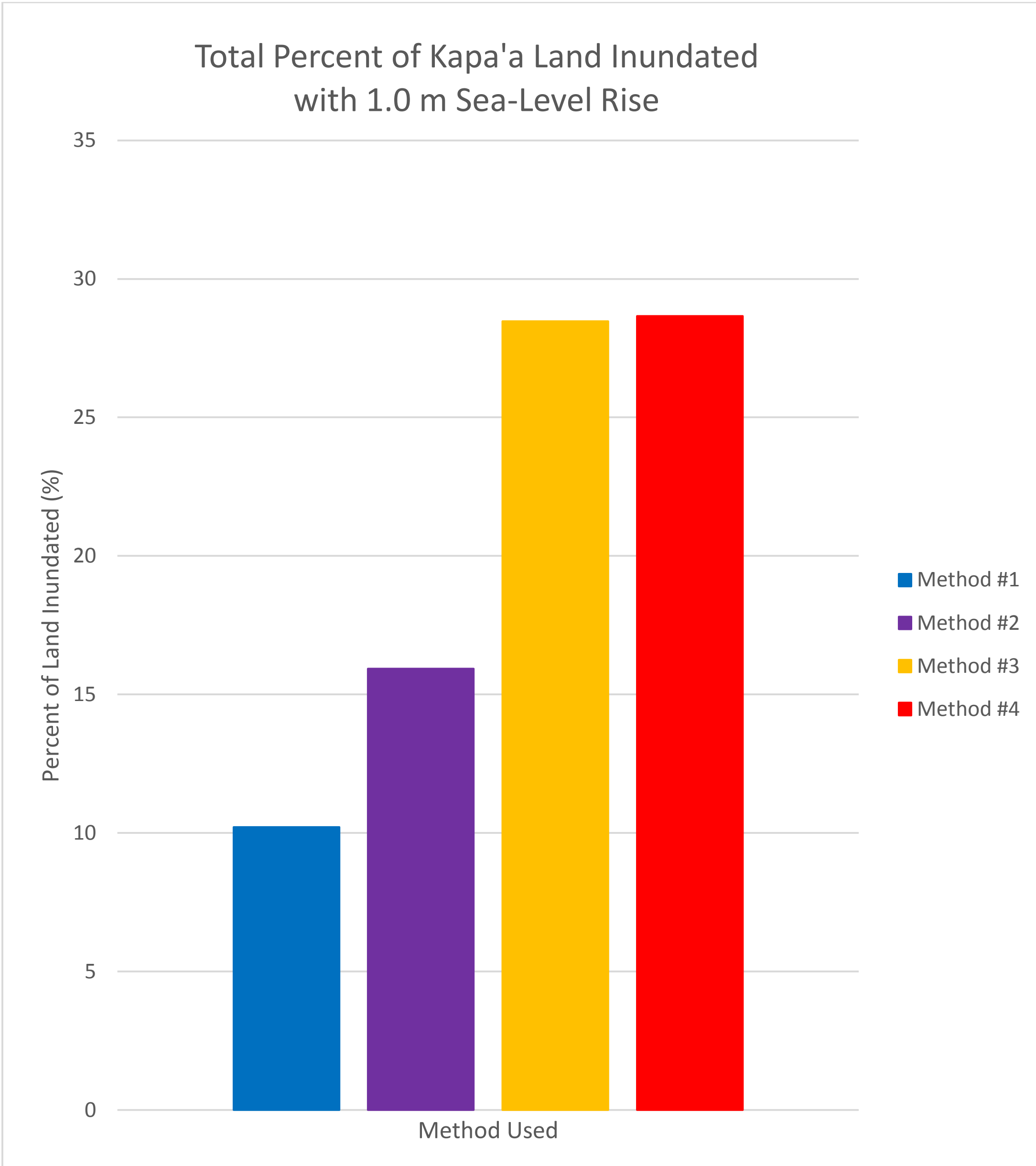

Figure 62 Percent of total Kapa’a land area in study site inundated by 1.5 m of sea-level rise using Methods #1-#4

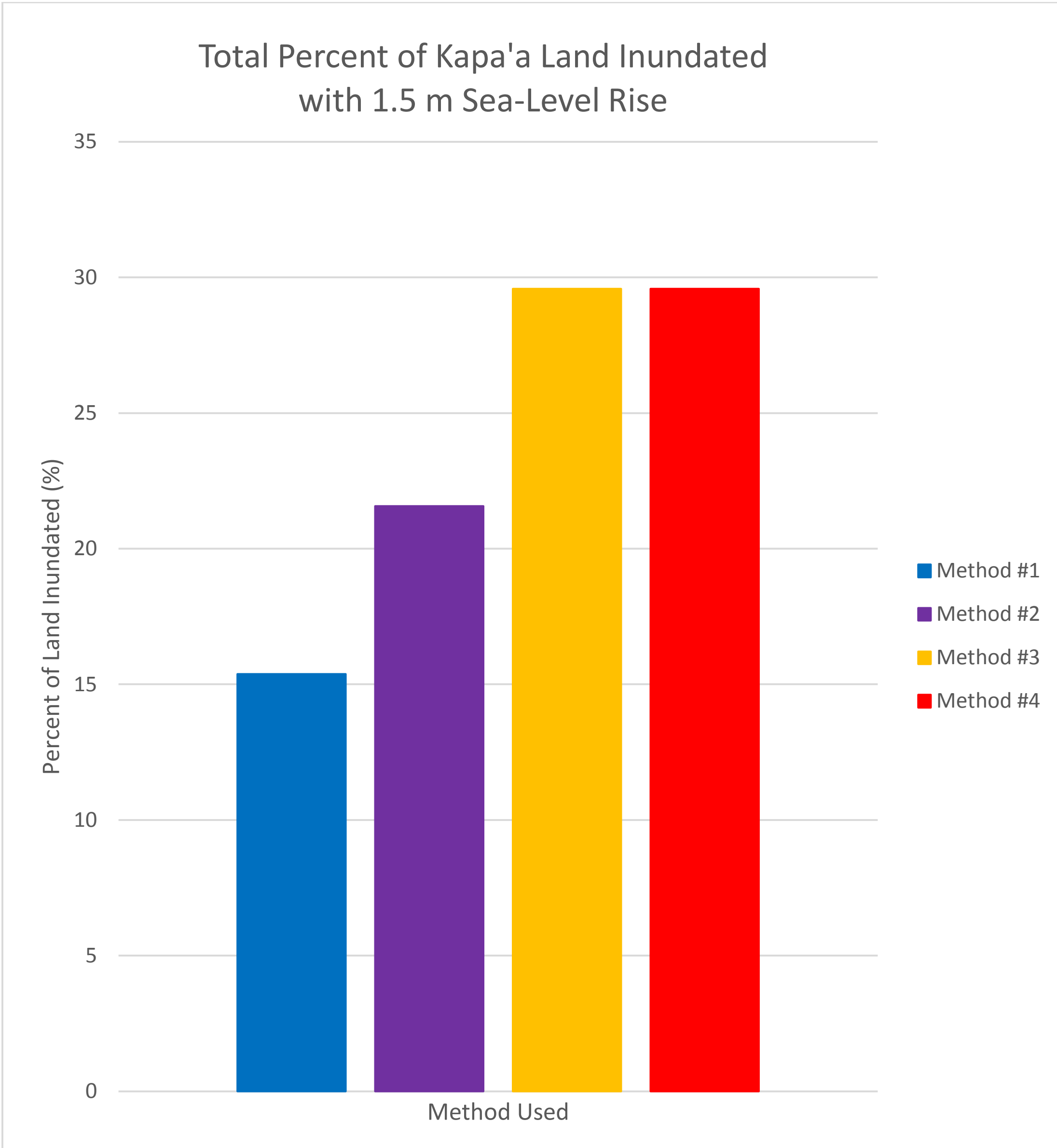

Figure 63 Percent of total Kapa'a land area in study site inundated by 2.0 m of sea-level rise using Methods #1-#4

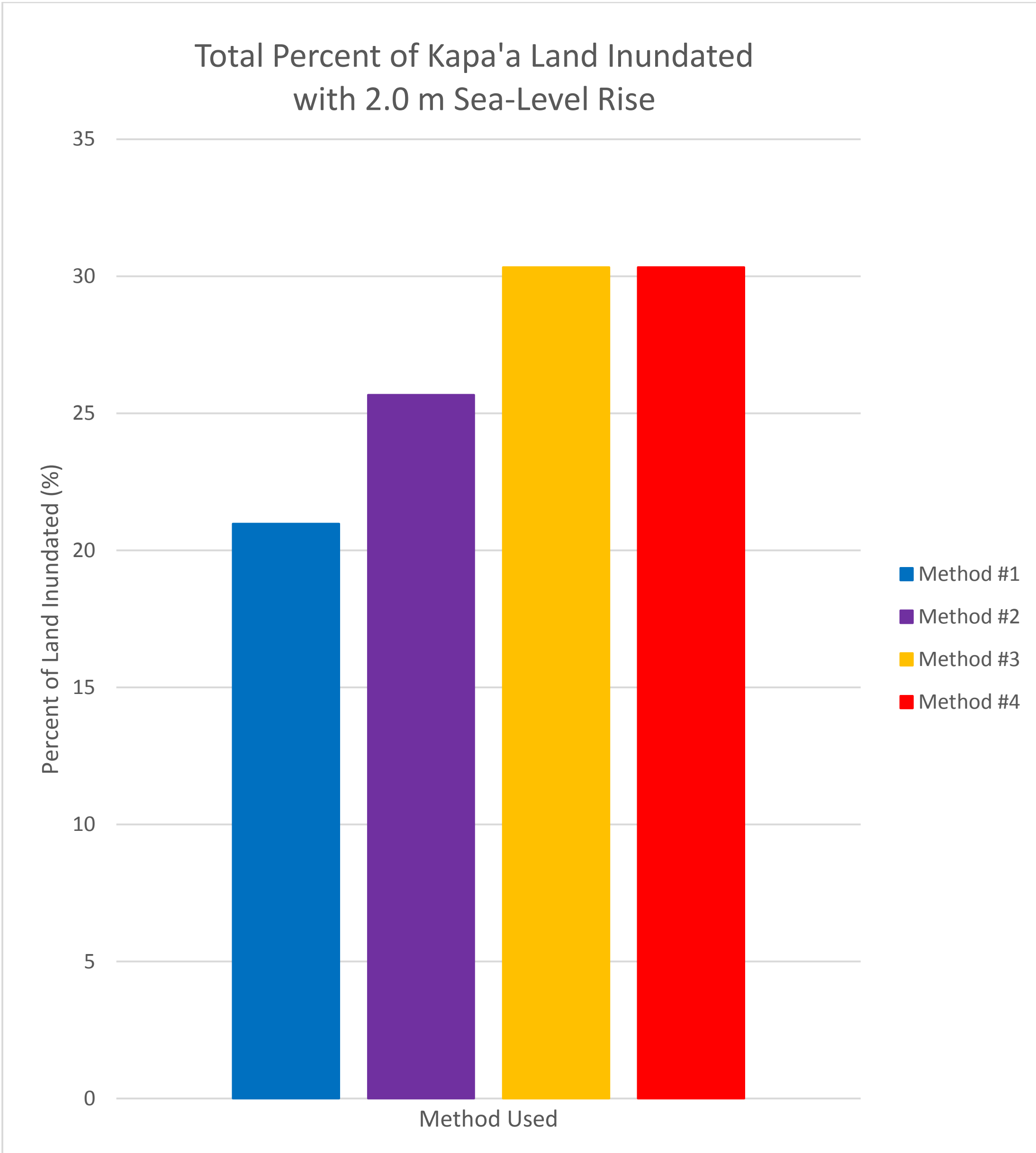

Appendix VI

Waimea Percent Inundation Graphs

Figure 64 Percent of total Waimea land area in study site inundated by 0.0 m of sea-level rise using Methods #1-#4

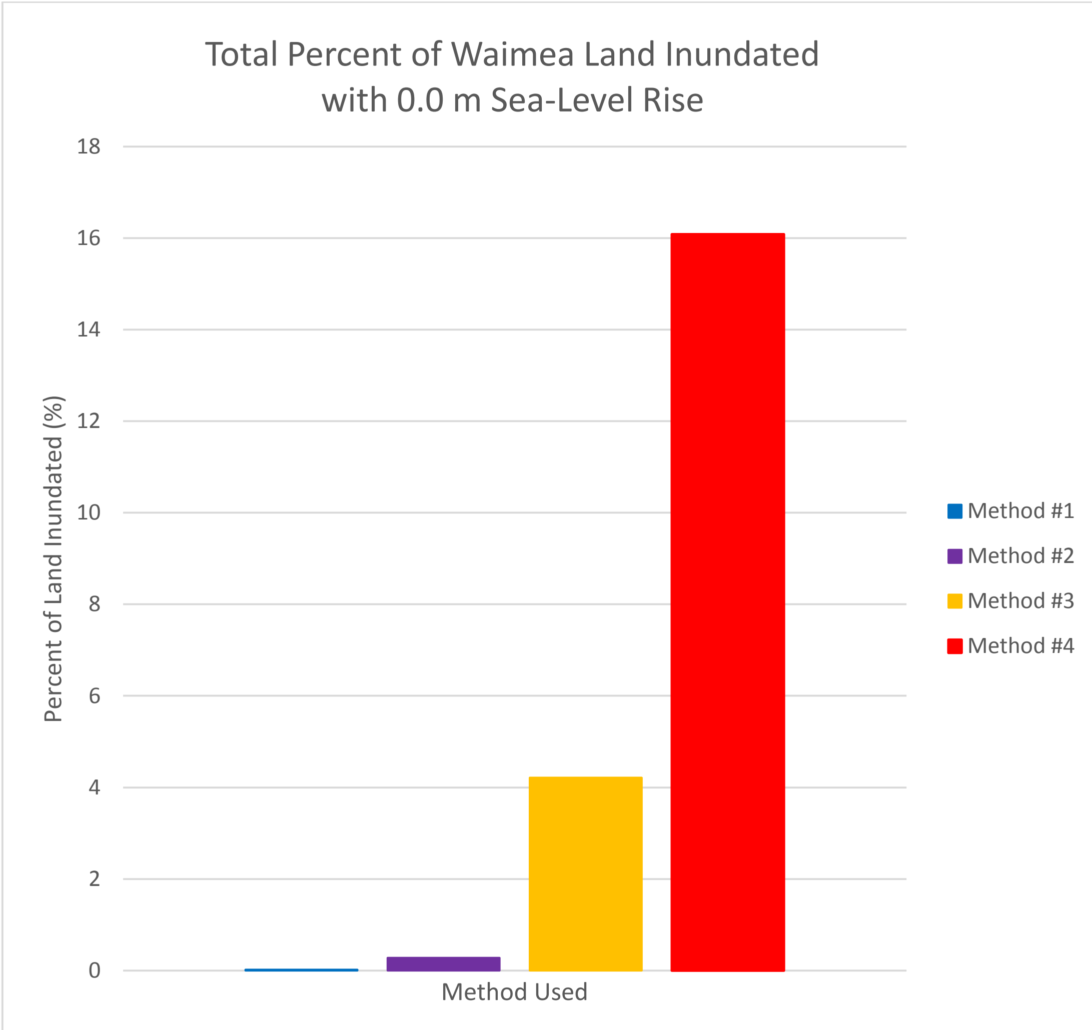

Figure 65 Percent of total Waimea land area in study site inundated by 0.5 m of sea-level rise using Methods #1-#4

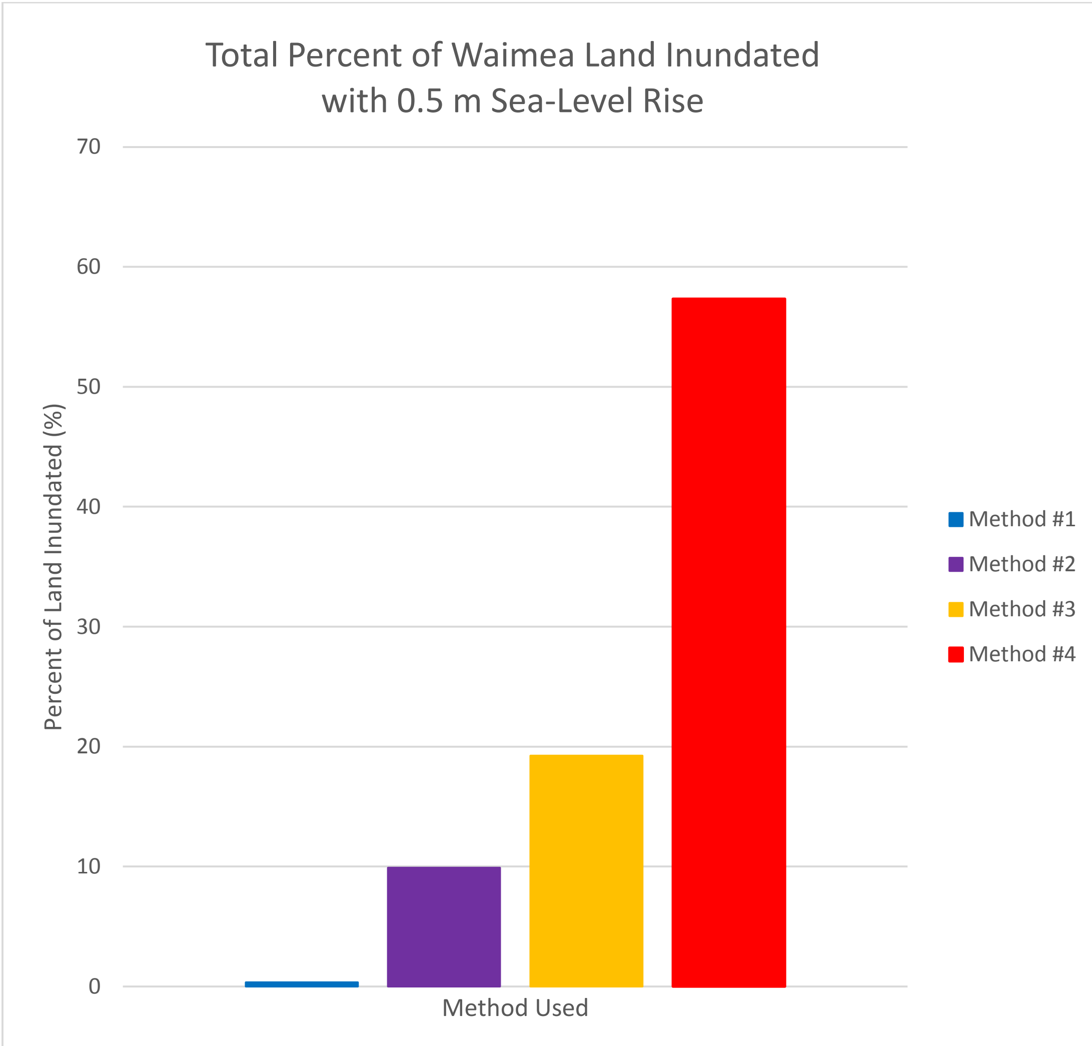

Figure 66 Percent of total Waimea land area in study site inundated by 1.0 m of sea-level rise using Methods #1-#4

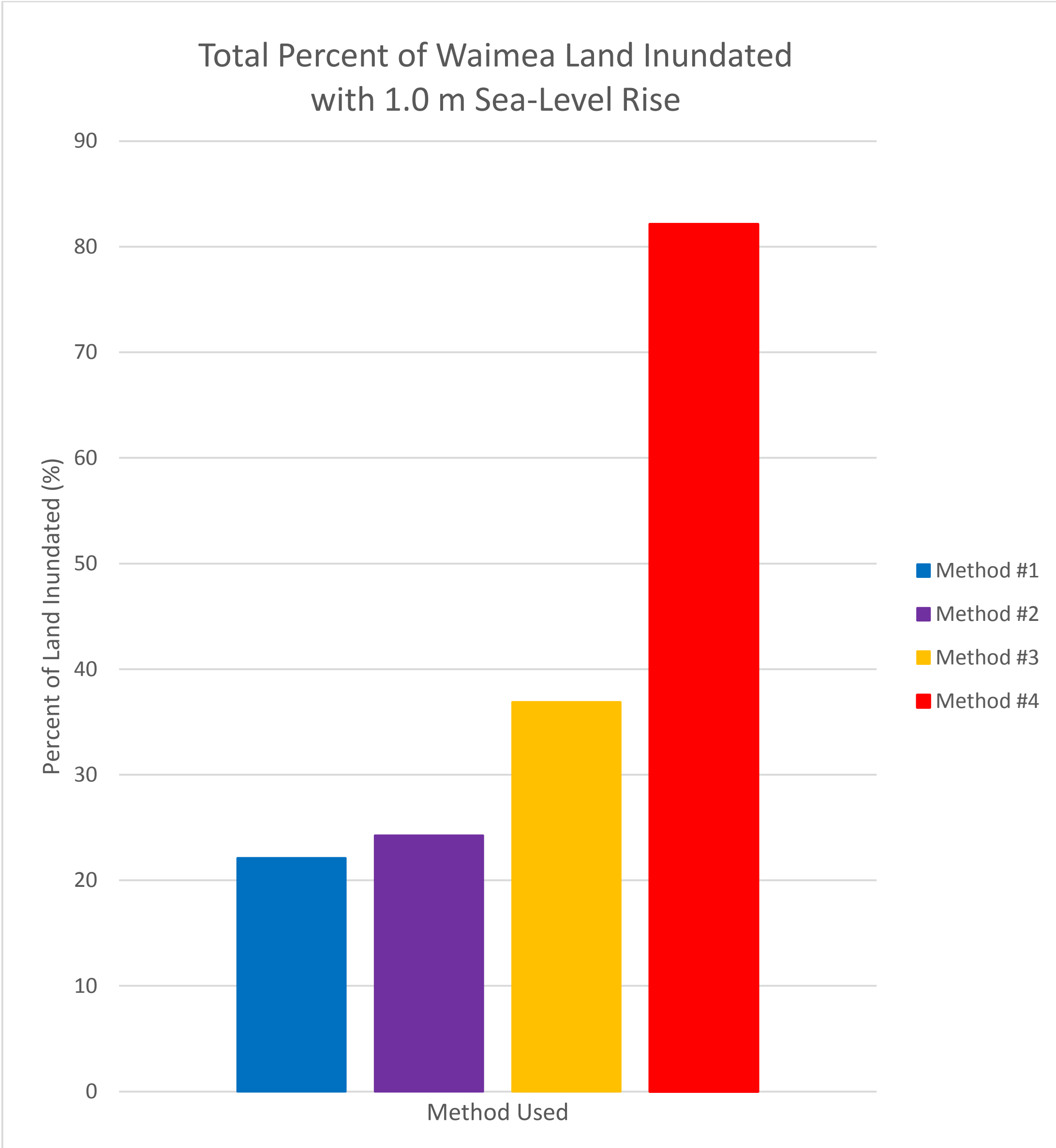

Figure 67 Percent of total Waimea land area in study site inundated by 1.5 m of sea-level rise using Methods #1-#4

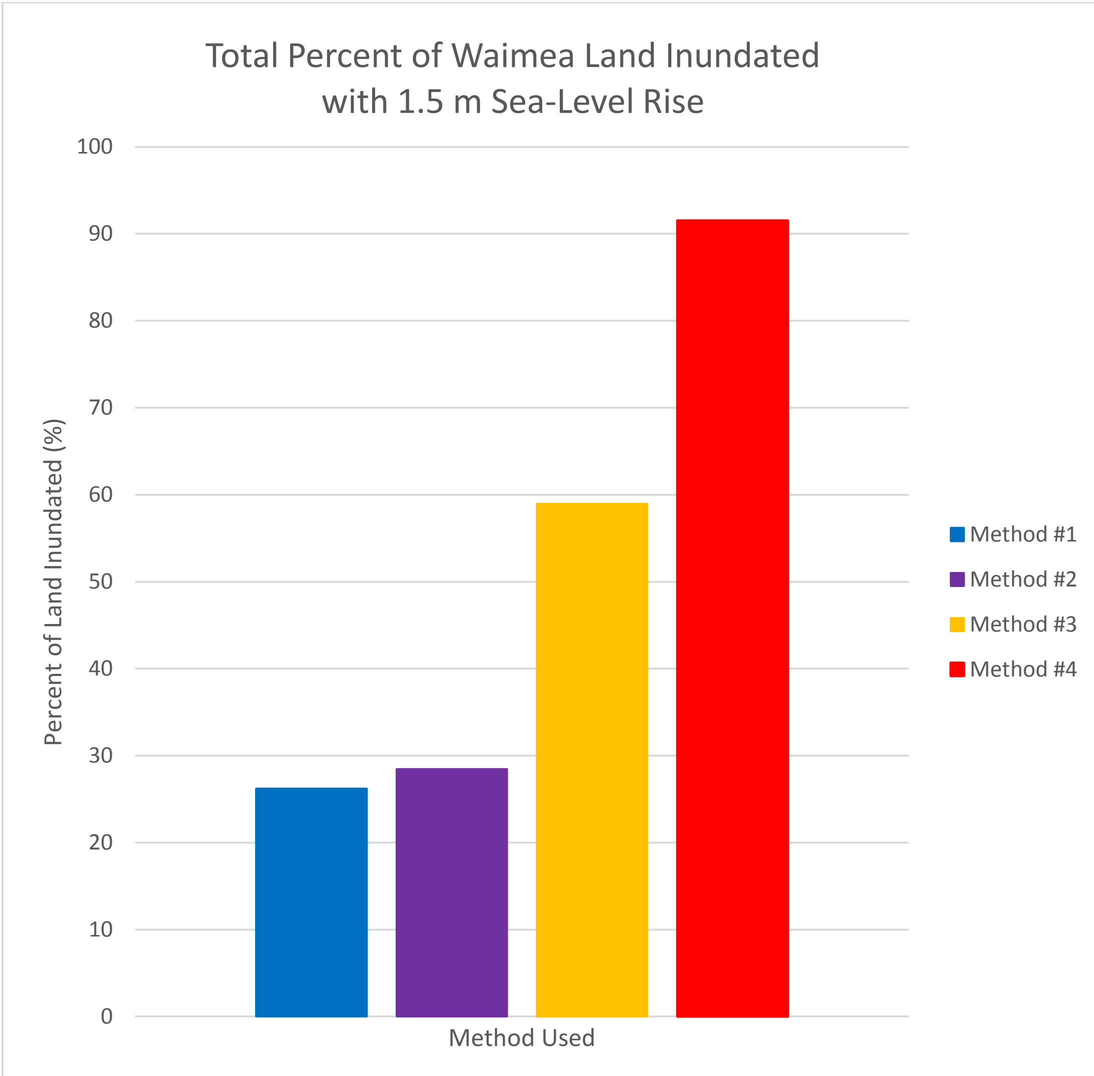

Figure 68 Percent of total Waimea land area in study site inundated by 2.0 m of sea-level rise using Methods #1-#4

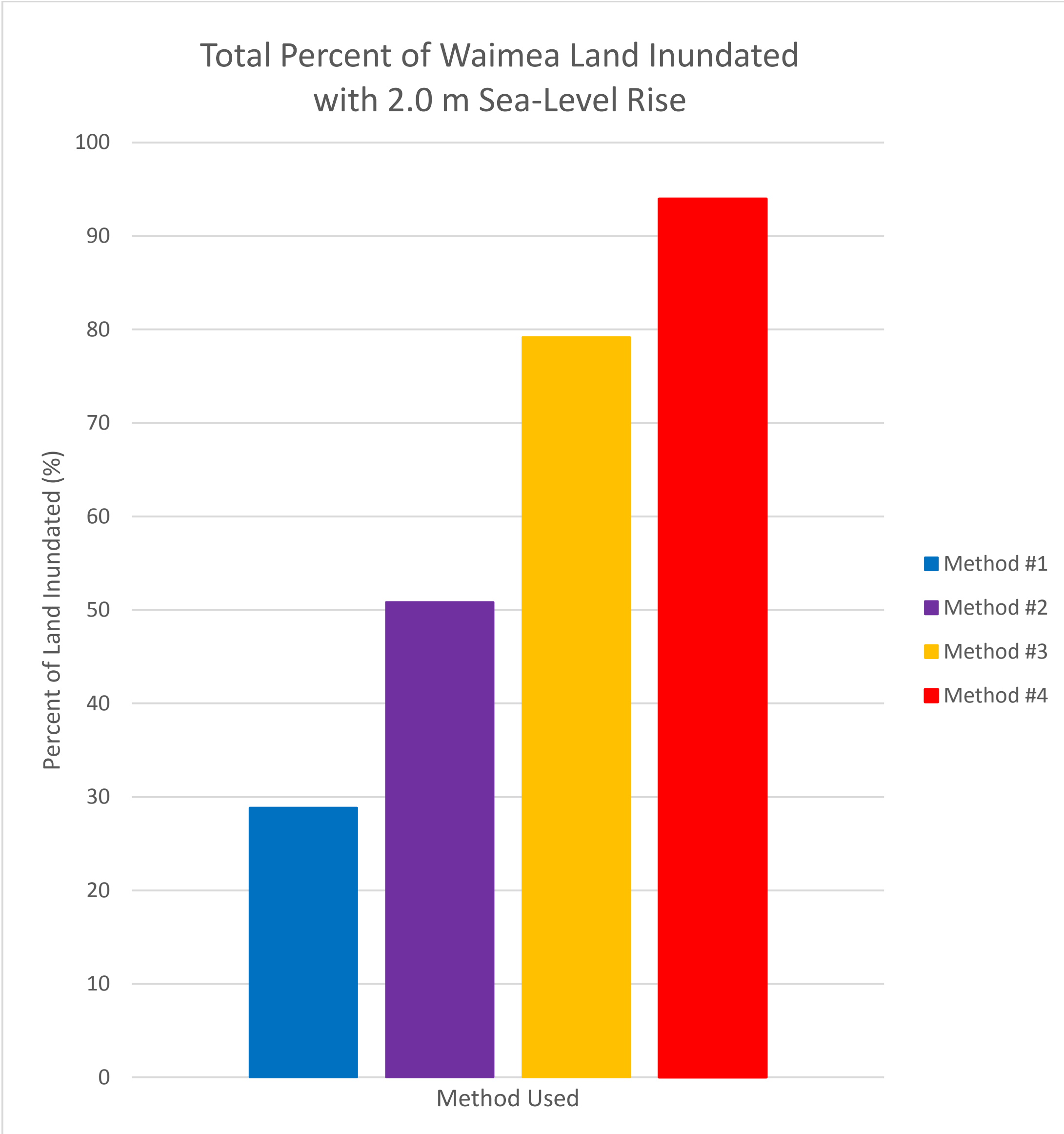

Appendix VII

Hanalei Percent Inundation by Land Cover Type

Figure 69 Land cover types inundated by each sea-level rise increment as a percent of total Hanalei land area in study site for Method #1

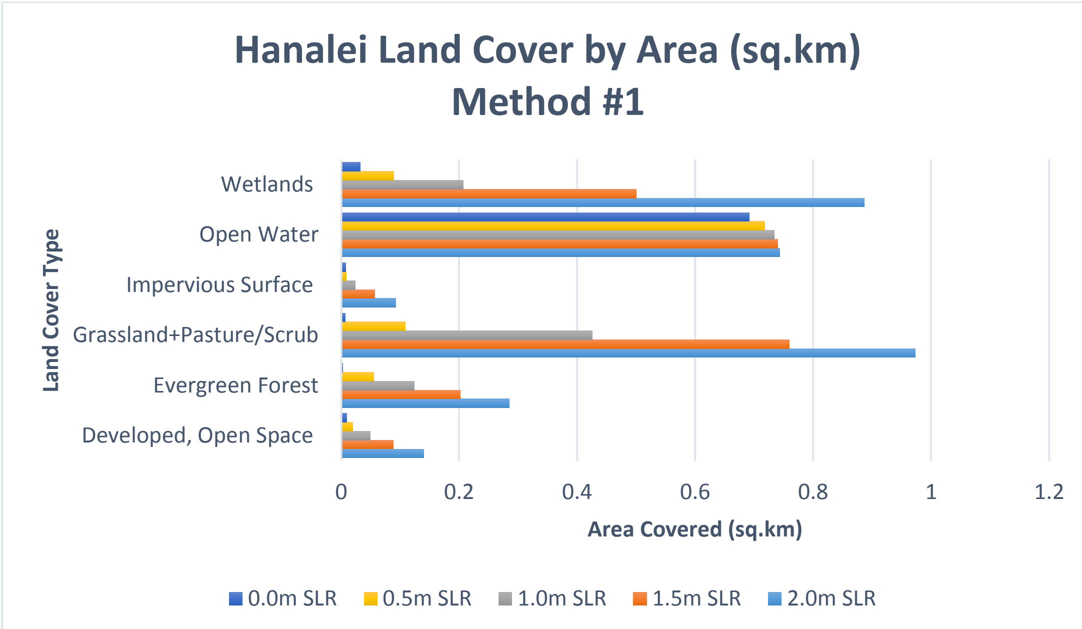

Figure 70 Land cover types inundated by each sea-level rise increment as a percent of total Hanalei land area in study site for Method #2

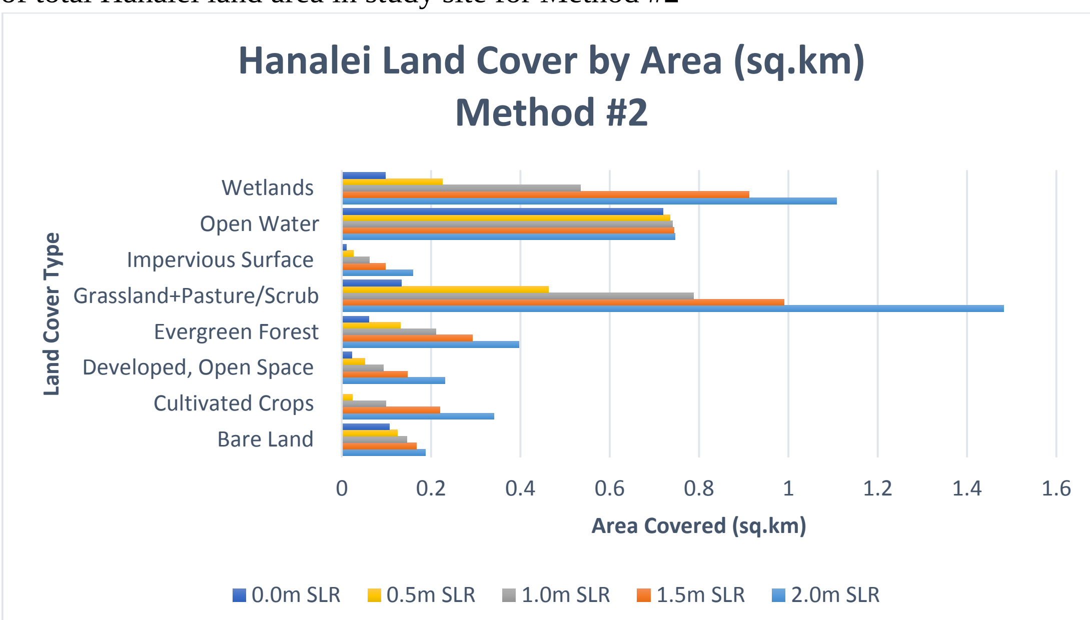

Figure 71 Land cover types inundated by each sea-level rise increment as a percent of total Hanalei land area in study site for Method #3

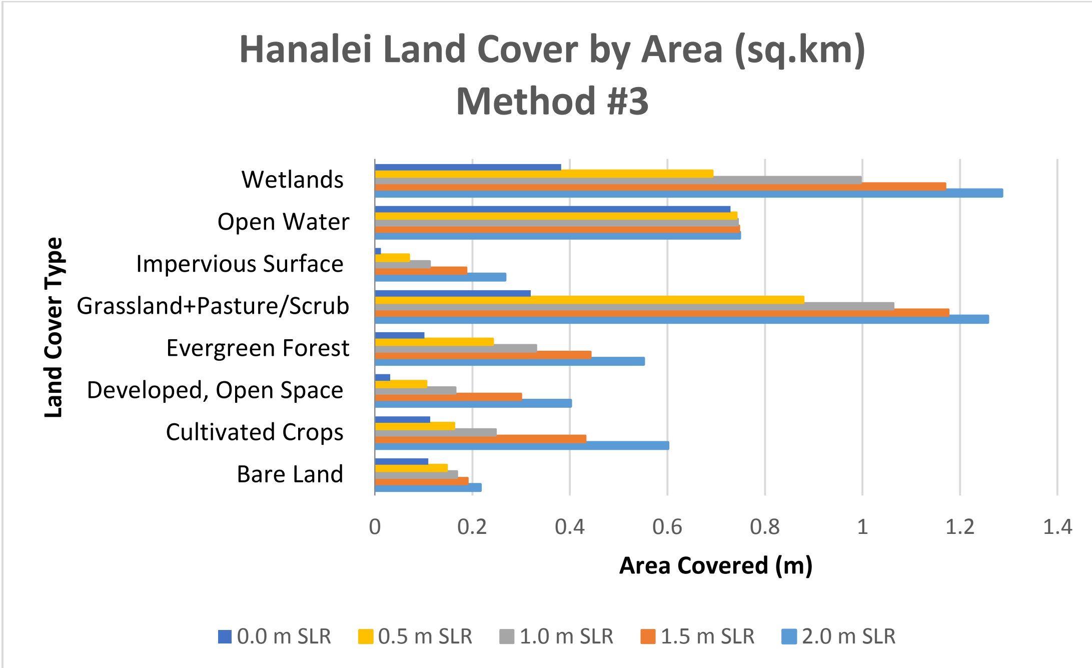

Figure 72 Land cover types inundated by each sea-level rise increment as a percent of total Hanalei land area in study site for Method #4

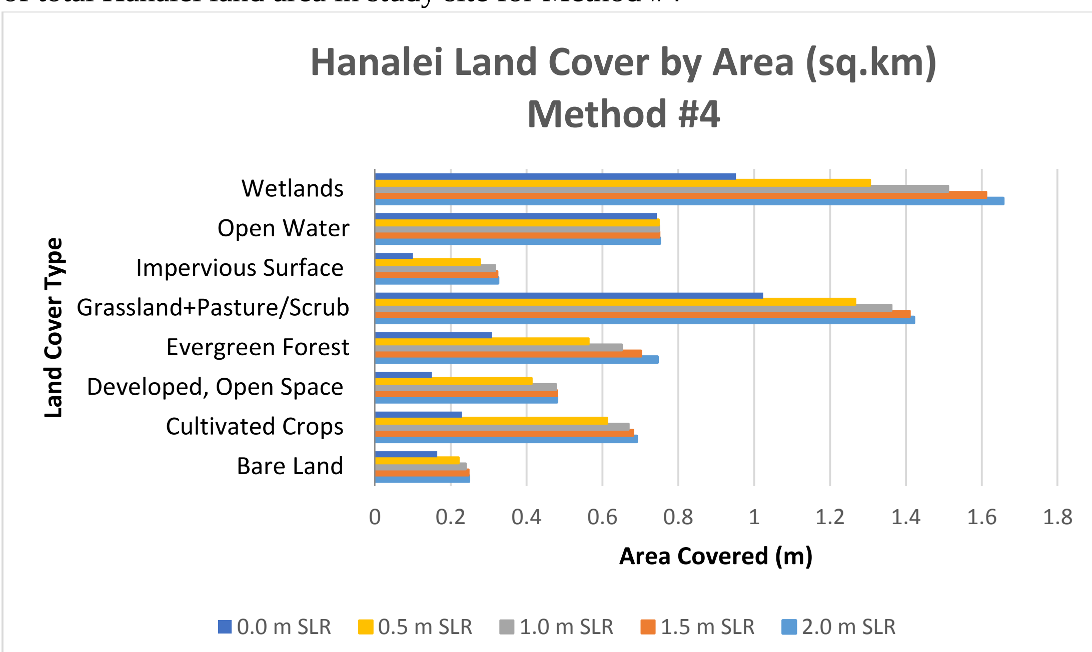

Appendix VIII
Kapa'a Percent Inundation by Land Cover Type

Figure 73 Land cover types inundated by each sea-level rise increment as a percent of total Kapa'a land area in study site for Method #1

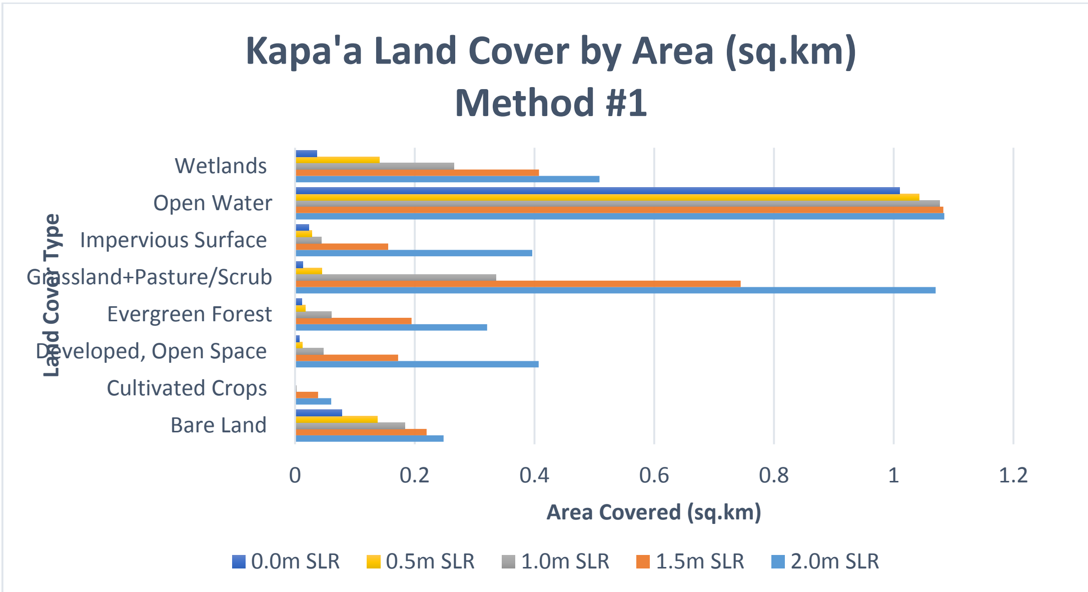

Figure 74 Land cover types inundated by each sea-level rise increment as a percent of total Kapa'a land area in study site for Method #2

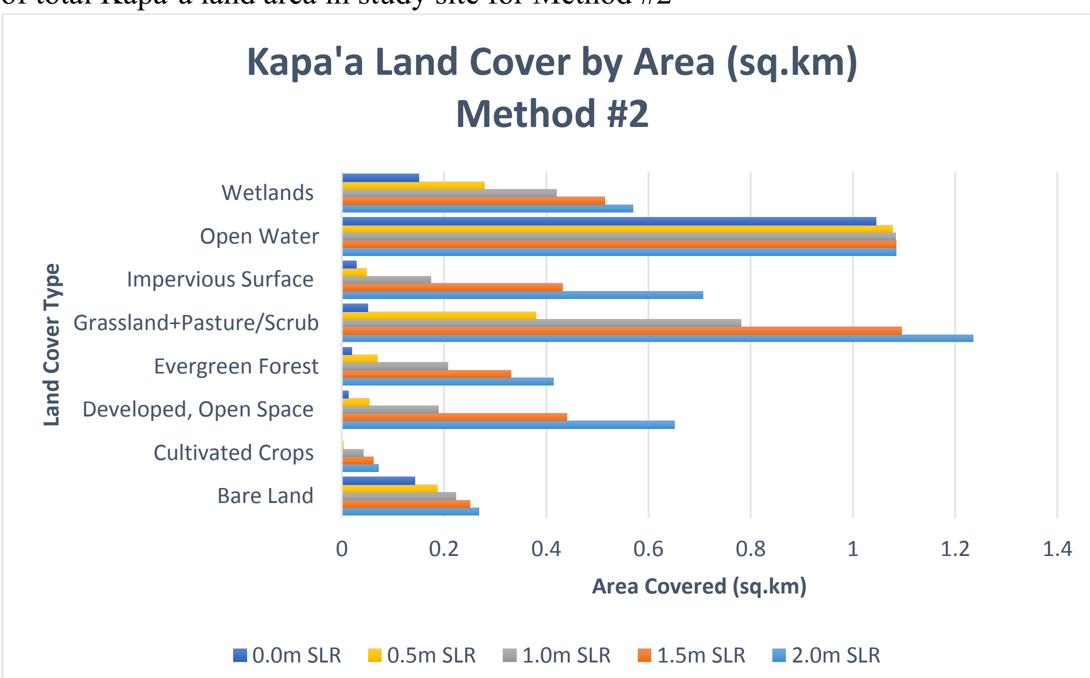

Figure 75 Land cover types inundated by each sea-level rise increment as a percent of total Kapa’a land area in study site for Method #3

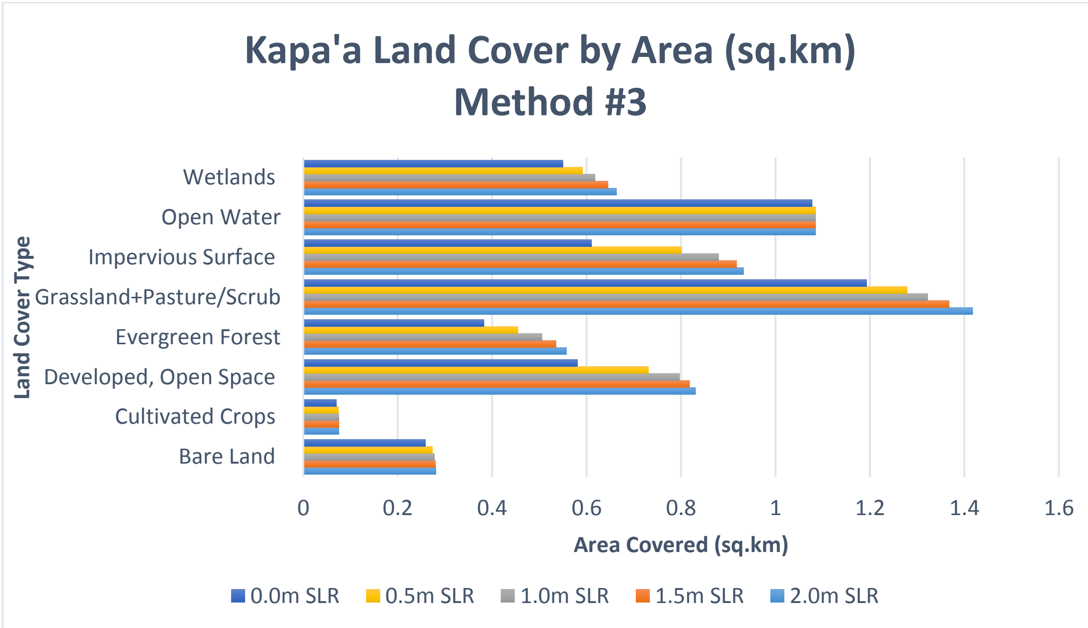

Figure 76 Land cover types inundated by each sea-level rise increment as a percent of total Kapa’a land area in study site for Method #4

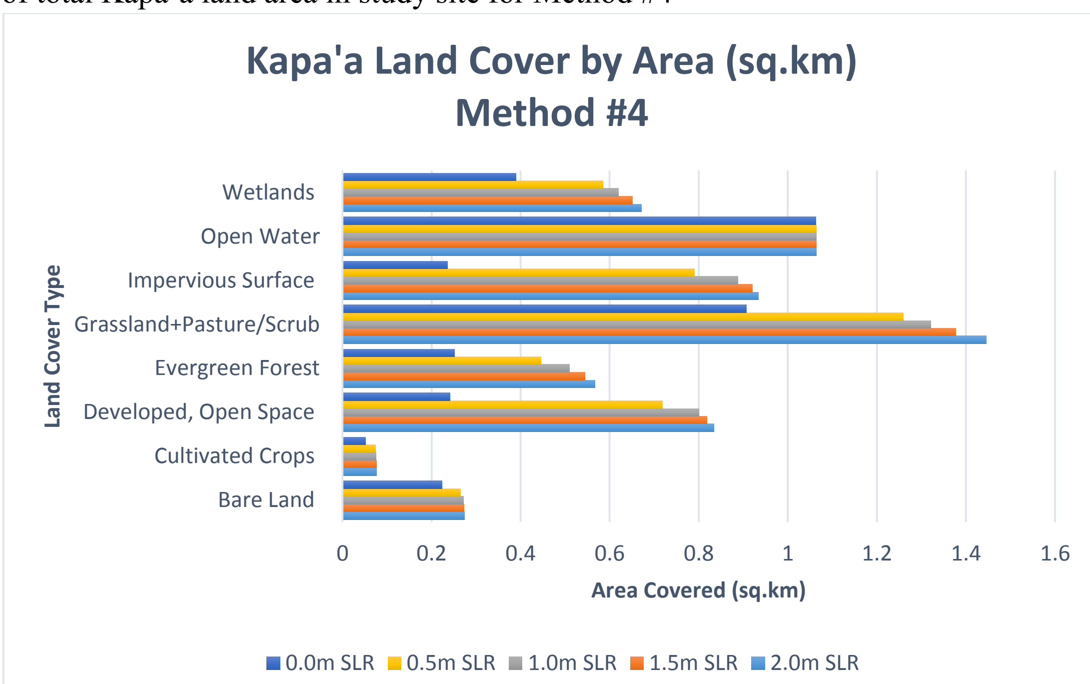

Appendix IX
Waimea Percent Inundation by Land Cover Type

Figure 77 Land cover types inundated by each sea-level rise increment as a percent of total Waimea land area in study site for Method #1

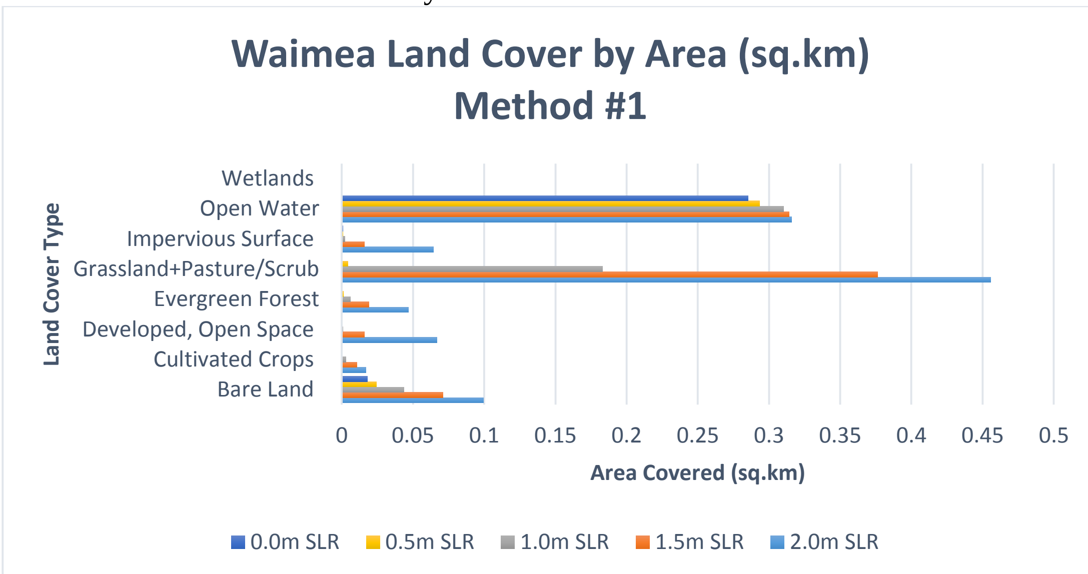

Figure 78 Land cover types inundated by each sea-level rise increment as a percent of total Waimea land area in study site for Method #2

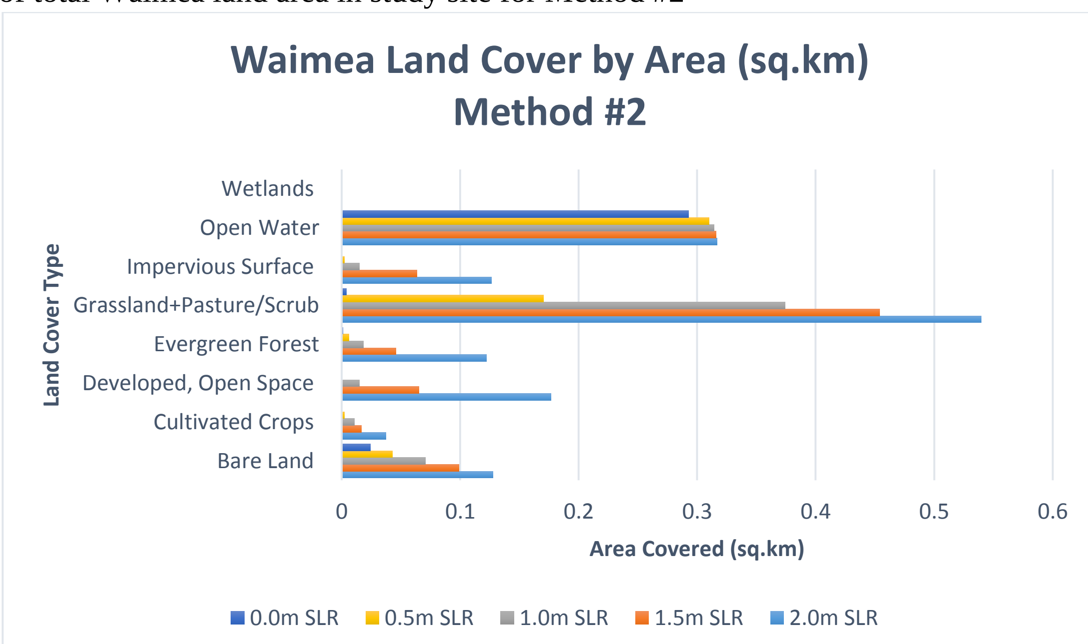

Figure 79 Land cover types inundated by each sea-level rise increment as a percent of total Waimea land area in study site for Method #3

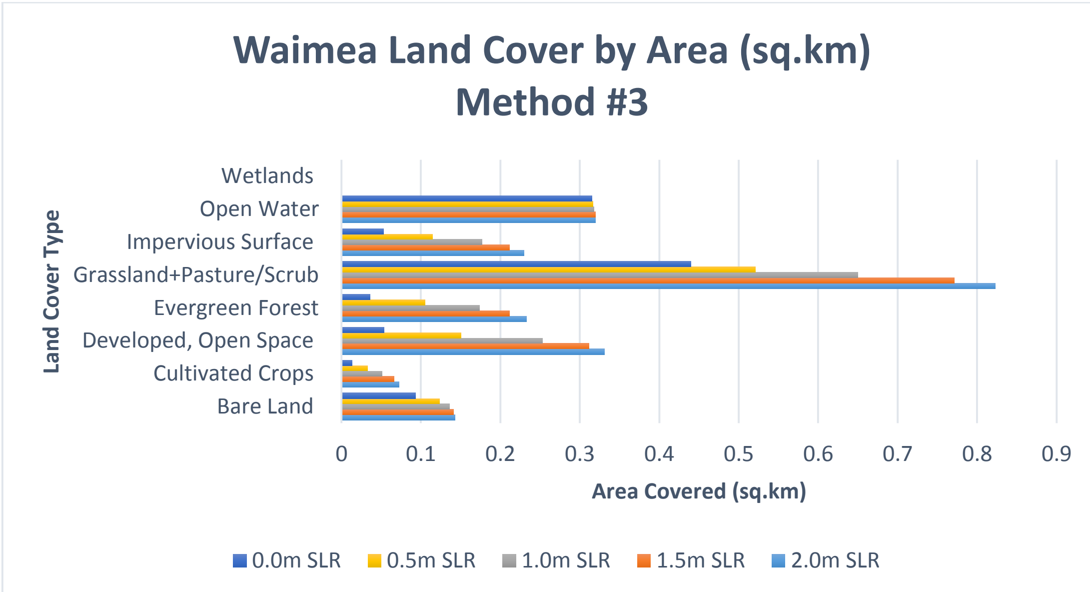

Figure 80 Land cover types inundated by each sea-level rise increment as a percent of total Waimea land area in study site for Method #4

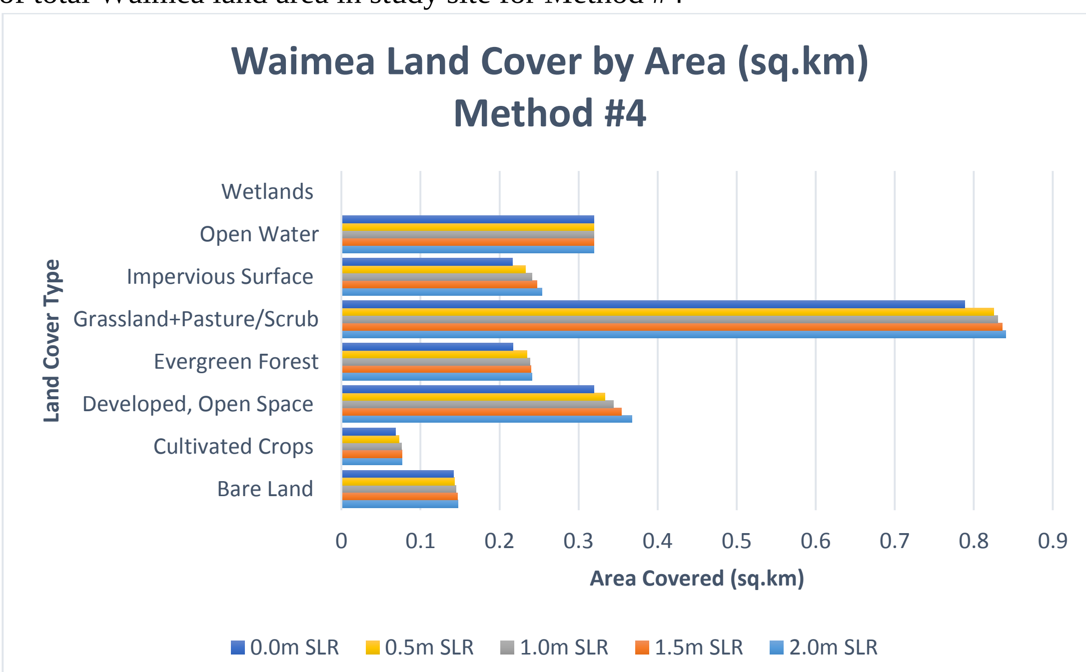

Appendix X

Data Tables

Table 1 Wave data information

Location	Mean Beach Slope	Sea Level Rise Increment (m)	Mean Wave Height (m)	Mean Period (sec)	Wavelength (m)	Wave Set-Up (m)	Wave Run-Up ($R_{2\%}$) (m)
Hanalei	0.4721	0.0	1.0	6.0	11.5	0.3	1.3
		0.5	1.5	6.0	11.5	0.7	1.6
		1.0	2.0	6.0	11.5	0.7	1.8
		1.5	2.5	6.0	11.5	0.7	2.0
		2.0	3.0	6.0	11.5	0.7	2.2
Kapa'a	0.3165	0.0	1.0	6.0	11.5	0.3	0.9
		0.5	1.5	6.0	11.5	0.7	1.1
		1.0	2.0	6.0	11.5	0.7	1.2
		1.5	2.5	6.0	11.5	0.7	1.4
		2.0	3.0	6.0	11.5	0.7	1.5
Waimea	0.2796	0.0	1.0	6.0	11.5	0.3	0.8
		0.5	1.5	6.0	11.5	0.7	0.9
		1.0	2.0	6.0	11.5	0.7	1.1
		1.5	2.5	6.0	11.5	0.7	1.2
		2.0	3.0	6.0	11.5	0.7	1.3

Table 2 Hanalei area covered by each method and all increments of sea-level rise

Total Area = 10.9969 sq.km	**Method #1**		**Method #2**		**Method #3**		**Method #4**	
Sea-level rise (m)	**Area Covered (sq.km)**	**Percent of total area covered**	**Area Covered (sq.km)**	**Percent of total area covered**	**Area Covered (sq.km)**	**Percent of total area covered**	**Area Covered (sq.km)**	**Percent of total area covered**
0.0	0.4462	4.1	0.7369	6.7	0.8523	7.8	3.0527	27.8
0.5	0.6912	6.3	1.3701	12.5	2.4205	22.0	4.7881	43.5
1.0	1.2960	11.8	2.2730	20.7	3.2093	29.2	5.3577	48.7
1.5	2.1741	19.8	3.1845	29.0	4.0252	36.6	5.5857	50.8
2.0	3.1102	28.3	3.9352	35.8	4.7082	42.8	5.6975	51.8

Table 3 Kapa'a area covered by each method and all increments of sea-level rise

Total Area = 19.2992 sq.km	Method #1		Method #2		Method #3		Method #4	
Sea-level rise (m)	**Area Covered (sq.km)**	**Percent of total area covered**	**Area Covered (sq.km)**	**Percent of total area covered**	**Area Covered (sq.km)**	**Percent of total area covered**	**Area Covered (sq.km)**	**Percent of total area covered**
0.0	0.3563	1.8	0.6910	3.6	1.6788	8.7	3.3978	17.6
0.5	0.6585	3.4	2.0334	10.5	3.4598	17.9	5.1374	26.6
1.0	1.9698	10.2	3.0740	15.9	5.4956	28.5	5.5320	28.7
1.5	2.9687	15.4	4.1638	21.6	5.7080	29.6	5.7080	29.6
2.0	4.0480	21.0	4.9552	25.7	5.8540	30.3	5.8540	30.3

Table 4 Waimea area covered by each method and all increments of sea-level rise

Total Area = 1.732 sq. km	**Method #1**		**Method #2**		**Method #3**		**Method #4**	
Sea-level rise (m)	**Area Covered (sq.km)**	**Percent of total area covered**	**Area Covered (sq.km)**	**Percent of total area covered**	**Area Covered (sq.km)**	**Percent of total area covered**	**Area Covered (sq.km)**	**Percent of total area covered**
0.0	0.0003	0.02	0.004877	0.3	0.1815	10.5	0.2786	16.1
0.5	0.005779	0.3	0.1713	9.9	0.3331	19.2	0.9931	57.3
1.0	0.3831	22.1	0.4200	24.2	0.6388	36.9	1.4228	82.1
1.5	0.4542	26.2	0.4929	28.5	1.0209	58.9	1.5852	91.5
2.0	0.4998	28.9	0.8802	50.8	1.3712	79.2	1.6276	94.0

Table 5 Hanalei land cover using Method #1

Sea-level rise (m)		**0**	**0.5**	**1.0**	**1.5**	**2.0**
Bare Land	**Area (sq.km)**	0.08922	0.1054	0.1228	0.1443	0.1657
	Percent of total area (%)	0.8	1.0	1.1	1.3	1.5
Cultivated Crops	**Area (sq.km)**	0.0000	0.0002480	0.002093	0.08507	0.2113
	Percent of total area (%)	0.0	0.002	0.2	0.8	1.9
Developed, Open Space	**Area (sq.km)**	0.009702	0.02002	0.04936	0.8815	0.1403
	Percent of total area (%)	0.09	1.8	0.4	0.8	1.3
Evergreen Forest	**Area (sq.km)**	0.002318	0.05500	0.1239	0.2022	0.2848
	Percent of total area (%)	0.02	0.5	1.1	1.8	2.6
Grassland/ Pasture/ Scrub	**Area (sq.km)**	0.006990	0.1089	0.4253	0.7595	0.9727
	Percent of total area (%)	0.06	0.1	0.4	0.8	1.0
Impervious Surface	**Area (sq.km)**	0.007710	0.008810	0.02396	0.05734	0.09270
	Percent of total area (%)	0.07	0.08	0.2	0.5	0.8
Open Water	**Area (sq.km)**	0.6920	0.7177	0.7340	0.7401	0.7435
	Percent of total area (%)	6.3	6.5	6.7	6.7	6.8
Wetland	**Area (sq.km)**	0.03205	0.08935	0.2070	0.5001	0.8872
	Percent of total area (%)	0.3	0.8	1.9	4.5	8.1

Table 6 Hanalei land cover using Method #2

Sea-level rise (m)		0	0.5	1.0	1.5	2.0
Bare Land	**Area (sq.km)**	0.1068	0.1249	0.1462	0.1675	0.1872
	Percent of total area (%)	1.0	1.1	1.3	1.5	1.7
Cultivated Crops	**Area (sq.km)**	0.0003629	0.02326	0.09893	0.2192	0.3410
	Percent of total area (%)	0.003	0.2	0.9	2.0	3.1
Developed, Open Space	**Area (sq.km)**	0.02257	0.05228	0.09351	0.1469	0.2316
	Percent of total area (%)	0.2	0.5	0.9	1.3	2.1
Evergreen Forest	**Area (sq.km)**	0.06070	0.1318	0.2106	0.2931	0.3973
	Percent of total area (%)	0.6	1.2	1.9	2.7	3.6
Grassland/ Pasture/ Scrub	**Area (sq.km)**	0.1332	0.4625	0.7880	0.9904	1.4820
	Percent of total area (%)	1.2	4.2	7.2	9.0	13.5
Impervious Surface	**Area (sq.km)**	0.009650	0.02604	0.06157	0.09781	0.1588
	Percent of total area (%)	0.09	0.2	0.6	0.9	1.4
Open Water	**Area (sq.km)**	0.7463	0.7439	0.7405	0.7349	0.7196
	Percent of total area (%)	6.5	6.7	6.7	6.8	6.8
Wetland	**Area (sq.km)**	0.09830	0.2254	0.5347	0.9127	1.1083
	Percent of total area (%)	0.9	2.0	4.9	8.3	10.1

Table 7 Hanalei land cover using Method #3

Sea-level rise (m)		**0**	**0.5**	**1.0**	**1.5**	**2.0**
Bare Land	**Area (sq.km)**	0.1099	0.1479	0.1689	0.1901	0.2165
	Percent of total area (%)	1.0	1.3	1.5	1.7	2.0
Cultivated Crops	**Area (sq.km)**	0.1133	0.1628	0.2480	0.4321	0.6012
	Percent of total area (%)	1.0	1.5	2.3	3.9	5.5
Developed, Open Space	**Area (sq.km)**	0.03123	0.1055	0.1656	0.3002	0.4015
	Percent of total area (%)	0.3	1.0	1.5	2.7	3.7
Evergreen Forest	**Area (sq.km)**	0.1014	0.2422	0.3306	0.4424	0.5513
	Percent of total area (%)	0.9	2.2	3.0	4.0	5.0
Grassland/ Pasture/ Scrub	**Area (sq.km)**	0.3194	0.8789	1.0636	1.1768	1.2570
	Percent of total area (%)	2.9	8.0	9.7	10.7	11.4
Impervious Surface	**Area (sq.km)**	0.01225	0.0703	0.1128	0.1878	0.2674
	Percent of total area (%)	0.1	0.6	1.0	1.7	2.94
Open Water	**Area (sq.km)**	0.72911	0.7417	0.7445	0.7469	0.7481
	Percent of total area (%)	6.6	6.7	6.8	6.8	6.8
Wetland	**Area (sq.km)**	0.3822	0.6926	0.9965	1.1700	1.2859
	Percent of total area (%)	3.5	6.3	9.1	10.6	11.7

Table 8 Hanalei land cover using Method #4

Sea-level rise (m)		**0**	**0.5**	**1.0**	**1.5**	**2.0**
Bare Land	**Area (sq.km)**	0.1645	0.2212	0.2396	0.2475	0.2480
	Percent of total area (%)	1.5	2.0	2.2	2.3	2.3
Cultivated Crops	**Area (sq.km)**	0.2297	0.6129	0.6695	0.6809	0.6901
	Percent of total area (%)	2.1	5.6	6.1	6.2	6.3
Developed, Open Space	**Area (sq.km)**	0.1504	0.4136	0.4777	0.4803	0.4804
	Percent of total area (%)	1.4	3.8	4.3	4.4	4.4
Evergreen Forest	**Area (sq.km)**	0.3090	0.5637	0.6512	0.7022	0.7452
	Percent of total area (%)	2.8	5.1	5.9	6.4	6.8
Grassland/ Pasture/ Scrub	**Area (sq.km)**	1.0242	1.2668	1.36239	1.4104	1.4211
	Percent of total area (%)	9.3	11.5	12.4	12.8	12.9
Impervious Surface	**Area (sq.km)**	0.1003	0.2767	0.3169	0.3229	0.3253
	Percent of total area (%)	0.9	2.5	2.9	2.9	3.0
Open Water	**Area (sq.km)**	0.7440	0.7483	0.7494	0.7504	0.7511
	Percent of total area (%)	6.8	6.8	6.8	6.8	6.8
Wetland	**Area (sq.km)**	0.9518	1.3056	1.5115	1.6118	1.6571
	Percent of total area (%)	8.7	11.9	13.7	14.7	15.1

Table 9 Kapa'a land cover using Method #1

Sea-level rise (m)		0	0.5	1.0	1.5	2.0
Bare Land	**Area (sq.km)**	0.07855	0.1374	0.1840	0.2200	0.2480
	Percent of total area (%)	0.4	0.7	1.0	1.1	1.3
Cultivated Crops	**Area (sq.km)**	0.0000001865	0.00001532	0.002377	0.03834	0.06044
	Percent of total area (%)	0.0	0.0	0.01	0.2	0.3
Developed, Open Space	**Area (sq.km)**	0.007114	0.01247	0.04785	0.1724	0.4069
	Percent of total area (%)	0.04	0.06	0.2	0.9	2.1
Evergreen Forest	**Area (sq.km)**	0.01109	0.01752	0.06063	0.1946	0.3209
	Percent of total area (%)	0.06	0.09	0.3	1.0	1.7
Grassland/ Pasture/ Scrub	**Area (sq.km)**	0.03492	0.1474	0.3039	0.5092	0.6764
	Percent of total area (%)	0.07	0.2	1.7	3.9	5.5
Impervious Surface	**Area (sq.km)**	0.02356	0.02831	0.04415	0.1554	0.3962
	Percent of total area (%)	0.1	0.1	0.2	0.8	2.1
Open Water	**Area (sq.km)**	1.0101	1.0424	1.0770	1.0830	1.0849
	Percent of total area (%)	5.2	5.4	5.6	5.6	5.6
Wetland	**Area (sq.km)**	0.03619	0.1404	0.2660	0.4076	0.5084
	Percent of total area (%)	0.2	0.7	1.4	2.1	2.6

Table 10 Kapa'a land cover using Method #2

Sea-level rise (m)		**0**	**0.5**	**1.0**	**1.5**	**2.0**
Bare Land	**Area (sq.km)**	0.1431	0.1870	0.2228	0.2502	0.2683
	Percent of total area (%)	0.7	1.0	1.2	1.3	1.4
Cultivated Crops	**Area (sq.km)**	0.00001533	0.003001	0.04215	0.06199	0.07207
	Percent of total area (%)	0.0	0.02	0.2	0.3	0.4
Developed, Open Space	**Area (sq.km)**	0.01320	0.05456	0.1893	0.4409	0.6508
	Percent of total area (%)	0.07	0.3	1.0	2.3	3.4
Evergreen Forest	**Area (sq.km)**	0.01917	0.06947	0.2081	0.3309	0.4147
	Percent of total area (%)	0.1	0.4	1.1	1.7	2.1
Grassland/ Pasture/ Scrub	**Area (sq.km)**	0.05070	0.3797	0.7818	1.0953	1.2354
	Percent of total area (%)	0.3	2.0	4.1	5.7	6.4
Impervious Surface	**Area (sq.km)**	0.02906	0.04828	0.1743	0.4323	0.7065
	Percent of total area (%)	0.2	0.3	0.9	2.2	3.7
Open Water	**Area (sq.km)**	1.0453	1.0781	1.0835	1.0848	1.0850
	Percent of total area (%)	5.4	5.6	5.6	5.6	5.6
Wetland	**Area (sq.km)**	0.1508	0.2792	0.4197	0.5151	0.5699
	Percent of total area (%)	0.8	1.4	2.2	2.7	3.0

Table 11 Kapa'a land cover using Method #3

Sea-level rise (m)		0	0.5	1.0	1.5	2.0
Bare Land	**Area (sq.km)**	0.1634	0.2247	0.2498	0.2729	0.2737
	Percent of total area (%)	0.8	1.2	1.3	1.4	1.4
Cultivated Crops	**Area (sq.km)**	0.008634	0.05235	0.06837	0.07582	0.07651
	Percent of total area (%)	0.04	0.3	0.4	0.4	0.4
Developed, Open Space	**Area (sq.km)**	0.2454	0.2536	0.5345	0.8182	0.8345
	Percent of total area (%)	1.3	1.3	2.8	4.2	4.3
Evergreen Forest	**Area (sq.km)**	0.04096	0.2594	0.3643	0.5443	0.5672
	Percent of total area (%)	0.2	1.3	1.9	2.8	2.9
Grassland/ Pasture/ Scrub	**Area (sq.km)**	0.7567	0.9276	1.1563	1.3768	1.4456
	Percent of total area (%)	3.9	4.8	6.0	7.1	7.5
Impervious Surface	**Area (sq.km)**	0.03299	0.2487	0.5480	0.9204	0.9344
	Percent of total area (%)	0.2	1.3	2.8	4.8	4.8
Open Water	**Area (sq.km)**	1.0535	1.0630	1.0637	1.0637	1.0637
	Percent of total area (%)	5.5	5.5	5.5	5.5	5.5
Wetland	**Area (sq.km)**	0.2225	0.4621	0.5352	0.6508	0.6716
	Percent of total area (%)	1.2	2.4	2.8	3.4	3.5

Table 12 Kapa'a land cover using Method #4

Sea-level rise (m)		**0**	**0.5**	**1.0**	**1.5**	**2.0**
Bare Land	**Area (sq.km)**	0.2233	0.2650	0.2718	0.2729	0.2737
	Percent of total area (%)	1.2	1.4	1.4	1.4	1.4
Cultivated Crops	**Area (sq.km)**	0.05143	0.07363	0.07552	0.07582	0.7651
	Percent of total area (%)	0.3	0.4	0.4	0.4	0.4
Developed, Open Space	**Area (sq.km)**	0.2421	0.7189	0.7998	0.8182	0.8345
	Percent of total area (%)	1.3	3.7	4.1	4.2	4.3
Evergreen Forest	**Area (sq.km)**	0.2516	0.4462	0.5101	0.5443	0.5672
	Percent of total area (%)	1.3	2.3	2.6	2.8	2.9
Grassland/ Pasture/ Scrub	**Area (sq.km)**	0.9071	1.2588	1.3211	1.3768	1.4456
	Percent of total area (%)	4.7	6.5	6.8	7.1	7.5
Impervious Surface	**Area (sq.km)**	0.2358	0.7910	0.8881	0.9204	0.9344
	Percent of total area (%)	1.2	4.1	4.6	4.8	4..8
Open Water	**Area (sq.km)**	1.0630	1.0637	1.0637	1.0637	1.0637
	Percent of total area (%)	5.5	5.5	5.5	5.5	5.5
Wetland	**Area (sq.km)**	0.3902	0.5847	0.6197	0.6508	0.6716
	Percent of total area (%)	2.0	3.0	3.2	3.4	3.5

Table 13 Waimea land cover using Method #1

Sea-level rise (m)		**0**	**0.5**	**1.0**	**1.5**	**2.0**
Bare Land	**Area (sq.km)**	0.01780	0.02451	0.04386	0.07111	0.09962
	Percent of total area (%)	1.0	1.4	2.5	4.1	5.8
Cultivated Crops	**Area (sq.km)**	0.0000	0.00003522	0.002881	0.01073	0.01693
	Percent of total area (%)	0.0	0.02	0.2	0.6	1.0
Developed, Open Space	**Area (sq.km)**	0.0000	0.00001228	0.0008962	0.01584	0.06695
	Percent of total area (%)	0.0	0.0	0.05	0.9	3.9
Evergreen Forest	**Area (sq.km)**	0.0005940	0.001087	0.006295	0.01897	0.04671
	Percent of total area (%)	0.03	0.06	0.4	1.1	2.7
Grassland/ Pasture/ Scrub	**Area (sq.km)**	0.0000	0.004290	0.1831	0.3764	0.4558
	Percent of total area (%)	0.0	0.2	10.6	21.7	26.3
Impervious Surface	**Area (sq.km)**	0.0007620	0.0008000	0.002134	0.01582	0.06454
	Percent of total area (%)	0.04	0.05	0.1	0.9	3.7
Open Water	**Area (sq.km)**	0.2854	0.2933	0.3101	0.3142	0.3157
	Percent of total area (%)	16.5	16.9	17.9	18.1	18.2
Wetland	**Area (sq.km)**	0.0000	0.0000	0.0000	0.0000	0.0000
	Percent of total area (%)	0.0	0.0	0.0	0.0	0.0

Table 14 Waimea land cover using Method #2

Sea-level rise (m)		0	0.5	1.0	1.5	2.0
Bare Land	**Area (sq.km)**	0.02416	0.04282	0.07038	0.09885	0.1277
	Percent of total area (%)	1.4	2.5	4.1	5.7	7.4
Cultivated Crops	**Area (sq.km)**	0.00003240	0.002251	0.01077	0.01651	0.03728
	Percent of total area (%)	0.002	0.1	0.6	1.0	2.2
Developed, Open Space	**Area (sq.km)**	0.000006160	0.0008369	0.01473	0.06522	0.1767
	Percent of total area (%)	0.0	0.05	0.9	3.8	10.2
Evergreen Forest	**Area (sq.km)**	0.001045	0.006015	0.01841	0.04551	0.1222
	Percent of total area (%)	0.06	0.3	1.1	2.6	7.1
Grassland/ Pasture/ Scrub	**Area (sq.km)**	0.003730	0.1705	0.3743	0.4542	0.5396
	Percent of total area (%)	0.2	9.8	21.6	26.2	31.2
Impervious Surface	**Area (sq.km)**	0.0008000	0.002070	0.01488	0.06347	0.1265
	Percent of total area (%)	0.05	0.1	0.9	3.7	7.3
Open Water	**Area (sq.km)**	0.2927	0.3100	0.3142	0.3157	0.3167
	Percent of total area (%)	16.9	17.9	18.1	18.2	18.3
Wetland	**Area (sq.km)**	0.0000	0.0000	0.0000	0.0000	0.0000
	Percent of total area (%)	0.0	0.0	0.0	0.0	0.0

Table 15 Waimea land cover using Method #3

Sea-level rise (m)		**0**	**0.5**	**1.0**	**1.5**	**2.0**
Bare Land	**Area (sq.km)**	0.03211	0.0797	0.1104	0.1329	0.1396
	Percent of total area (%)	1.9	4.6	6.4	7.7	8.1
Cultivated Crops	**Area (sq.km)**	0.000391	0.01115	0.02479	0.04406	0.06080
	Percent of total area (%)	0.02	0.6	1.4	2.5	3.5
Developed, Open Space	**Area (sq.km)**	0.0002468	0. 03367	0.1052	0.2157	0.2933
	Percent of total area (%)	0.01	1.9	6.1	12.5	16.9
Evergreen Forest	**Area (sq.km)**	0.002204	0.02408	0.07274	0.1504	0.1983
	Percent of total area (%)	0.1	1.4	4.2	8.7	11.4
Grassland/ Pasture/ Scrub	**Area (sq.km)**	0.04382	0.4042	0.4853	0.5923	0.7303
	Percent of total area (%)	2.5	23.3	28.0	34.2	42.2
Impervious Surface	**Area (sq.km)**	0.001439	0.03292	0.08863	0.1527	0.2006
	Percent of total area (%)	0.1	1.9	5.1	8.8	11.6
Open Water	**Area (sq.km)**	0.3051	0.3142	0.3153	0.3167	0.3184
	Percent of total area (%)	17.6	18.1	18.2	18.3	18.4
Wetland	**Area (sq.km)**	0.0000	0.00000	0.0000	0.0000	0.0000
	Percent of total area (%)	0.0	0.0	0	0.0	0.0

Table 16 Waimea land cover using Method #4

Sea-level rise (m)		0	0.5	1.0	1.5	2.0
Bare Land	**Area (sq.km)**	0.07294	0.1318	0.1405	0.1427	0.1451
	Percent of total area (%)	4.2	7.6	8.1	8.2	8.4
Cultivated Crops	**Area (sq.km)**	0.01088	0.04236	0.06391	0.07244	0.07585
	Percent of total area (%)	0.6	2.4	3.7	4.2	4.4
Developed, Open Space	**Area (sq.km)**	0.2062	0.2099	0.3019	0.3315	0.3441
	Percent of total area (%)	11.9	12.1	17.4	19.1	19.9
Evergreen Forest	**Area (sq.km)**	0.04330	0.2045	0.2051	0.228	0.2382
	Percent of total area (%)	2.5	11.8	11.8	13.4	13.8
Grassland/ Pasture/ Scrub	**Area (sq.km)**	0.3854	0.5737	0. 7543	0.8228	0.8307
	Percent of total area (%)	22.2	33.1	43.6	47.5	48.0
Impervious Surface	**Area (sq.km)**	0.1461	0.2057	0.2114	0.2299	0.2409
	Percent of total area (%)	8.4	11.9	12.2	13.3	13.9
Open Water	**Area (sq.km)**	0.3137	0.3165	0.3187	0.3196	0.3196
	Percent of total area (%)	18.1	18.3	18.4	18.5	18.5
Wetland	**Area (sq.km)**	0.0000	0.0000	0.0000	0.0000	0.0000
	Percent of total area (%)	0.0	0.0	0.0	0.0	0.0

References

Clague, D.A., and Dalrymple, G.B., 1989, Tectonics, geochronology, and origin of the Hawaiian Emperor Volcanic Chain, *in* Winterer, E.L., Hussong, D.M., and Decker R.W. (eds.), The Eastern Pacific Ocean and Hawaii: Geological Society of America, Boulder, Colorado, p. 188–217.

Courtillot, V., Davaille, A., Besse, J. & Stock, J. 2003 Three distinct types of hotspots in the Earth's mantle. Earth Planet. Sci. Lett. 205, 295–308. (doi:10.1016/S0012-821X(02)01048-8)

Department of Commerce (DOC), National Oceanic and Atmospheric Administration (NOAA), National Ocean Service (NOS), Coastal Services Center (CSC), 2005, C-CAP Land Cover, Kauai, Hawaii 2005, Charleston, SC, NOAA's Ocean Service, Coastal Services Center (CSC),(Also available at http://www.csc.noaa.gov/digitalcoast/data/ccaphighres/index.html).

Eversole, Dolan, and Lemmo, Sam, 2007, Waikiki beach nourishment: A demonstration of offshore sand recycling, State of Hawaii Department of Land and Natural Resources, Honolulu, Hawaii, (Also available at www6.hawaii.gov/dlnr/occl/files/Waikiki/summary.pdf).

Feirstein, E., and Fletcher, C.H., 2004, Hawaii's coastline: Chapter for the world's coastline, ed. Eric Bird, p.44, (Also available at http://www.wkap.nl/subjects/TWCO).

Fletcher, Charles, Boyd, Robynne, Grober-Dunsmore, Rikki, Neal, William J., and Tice, Virginia, 2010, On the Shores of Paradise. Hawaii: University of Hawaii Press, SOEST.

Fletcher, C.H., Romine, B.M., Genz, A.S., Barbee, M.M., Dyer, Matthew, Anderson, T.R., Lim, S.C., Vitousek, Sean, Bochicchio, Christopher, and Richmond, B.M., 2012, National assessment of shoreline change: Historical shoreline change in the Hawaiian Islands: U.S. Geological Survey Open-File Report 2011–1051, p.55, (Also available at http://pubs.usgs.gov/of/2011/1051).

Garvey, Kim, Sloop, Robert, Smith, Thomas, and Podoski, Jessica, 2012, Regional sediment management- Hawaii style: Studies on Maui and Kauai, State of Hawaii Department of Land and Natural Resources, US Army Corps of Engineers, Honolulu District, H20 Conference, San Diego, California

Gibbs, A.E., Richmond, B.M., Fletcher, C.H., and Hilman, K.P, 2001, Hawaii Beach Monitoring Program: Beach Profile Data: USGS Open File Report 01-308, ver. 1.0.

Griggs, G. B., J. F. Tait, L. J. Moore, K. Scott, W. Corona and D. Pembrook , 1997, The Interaction of Seawalls and Beaches: Eight years of field monitoring, Monterey Bay, California, U.S. Army Corps of Engineers, Waterways Experiment Station Contract Report CHL-97-1: 34.

Griggs, G.B., 2005, The impacts of coastal armoring, 2005, Shore and Beach, 73:1: p.13-22.

Guiles, Martin, Luther, Douglas S., and Merrifield, Mark, 2012, Sea level forecasts at harbors in Hawaii and on other Pacific islands, PacIOOS-Sea Level Public Information Products, SOEST Technical Report, Honolulu, Hawaii, School of Ocean and Earth Science and Technology, University of Hawaii at Manoa, p. 1-72.

Hoeke, R., C. Storlazzi, and P. Ridd, 2011, Hydrodynamics of a bathymetrically complex fringing coral reef embayment: Wave climate, in situ observations, and wave prediction, J. Geophys. Res., 116, C04018, doi:10.1029/2010JC006170.

Jensen, Dr.Robert. 2010, Wave Information Studies Project. Coastal and Hydraulics Laboratory; Engineer Research and Development Center, US Army Corps of Engineers, National Oceanic and Atmospheric Administration (NOAA), National Ocean Service (NOS). 2010. Technical Considerations for Use of Geospatial Data in Sea Level Change Mapping and Assessment. NOAA NOS Technical Report. Silver Spring, MD: NOAA NOS.

Komar, Paul D., 1976, Beach processes and sedimentation. Prentice-Hall, Englewood Cliffs, New Jersey.

Miller, T.L. and Fletcher, C.H., 2003, Waikiki: Historical analysis of an engineered Shoreline, Journal of Coastal Research, v. 19.4, p. 1026-1043.

National Research Council, 2012, Sea-Level Rise for the Coasts of California, Oregon and Washington: Past, Present and Future. The National Academies Press, Washington, D.C. p.274.

Neall, Vincent E. and Trewick, Steven A., 2008, The age and origin of the Pacific Islands: A geological overview. Phil. Trans. R. Soc. B 363 (1508): 3293–3308. doi:10.1098/rstb.2008.0119

NOAA, 2012, Detailed Methodology for Mapping Sea-level rise Inundation, NOAA Coastal Services Center, (Also available at www.csc.noaa.gov/slr/viewer/assests/pdfs/Inundation_Methods.pdf).

Office of Ocean and Coastal Resource Management, 2012, Shoreline management: Construction setbacks, ocean and coastal resource management, National Oceanic and Atmospheric Administration,(Also available at http://coastalmanagement.noaa.gov/initiatives/shoreline_ppr_setbacks.html).

Rahmstorf, S. 2007, A semi-empirical approach to projecting future SLR: Science, v. 315, no. 5810, p. 368–370.

Reynolds, M.H., Berkowitz, P., Courtot, K.N., and Krause, C.M., eds., 2012, Predicting sea-level rise vulnerability of terrestrial habitat and wildlife of the Northwestern Hawaiian Islands: U.S. Geological Survey Open-File Report 2012–1182, p.139.

Ruggiero P., Komar, P.D., McDougal, W.G., Marra, J.J., and Beach, R.A., 2001, Wave runup, extreme water levels and the erosion of properties backing beaches, Journal of Coastal Research, 17(2), p. 407-419.

Stamski, Rebecca, 2005,The impacts of coastal protection structures in California's Monterey Bay National Marine Sanctuary, Marine Sanctuaries Conservation Series MSD-05-3, U.S. Department of Commerce, National Oceanic and Atmospheric Administration, Marine Sanctuaries Division, Silver Spring, MD. p.18.

Stockdon, H.F., Holman, R.A., Howd, P.A., and Sallenger, A.H., 2006, Empirical parameterization of setup, swash, and runup: Coastal Engineering, v. 53, p. 573–588.

Storlazzi, C.D., Berkowitz, P., Reynolds, M.H., and Logan, J.B., 2013, Forecasting the impact of storm waves and sea-level rise on Midway Atoll and Laysan Island within the Papahānaumokuākea Marine National Monument—a comparison of passive versus dynamic inundation models: U.S. Geological Survey Open-File Report 2013-1069, p. 78.

Storlazzi, C.D., Elias, E., Field, M.E., and Presto, M.K., 2011, Numerical modeling of the impact of SLR on fringing coral reef hydrodynamics and sediment transport: Coral Reefs, v. 30, no. 1, p. 83–96.

Tarduno, John, Bunge, Hans-Peter, Sleep, Norm, and Hansen, Ulrich, 2009, The bent Hawaiian-Emperor hotspot track: Inheriting the mantle wind, Science 3 April 2009: 324 (5923), 50-53. [DOI:10.1126/science.1161256].

Vitousek, Sean, Fletcher, Charles H., and Barbee, Matthew M., 2008, A practical approach to mapping extreme wave inundation: Consequences of sea-level rise and coastal erosion, Proceedings: Solution to Coastal Disaster 2008, Oahu, Hawaii, April 13-16, p.85-96.

http://csc.noaa.gov/slr/data/

www.meted.ucar.edu/marine/

http://wis.usace.army.mil/pac